

科研论文一览表

序号	论文题目	第一作者	发表/出版时间	发表刊物名称	论文收录
1	Mechanisms of Paeoniflorin against myocardial ischemia reperfusion injury based on network pharmacology	赵成国	2021-09-26	Mater. Express	SCI
2	The mechanism of radix paeoniae rubra in treatment of myocardial ischemia-reperfusion injury based on network pharmacology and molecular docking	尹美芳	2021-08-30	Materials Express	SCI
3	Self-assembled drug-polymer micelles with NO precursor loaded for synergistic cancer therapy	金元宝	2021-08-01	Journal of Polymer Research	SCI
4	Effect of starter cultures mixed with different autochthonous lactic acid bacteria on microbial, metabolome and sensory properties of Chinese northeast sauerkraut	胡文忠	2021-07-14	Food Research International	SCI
5	The p-Anisaldehyde/beta-cyclodextrin inclusion complexes as fumigation agent for control of postharvest decay and quality of strawberry	林莹	2021-06-12	Food Control	SCI
6	Phytochemical and chemotaxonomic studies on Pteris wallichiana J. Agardh	胡文忠	2021-02-10	Biochemical Systematics and Ecology	SCI
7	Cloning and functional analysis of HMGR gene in Ligularia fischeri	杜娟	2020-12-11	IOP Conference Series: Earth and Environmental Science	EI国际
8	Study on the anticancer biological mechanism of Resveratrol	杜娟	2020-12-11	E3S Web of Conferences	EI国际
9	Study on the Mechanism of Paeoniflorin Against Atherosclerosis Through Network Pharmacology and Molecular Docking	赵成国	2020-12-08	Journal of Biobased Materials and Bioenergy?	SCI
10	The protection of forsythin against L-Glu-induced HT22 cells damage and AD symptoms in APP/PS1 mice	王艳珍	2020-11-15	Basic & Clinical Pharmacology & Toxicology	SCI
11	Identification of Chemical Components in Pericarpium Citri Reticulatae by HPLC-MS/MS	刘明石	2020-10-29	Earth and Environmental Science	EI国际
12	The hypoglycemic and renal protective effects of Grifola frondosa polysaccharides in early diabetic nephropathy	姜涛	2020-10-01	journal of food biochemistry	SCI
13	Modern research progress on pharmacological effects of paeoniflorin	赵成国	2020-09-03	IOP Conference Series: Earth and Environmental Science	EI国际
14	Research progress of detection technology for illegal addition of prohibited substances in cosmetics	张瑶	2020-09-03	Earth and Environmental Science	EI国际
15	The Potential of Chlorine Dioxide Gas for Postharvest Diplodia Stem-End Rot Control on Citrus Fruit	钟恬	2020-09-01	HORTSCIENCE	SCI
16	Comparative study on main components and detection methods of pericarpium citri reticulatae from different habitats	刘明石	2020-08-31	Earth and Environmental Science	EI国际

17	WD105, a novel decursin derivative, showed greater growth inhibition and androgen receptor suppression in LNCaP human prostate cancer cells	吴威	2020-08-20	Cancer Res	SCI
18	Antimicrobial efficacy of liposome encapsulated citral and effect on the shelf life of Shatangju mandarin	陈沛洲	2020-08-01	JOURNAL OF FOOD PROTECTION	SCI
19	Determination of the Content of Amlodipine Desylate Tablets and Its Application in the Treatment of Hypertension	张瑶	2020-07-23	Medical Development and Human Health	SCI
20	Preparation and Physical Properties of Gelatin-based film Containing carvacrol/ β -cyclodextrin Inclusion Complex	钟恬	2020-07-01	JOURNAL OF THE PAKISTAN MEDICAL ASSOCIATION	SCI
21	Preparation, Characterization and in vitro Antibacterial Activities of Citral-Loaded Liposome	钟恬	2020-07-01	JOURNAL OF THE PAKISTAN MEDICAL ASSOCIATION	SCI
22	Effects of Dietary Supplementation of Lauric Acid on Lactation Function, Mammary Gland Development, and Serum Lipid Metabolites in Lactating Mice	杨林	2020-03-22	animals	SCIE
23	A metabolomic study of the urine of rats with Alzheimer's disease and the efficacy of Ding-Zhi-Xiao-Wan on the afflicted rats	何洋	2020-02-20	Journal of Separation Science	SCI
24	Anti-fatigue Evaluation of Rehmanniae Radix	赵成国	2020-02-01	Basic & Clinical Pharmacology & Toxicology	SCI
25	Preparation and In Vitro Performance Evaluation of Ellagic Acid	秦书芝	2020-02-01	Basic & Clinical Pharmacology & Toxicology	SCI
26	Chemical characterization of small-molecule inhibitors of monoamine oxidase B synthesized from the Acanthopanax senticosus root with affinity ultrafiltration mass spectrometry	何洋	2020-01-20	Rapid Commun Mass Spectrom.	SCI
27	The anti-fatigue and anti-anoxia effects of Tremella extract	杨东生	2019-12-30	SAUDI JOURNAL OF BIOLOGICAL SCIENCES	SCI
28	Study on the antioxidation of mango polyphenols	李晶莹	2019-11-01	IOP Conference Series: Earth and Environmental Science	EI国际
29	Pharmacological Basis for Application of Purified Polysaccharides Obtained Sparassis crispa Fruitbodies in Alzheimer's Disease	王艳珍	2019-11-01	Basic & Clinical Pharmacology & Toxicology	SCI
30	Microfluidic-Based Approaches for Foodborne Pathogen Detection	刘焱	2019-09-23	Microorganisms	SCI
31	Protective Effects of Fagopyrum cymosum against DSS-Induced colitis in Mice	王兰英	2019-08-19	Indian Journal of Pharmaceutical Sciences	SCI
32	Preparation and characterization of medical gelatin matrix composites	张瑶	2019-03-22	Materials Science and Engineering	EI国内
33	Optimization of Liquid Fermentation Medium for Mycelium of Pleurotus djamor	王亮	2019-02-05	Indian Journal of Pharmaceutical Sciences	SCI
34	Effects of Paeoniflorin on Oxidative Stress and Inflammatory Response in Rats with Ischemia-reperfusion Injury	秦书芝	2019-02-01	Indian Journal of Pharmaceutical Sciences	SCI

35	Analysis of Different Processed Products Volatile Oil Magnolia officinalis and their Antibacterial Effects in vitro	赵成国	2019-02-01	Indian Journal of Pharmaceutical Sciences	SCI
36	preparation and in vitro Release of Lutein Ophthalmic in situ Gel	吴丽艳	2019-02-01	INDIAN PHARMACEUYICAL ASSOC	SCIE
37	Identification of the Main Components of Coriolus Versicolor Fruiting Body	孟凡欣	2019-01-30	Indian Journal of Pharmaceutical Sciences	SCI
38	Adsorption Kinetics and Isotherms of Flavonoids from Pteris esquiroliiion Macroporous Resin	胡文忠	2019-01-30	Indian Journal of Pharmaceutical Sciences	SCI
39	The Phytochemical Constituents of the Rhizomes of Sophora tonkinensis	胡文忠	2019-01-30	Indian Journal of Pharmaceutical Sciences	SCI
40	Research Progress on Antioxidant Activity of Phenolic Compounds in Fresh-cut Vegetables Induced by Injury Stress	胡文忠	2019-01-30	Indian Journal of Pharmaceutical Sciences	SCI
41	Effect of Chitosan Coating on the Quality and Antioxidant Enzymes of the Sweet Cherry (Prunus avium L.) During Storage	胡文忠	2019-01-30	Indian Journal of Pharmaceutical Sciences	SCI
42	Oral Administration of Tanshinone IIA Does Not Attenuate Two Lineages of Transgenic Adenocarcinoma of Mouse Prostate Carcinogenesis	吴威	2019-01-10	Indian Journal of Pharmaceutical Sciences	SCI
43	Effects of Rhodiola sachalinensish Herbal Residues on Antioxidant Activity of Polysaccharides and Cultivated of Pleurotus djamor	王兰英	2019-01-10	Indian Journal of Pharmaceutical Sciences	SCI
44	Antioxidant Activity of Pleurotus djamor Polysaccharides Cultivated in Litchi Hull	王兰英	2019-01-10	Indian Journal of Pharmaceutical Sciences	SCI
45	Lewis lung carcinoma allograft efficacy test outcomes may be confounded by variable inoculum viability	吴威	2019-01-09	Indian Journal of Pharmaceutical Sciences	SCI
46	Paeoniflorin alleviates myocardial ischemia reperfusion injury through regulating autophagy	赵成国	2018-12-17	Basic & Clinical Pharmacology & Toxicology	SCI
47	Extraction process optimization and comparative analysis of components of volatile oil from citri reticulatae pericarpium and citri reticulatae pericarpium viride	赵成国	2018-12-17	Basic & Clinical Pharmacology & Toxicology	SCI
48	Studies on the protective properties of polysaccharides purified from sparassis crispa in the mouse with alzheimer's disease	孟凡欣	2018-11-20	BASIC & CLINICAL PHARMACOLOGY & TOXICOLOGY	SCIE
49	From analysis of ischemic mouse brain proteome to identification of human serum clusterin as a Potential biomarker for severity of acute ischemic stroke	周慧	2018-11-15	Translational Stroke Research	SCI
50	Dynamic Analysis of Nucleosides and Carbohydrates during Developmental Stages of Cordyceps militaris in Silkworm (Bombyxmori)	王兰英	2018-11-15	Journal of AOAC International	SCI
51	Investigation on the neuro-protective effects of hericium erinaceus polysaccharides against MPP+ -damaged HT22 cells via ERKs -mediated mitochondria apoptotic pathway	杨东生	2018-11-01	USING e-ANNOTATION TOOLS FOR ELECTRONIC PROOF CORRECTION	SCIE

52	Preparation, characterization and in vitro release study of drug-loaded sodium carboxy-methylcellulose/chitosan composite sponge	蔡宝宜	2018-10-22	Plos One	SCI
53	亲和超滤质谱技术在中药活性成分筛选中的研究进展	周慧	2018-09-20	质谱学报	EI国内
54	Effect of Binary Organic Solvents Together with Emulsifier on Particle Size and In vitro Behavior of Paclitaxel-Encapsulated Polymeric Lipid Nanoparticles	秦书芝	2018-08-01	CURRENT DRUG DELIVERY	SCI
55	Study on the extraction conditions of polyphenol in mango leaves	李晶莹	2018-06-21	Indian Journal of Pharmaceutical Sciences	SCI
56	Sustained Drug Release Attained by Tartaric Acid Cross-linked Poly(Lactic Acid)	王亮	2018-06-21	Indian Journal of Pharmaceutical Sciences	SCI
57	Phenylbutyl isoselenocyanate induces reactive oxygen species to inhibit androgen receptor and to initiate p53-mediated apoptosis in LNCaP prostate cancer cells.	吴威	2018-05-02	Mol Carcinog	SCI
58	CAMPTOTHECIN-LOADED MAGNETIC NANOSPHERES FOR TARGETED CANCER THERAPY AND MAGNETIC RESONANCE IMAGING	金元宝	2018-02-13	Indian Journal of Pharmaceutical Sciences	SCI
59	THE INVOLVEMENT OF MITOCHONDRIA-MEDIATED PATHWAY IN PROTECTIVE ACTION OF	金元宝	2018-02-13	Indian Journal of Pharmaceutical Sciences	SCI
60	The influence of lipid self-association in polysaccharide matrix on controlled-release of butyl hydroxy anisid	王立英	2018-02-13	Indian Journal of Pharmaceutical Sciences	SCI
61	Preparation and pharmacokinetics of gambogic acid long-circulating liposomes	王立英	2018-02-13	Indian Journal of Pharmaceutical Sciences	SCI
62	Novel Biodegradable Star Copolymer 2PLA-(Trimesic Acid)-IPEG as Hydrophilic Drug Carrier	钟恬	2018-02-01	Indian Journal of Pharmaceutical Sciences	SCI
63	Preparation and Characterization of Hydroxyapatite-ivermectin Nanocomposite	吴丽艳	2018-02-01	Indian Journal of Pharmaceutical Sciences	SCI
64	CELL PENETRATING PEPTIDES AND TRASTUZUMAB MODIFIED PROTAMINE-SIRNA MULTIFUNCTIONAL LIPID NANOPARTICLES TARGETING HER2 IN BREAST CANCER	秦书芝	2018-02-01	Indian Journal of Pharmaceutical Sciences	SCI
65	INFLUENCE AND COMPARISON OF DIFFERENT GINGER PROCESSING METHODS ON MAGNOLIA OFFICINALIS VOLATILE INGREDIENTS	赵成国	2018-02-01	Indian Journal of Pharmaceutical Sciences	SCI
66	AMPHIPHILIC DRUG-POLYMER ASSEMBLED MICELLES CONTAINING ACID-CLEAVABLE LINKER FOR ANTICANCER DRUG DELIVERY	刘垚	2018-01-30	Indian Journal of Pharmaceutical Sciences	SCI
67	MICROFLUIDIC HYDRODYNAMIC FOCUSING SYNTHESIS OF LIPOSOMES FOR VITAMIN D-3 DELIVERY	孟凡欣	2018-01-30	Indian Journal of Pharmaceutical Sciences	SCI
68	CARNOSIC ACID EXHIBITS ANTITUMOR PROPERTIES IN PITUITARY ADENOMA CELLS VIA ROS-DEPENDENT MITOCHONDRIAL SIGNALING PATHWAYS	孟凡欣	2018-01-30	Indian Journal of Pharmaceutical Sciences	SCI

69	Phylogenetic relationship of <i>Lepista sordida</i> JZ01 and antimicrobial activity of its fermentation broth extract	王兰英	2018-01-27	Indian Journal of Pharmaceutical Sciences	SCI
70	A Novel Synthetic Compound Induces Hepatocellular Carcinoma Cell Apoptosis via Mitochondrial Pathway	杨东生	2018-01-01	Indian Journal of Pharmaceutical Sciences	SCI
71	Rhodiola Extraction (RE) induces apoptosis in A549 cells via ROS-related mitochondrial pathways	杨东生	2018-01-01	Indian Journal of Pharmaceutical Sciences	SCI
72	DISCRIMINATION OF POPLAR GUM FROM PROPOLIS-A METHOD BASED ON CHROMATOGRAPHIC FINGERPRINTS COUPLED WITH MULTIVARIATE STATISTICAL ANALYSIS	耿璐璐	2018-01-01	Indian Journal of Pharmaceutical Sciences	SCI



Effect of starter cultures mixed with different autochthonous lactic acid bacteria on microbial, metabolome and sensory properties of Chinese northeast sauerkraut

Wenzhong Hu^{a,b,c,*}, Xiaozhe Yang^{c,d,1}, Yaru Ji^{c,d}, Yuge Guan^{c,d}

^a School of Pharmacy and Food Science, Zhuhai College of Jilin University, Zhuhai 519041, China

^b Department of Food Engineering, College of Life Science, Dalian Minzu University, Dalian 116600, China

^c Key Laboratory of Biotechnology and Bioresources Utilization, Ministry of Education, Dalian 116600, China

^d School of Bioengineering, Dalian University of Technology, Dalian 116024, China

ARTICLE INFO

Keywords:

Mix-culture fermentation
qPCR
Metabolome
E-nose
E-tongue
Sensory characteristics

ABSTRACT

Effects of mixed cultures composed of any two of four autochthonous lactic acid bacteria on fermentation of Chinese northeast sauerkraut were investigated in this study. Results indicated that different mixed cultures inoculation generated diversified physicochemical, microbiological and flavor quality of sauerkraut. Compared to spontaneous fermentation, mix-culture fermentation showed significant higher population of lactic acid bacteria and lower amounts of undesirable microorganisms. Free amino acids increased by 2- to 5-fold from initial level in spontaneous and mix-culture fermentation, with the lowest production by spontaneous fermentation. Moreover, mix-culture fermentation promoted the flavor formation based on the analysis of HS-SPME/GC-MS, E-nose, E-tongue and sensory evaluation, especially for the mixed culture of *Leu. mesenteroides* and *L. plantarum*. These results highlighted that using a mixed culture made up with *Leu. mesenteroides* and *L. plantarum* could be a potential way to improve the quality of sauerkraut, which could provide an alternative way to meet consumers' requirement.

1. Introduction

Northeast sauerkraut is a famous traditional Chinese fermented food made from Chinese cabbage (*Brassica rapa* L. pekinensis, cv. Wombok) in a certain concentration of brine, being very popular in the northeast region of China for the nutritional value, pleasant flavor and health benefits. Sauerkraut contains not only high amounts of vitamins and minerals, but also high levels of glucosinolate hydrolysis products, and is known to have various functions such as anti-obesity, anti-oxidant, anti-cancer and cholesterol reduction (Park et al., 2019). Fermentation improves the flavor properties with the production of aromatic metabolites including organic acids, free amino acids (FAAs) and volatile compounds (Chen et al., 2019). At present, the annual output of northeast sauerkraut has reached several hundred thousand tons, with an output value of nearly 5 billion CNY (Wang, Zhang, Gao, Han, & Wu, 2021).

Nonetheless, until now, northeast sauerkraut is still produced by the natural fermentation which is made based on empirical knowledge and

relies on the microbiota originated from raw materials and environment. Fresh and good quality cabbages are pretreated (washed, cut and blanched) and then stacked with salt into jars, and finally left at ambient temperature for at least one month (Liang et al., 2020). Generally, the microbiota of northeast sauerkraut includes members of lactic acid bacteria (LAB), which are the dominant microbial group throughout the fermentation, whereas yeasts, molds, *Enterobacteriaceae*, *Clostridium*, *Pseudomonadaceae* and *Staphylococcus* may appear at the beginning of fermentation (Vaccaluzzo et al., 2020). Liang, Yin, Zhang, Chang, and Zhang (2018) have reported that the spontaneous fermentation process is initiated by heterofermentative LAB such as *Leu. mesenteroides*, and terminated by homofermentative LAB such as *L. plantarum*. However, spontaneous fermentation usually results in products with poor quality, due to the contamination with spoilage microorganisms or pathogens, which has been a significant bottleneck for industrial production. Meanwhile, the consumers' consumption trend toward fresh-tasting, high-nutritional and health-promoting foods, with satisfactory

* Corresponding author.

E-mail address: hwz@dlnu.edu.cn (W. Hu).

¹ These authors contributed equally to this work.

organoleptic properties, is increasing.

LAB, as one of the most important microorganisms in fermented foods, have been given the Generally Recognized as Safe (GRAS) status by the US Food and Drug Administration (FDA) and the Qualified Presumption of Safety (QPS) status by the European Food Safety Authority (EFSA) (Hossain et al., 2020). LAB are able to metabolize chemical components of vegetables, which contributes to the nutritional value, flavor and texture of final products, and improves the digestibility. Additionally, LAB exhibit probiotic effects by producing antimicrobial compounds, such as organic acids, carbon dioxide, hydrogen peroxide and bacteriocins. Recently, LAB have been used as starters to drive the fermentation process, prolong the shelf life and improve the organoleptic characteristics of fermented products, such as yoghurt (Soni et al., 2020), kimchi (Lee, Choi, Lee, Park, Oh, Yun, & Lee, 2020) and sour meat (Zhang, Hu, Xie, & Wang, 2020). Minervini, Missaoui, Celano, Calasso, Achour, Saidane, and De Angelis (2019) developed a co-culture system composed of *L. paraplantarum* and *L. plantarum* for the fermentation of zougou, and the result demonstrated that co-culture fermentation improved the antioxidant activity, color, odor and safety of products. Lee et al. (2020) established a mixed culture made up with *Leu. mesenteroides* and *L. sakei* to investigate the effects of mixed culture on the overall fermentation process of kimchi, and the result demonstrated the mixed culture had great potential for the standardized manufacture of kimchi. These studies demonstrated that fermentation with mixed culture made important contributions to improve the quality of fermented foods. Thus, the use of mixed cultures in the fermentation of northeast sauerkraut would be one of the most effective approaches to control the fermentation process, standardize the quality, ensure the safety, and optimize the benefits of final products.

However, up to now, no systematic study has been performed on the effects of mixed-cultures on the fermentation of northeast sauerkraut. In our previous study, several potential LAB strains were isolated from spontaneous sauerkraut in northeast China. The previous experimental results showed that they possessed excellent fermentative properties, including good growth activity, high capacity of acid production and nitrite degradation, and significant antimicrobial activity (Yang et al., 2020). Hence, the aim of this study was to explore, in-depth, the effects of mix-culture fermentation by different combinations of selected LAB species on the quality of northeast sauerkraut. Alterations in the growth of microorganisms, pH and the contents of nonvolatile and volatile compounds before and after fermentation were determined. Furthermore, the sensory characteristics of final products were evaluated by E-tongue, E-nose and trained panelists, respectively.

2. Materials and methods

2.1. Starter preparation

Four autochthonous LAB strains used in this study were *Leuconostoc mesenteroides* (*Leu. mesenteroides*), *Lactobacillus plantarum* (*L. plantarum*), *Lactobacillus paracasei* (*L. paracasei*) and *Weissella cibaria* (*W. cibaria*), which were previously isolated in our lab from homemade spontaneous sauerkraut in Dalian, Jinzhou, Liaoning Province (Yang et al., 2020). These strains were stored at $-80\text{ }^{\circ}\text{C}$ in MRS broth supplemented with glycerol (20%, v/v). Prior fermentation, the four strains were pre-cultured into sterile MRS broth and incubated at $30\text{ }^{\circ}\text{C}$ for 24 h to obtain a final cell density of 9 log cfu/mL . Then cells were harvested by centrifugation at $12,000g$ for 20 min at $4\text{ }^{\circ}\text{C}$, washed twice with sterile 0.85% (w/v) saline, and suspended in sterile 0.85% (w/v) saline to obtain a concentration of 7 log cfu/mL for inoculation.

2.2. Sauerkraut fermentation and sampling procedures

Northeast sauerkraut was fermented according to the method described by Yang et al. (2020). Briefly, the raw materials, fresh Chinese cabbages, were cut into halves along the long axis and blanched for 1

min in boiling water. Then, the pretreated cabbages were transferred to 7.3-L ceramic jars together with sterile salt solution (1%, w/w). Meanwhile, different starter cultures were mixed at the ratio of 1:1 and inoculated at 10^6 cfu/g cabbage approximately. Finally, all jars were sealed tightly and placed at $18\text{--}20\text{ }^{\circ}\text{C}$ for 30 days. Seven batches were performed as follows: (I) spontaneous fermentation (Spo), (II) inoculated with mixed culture of *Leu. mesenteroides* and *L. plantarum* (MP), (III) inoculated with mixed culture of *Leu. mesenteroides* and *L. paracasei* (MA), (IV) inoculated with mixed culture of *Leu. mesenteroides* and *W. cibaria* (MW), (V) inoculated with mixed culture of *L. plantarum* and *L. paracasei* (PA), (VI) inoculated with mixed culture of *L. plantarum* and *W. cibaria* (PW), (VII) inoculated with mixed culture of *L. paracasei* and *W. cibaria* (AW). The brine and solid sauerkraut were sampled at day 1, 3, 5, 7, 12, 17, 23 and 30 for subsequent experimental analysis, according to the sampling method as described previously (Yang et al., 2020). Sauerkraut brine was collected using sterile pipette from upper, middle and under layer of jar respectively, and five subsamples collected from each layer were combined and mixed well. Then collected samples were centrifugated at $12,000g$ for 15 min at $4\text{ }^{\circ}\text{C}$. The separated pellets and supernatants were stored at $-80\text{ }^{\circ}\text{C}$ for further analysis.

2.3. pH measurement

The pH value was measured by placing a pH electrode of the pH meter directly (PHS-3G, INESA Scientific Instrument Co., Ltd., Shanghai, China) into samples at room temperature.

2.4. Microbiological analysis

2.4.1. Counts of viable cells using the plating method

The microbiological analysis of the viable cells during the fermentation was performed by the standard plate-counting method. 1 mL of sauerkraut brine was subjected to serial dilutions ranging from 10^{-1} to 10^{-9} , and then cultured on plates by pouring method, including De Man Rogosa Sharpe (MRS, Hopebio, Qingdao, P. R. China) agar plates incubated at $30\text{ }^{\circ}\text{C}$ for 48 h for LAB count and Violet Red Bile Glucose (VRBG, Hopebio, Qingdao, P. R. China) agar plates incubated at $37\text{ }^{\circ}\text{C}$ for 24 h for Enterobacteriaceae count.

2.4.2. Quantification by the real-time quantitative PCR (qPCR) method

2.4.2.1. Genomic DNA extraction. DNA was extracted from all samples at day 1, 3, 5, 7, 12, 17, 23 and 30 using the MiniBEST Bacterial Genomic DNA Extraction kit Ver. 3.0 (Takara, Shiga, Japan) as per the manufacturer's recommendations for Gram-positive bacteria.

2.4.2.2. Amplification conditions. The qPCR reactions were performed in 96-well plates on a Biorad ICycler instrument (Biorad) using SYBR Green as the fluorophore. Primers and standard curves were the same as that used in our previous study (Yang et al., 2020). Amplification reactions were performed in replicate in a final volume of 20 μL containing 10 μL of SYBR Green Premix Pro Taq HS qPCR Kit (AG11701, ACCURATE BIOTECHNOLOGY, HUNAN, Co., Ltd), 0.4 μL of each primer, 7.2 μL of RNase-free water and 2 μL of template DNA. The conditions of amplification reactions were: $95\text{ }^{\circ}\text{C}$ for 30 s, followed by 39 cycles of denaturation at $95\text{ }^{\circ}\text{C}$ for 5 s, annealing at $60\text{ }^{\circ}\text{C}$ for 30 s and extension at $95\text{ }^{\circ}\text{C}$ for 10 s. Melting curve analysis was performed automatically by continuous heating from $65\text{ }^{\circ}\text{C}$ to $95\text{ }^{\circ}\text{C}$. All qPCR runs were analyzed using automatic software settings. Standard curves were generated using serial DNA dilutions of four LAB strains (ranging from 10^9 to 10^2 cfu/mL) and were constructed by plotting mean C_q values against $\log\text{ cfu}$ of them.

2.5. Analysis of metabolome profiles

2.5.1. Determination of non-volatile compounds

High-performance liquid chromatography (HPLC) with a differential refractometer CTO-10vp detector (Agilent Instruments, USA) was conducted to determine the concentrations of non-volatile compounds (glucose, fructose, lactic acid and citric acid) following the method described previously (Yang et al., 2020). Before determination, sauerkraut brine was centrifuged at 12,000g for 10 min and then filtered through 0.22 µm micropore filter (Jin Teng Corp., Tian Jin, China). The Aminex 300 mm × 7.8 mm HPX-87H column (Bio-Rad Laboratories, USA) was used to separate the non-volatile metabolites at 65°C. The mobile phase was 0.005 M H₂SO₄. The non-volatiles were identified by comparing their retention times with their standard solutions, and quantified using calibration curves generated from the peak areas of the standards.

The content of FAAs was determined according to the method described by Yang et al. (2020). 10% sulfosalicylic acid was added to the precipitation of proteins and peptides, and the sample was centrifuged at 12,000g for 20 min at 4 °C. Then, 1 mL of supernatant was filtered through a 0.22 µm micropore filter (Jin Teng Corp., Tian Jin, China) and analyzed by an automatic amino acid analyzer (Biochrom Ltd., Cambridge Science Park, England) with a Hitachi 2622c exchange column (4.6 mm × 6.0 m), at wavelengths of 440 nm for Proline (Pro) detection and 570 nm for all the other FAAs detection. The concentration of each FAA was calculated by the external standard method (Wu et al., 2015).

2.5.2. Determination of volatile compounds and odor activity values (OAVs) calculation

The content of volatile metabolites was determined by the method reported previously (Yang et al., 2020). Briefly, 5 mL of the sauerkraut brine and 1.6 g NaCl were transferred into a 20 mL headspace vial. The vial was tightly capped, heated in a water bath at 60 °C and stirred every 5 min for 40 min. Then a solid-phase microextraction (SPME) fiber (divinylbenzene/carboxen/polydimethyl siloxane, DVB/CAR/PDMS, 50/30 µm, Supelco, Inc., Bellefonte, PA, USA) was inserted into the headspace vial to adsorb volatiles for 40 min at 60 °C and then was injected into the GC injector for desorption. A Shimadzu gas chromatograph (Shimadzu, Kyoto, Japan) with a Rxi-5Sil MS column (30 m × 0.25 mm × 0.25 µm, Restek, Bellefonte, PA, USA) was used for GC/MS analysis. High-purity helium was used as carrier gas at a constant flow rate of 1.0 mL/min. The injector temperature was 250 °C, while the oven temperature was increased from 35 °C (3 min) to 160 °C at a rate of 6 °C/min, and then increased at 10 °C/min to 250 °C. The interface and ion source temperature were set at 230 °C and 200 °C, respectively. The mass detector operated in electron impact (EI) mode was generated at 70 eV with a scan range of 35–500 *m/z*. Volatiles were identified using the National Institute of Standard and Technology (NIST) and Wiley libraries (similarity index > 85%), and quantified using 2-octanol (19.656 µg/L) as the internal standard. The concentration of volatile was calculated as: concentration of volatile = (concentration of standard × MS peak area of volatile)/MS peak area of standard. All analyses were repeated three times.

The OAVs of volatile compounds were calculated by dividing their concentrations with odor thresholds, which were obtained from previous studies collected in literatures (Wei, Xiao, Wei, Li, Li, Liu, & Zhong, 2021; Yun et al., 2020a; 2020b). To some extent, OAVs can reflect the contribution of volatile compounds to the characteristic flavor of sample. Generally, compound with OAV > 1 contributes to the overall aroma significantly.

2.6. E-nose analysis

E-nose analysis was performed with a PEN 3.0 E-nose device (Winmuster Airsense Analytics Inc., Schwerin, Germany) equipped with a sensor array system containing ten metal-oxide semiconductors with

different chemical composition and thickness. The sensors were W1C, W5S, W3C, W6S, W5C, W1S, W1W, W2S, W2W and W3S, and were constructed to measure aromatic compounds, oxynitride, ammonia and aromatic compounds, hydrogen, alkane and aromatic compounds, methane, sulfur compounds, ethanol, aromatic and organic sulfur compounds, and alkanes, respectively. Briefly, 5 mL of sauerkraut brine was placed into a 20 mL headspace vial, capped with a PTFE septum and then equilibrated at room temperature before testing. The headspace gas was injected into the E-nose carried by air for 60 s at a constant flow rate of 300 mL/min, and during the test, the sensor signals were recorded at each second. After each test, the sensor system was purged with filtered air for 120 s, to reestablish the instrument baseline prior to the next sample injection. Data was collected by the pattern recognition software (WinMuster, v.1.6, Airsense Analytics GmbH, Germany). Each sample was analyzed three replicates and the average was used for the subsequent statistical analysis.

2.7. E-tongue analysis

The SA-402B electronic tongue system (E-tongue, Intelligent Sensor Technology, Inc., Kanagawa, Japan) was used to determine the taste profile of sauerkraut products. The system consists of five taste sensors (AAE, CTO, CAO, AE1 and C00) and is used to test umami, saltiness, sourness, aftertaste, astringency, richness and bitterness, respectively. All sensors were activated for 24 h using an internal solution (3.3 M KCl and saturated silver chloride) and a reference solution (30 mM KCl and 0.3 mM tartaric acid). Sauerkraut sample was homogenized, filtered through gauze to collect the juice and centrifuged at 12,000g for 10 min. After a successful self-test, the detection method was set and the supernatant was analyzed from eight taste values (sourness, bitterness, saltiness, umami, aftertaste-A, aftertaste-B, astringency and richness). Three replicates were performed for each sauerkraut sample.

2.8. Sensory analysis

Sensory evaluation of the final sauerkraut products was conducted by 15 trained panelists including 7 men and 8 women with an average age of 28 (from age 20 to 40). Training sessions were carried out for panelists prior to sensory evaluation to ensure that each panelist could consistently clarify and detect the attribute of each sauerkraut product. During the training session, panelists defined and developed sensory attributes of the samples until they reached an agreement. Commercial sauerkraut products were used for the training, and each of the sensory notes and its score distribution was thoroughly discussed until a consensus among panel members was reached (Yi et al., 2019). During formal sensory evaluation, each sample (10 g) composed of solid sauerkraut and brine, was randomly presented to panelists in clear plastic cups coded with three-digit codes in a random order to prevent bias. The measurements were carried out at room temperature. Water and crackers were provided for the panel to rinse their palates between samples. The overall preference (color, sourness, crispness, flavor, taste and overall acceptability) was scored using a 9-point scale (1, extremely dislike; 3, dislike; 5, neither like nor dislike; 7, like; 9, extremely like) (Choi, Yong, Lee, Park, Yun, Park, & Lee, 2019).

2.9. Statistical analysis

The experimental results were expressed as means ± standard error of the mean, derived from three repeated measurements from each fermentation vessel. SPSS 19.0 software (SPSS Inc., Chicago, IL, USA) was used to perform a one-way analysis of variance (ANOVA), while Turkey's test was performed to test for significant differences (*p* < 0.05). The data of volatilome determination and E-nose analysis were subjected to a principal component analysis (PCA) using SIMCA software (version 11.0, Umetrics, Umea, Sweden). The cluster analysis was conducted by R (version 3.4.4). The type of linkage method and distance

measurement were “complete” and “Euclidean”, respectively. Z-transformation of raw data was required to be processed before constructing a heatmap. The phylogenetic tree was calculated using the neighbor-joining method.

3. Results and discussion

3.1. Microbiological analysis during fermentation

3.1.1. Enumeration of microorganisms using plating method

To monitor the whole fermentation process and evaluate the safety of sauerkraut, it is necessary to investigate the microbial dynamics. LAB is a dominant group in acid production and of great importance in fermented foods. The population of LAB at day 1 was approximately 8.40 log cfu/mL in all mix-cultured samples, whereas that in Spo samples was only 7.11 log cfu/mL (Supplementary Table S1). Among all samples, LAB increased rapidly from day 1 and then gradually decreased until the fermentation finished. The population of LAB showed a decrease in the later stage of fermentation, likely due to the low pH value and limited nutrient availability as fermentation progressed. The time to reach the peak value of LAB population varied among different samples, at day 5 in PW fermented samples, at day 3 in four treatment groups (Spo, MP, PA and AW), and at day 1 in MW samples. This difference was inferred to be caused by the homolactic or heterolactic acid fermentation performed by the starter strains. In addition, it was also related to the difference in growth ability of starter strains. In the early stage of fermentation, a fast growth of LAB could lead to a rapid decline in pH value, which is necessary to prevent the growth of spoilage microorganisms (Zhang et al., 2020). The minimum of LAB number at the peak and at the end of fermentation were all detected in the Spo samples. At the end of fermentation, the PW samples contained the largest number of LAB, followed by the PA samples. These results suggested that it was necessary to inoculate the starters of LAB for the rapid and vigorous fermentation.

As the fermentation progressed, the population of Enterobacteriaceae in all samples gradually decreased and was not detected at the end of fermentation (Supplementary Table S1). However, the time taken to decrease below the detection limit was different, depending on the type of mixed culture inoculated. Compared with the Spo fermentation, mix-culture fermentation allowed the number of Enterobacteriaceae below the limit of detection within a shorter period. The population of Enterobacteriaceae decreased below the detection limit after 24 h of fermentation in three mix-cultured groups (MP, MA and MW), at day 3 in two groups (PA and PW), at day 5 in AW samples, whereas at day 7 in Spo samples. These results suggested that mix-culture fermentation could promote the rapid growth of beneficial bacteria and inhibit the growth of undesirable bacteria.

3.1.2. qPCR analysis

The dynamic behavior of the starter strains during fermentation was monitored by qPCR, which was a faster and more reliable alternative method to identify and quantify microorganisms during fermentation. Additionally, mix-cultured strains might compete for nutrients or produce metabolites that stimulate or inhibit each other's growth. Thus, it was helpful to determine the possible population interactions between the starter cultures.

It was expected that significant ($p < 0.05$) higher numbers of all starter strains were detected in the mix-cultured samples compared to the Spo samples (Supplementary Table S1), which meant that the fermentation with mixed cultures was effective. Regarding the mix-cultured models with *Leu. mesenteroides* (MP and MA), the population of *Leu. mesenteroides* was lower than that of *L. plantarum* and *L. paracasei*, especially in the mid-late stage of fermentation. The result could be explained by the rapid acidification of *L. plantarum* and *L. paracasei*, which was due to their homolactic fermentation. In other terms, lactic acid produced by *L. plantarum* and *L. paracasei* made *Leu. mesenteroides*

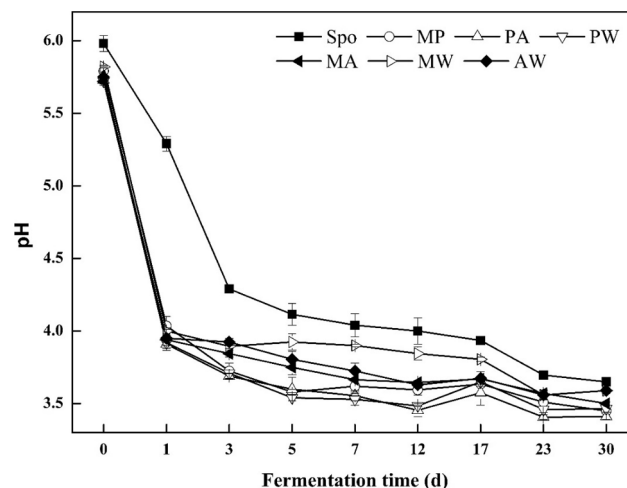


Fig. 1. Changes of pH during the fermentation of northeast sauerkraut by spontaneous (Spo) and different mixed cultures (MP, MA, MW, PA, PW and AW).

disadvantageous in the competition for substrates in mix-culture fermentation. This result was in good agreement with a previous study regarding the effect of single and mixed inoculation of *L. lactis* and *Leu. mesenteroides* on the fermentation of skim milk (Özcan et al., 2020). During the MW mix-culture fermentation, *Leu. mesenteroides* and *W. cibaria* showed similar behavior, increasing during the first 12 days and then decreasing until the fermentation finished, and no significant difference was found between their population. This result supported the statement of previous study that *Leuconostoc* and *Weissella* appeared in pairs or in chains, and co-existed in a variety of fermented foods (Zhang et al., 2019a).

As homofermentative LAB, *L. plantarum* showed a significant ($p < 0.05$) higher growth performance compared to that of *L. paracasei* in PA mix-cultured fermentation, which was likely due to the growth of *L. paracasei* was suppressed by *L. plantarum*. Significant ($p < 0.05$) higher number of *L. plantarum* was found in the MP and PW samples, with respect to that in PA samples. This finding was in good agreement with Xu, He, Zhang, and Kong (2017), who reported that heterofermentative LAB accelerated the growth of *L. plantarum* and resulted in a rapid decrease in pH value. During the process of PW mix-culture fermentation, the changes of *L. plantarum* and *W. cibaria* population were almost synchronous, showing an order-of-magnitude increase at day 23. *L. plantarum* showed a higher and *W. cibaria* showed a lower growth performance in PW samples, while in AW samples, the population of *W. cibaria* was higher than that of *L. paracasei*. This result indicated that the presence of *W. cibaria* exhibited different effects on the growth of *L. plantarum* and *L. paracasei* in mix-culture fermentation, although the underlying mechanism was still unclear. *L. paracasei* grew better in the presence of heterofermentative LAB (*Leu. mesenteroides* and *W. cibaria*) compared with that mixed with *L. plantarum*. This difference could be attributed to a better competitiveness of *L. paracasei* in MA and WA mixed cultures when compared with that in PA mixed culture.

Overall, among all mix-cultured samples, the population of *L. plantarum* and *W. cibaria* were higher compared to all the other starters, which might be related to their strong acid tolerance capacity. These results were in accordance with previous report (Jung et al., 2012), which had been explained by the hypothesis that members of *Leuconostoc* grew well under less acidic and anaerobic condition, while members of *Lactobacillus* and *Weissella* were more competitive under acidic condition.

Compared to the plating method, the population of LAB quantified by qPCR was higher. According to the statement of Fittipaldi, Nocker, and Codony (2012), firstly, this meant that DNA was easily extracted

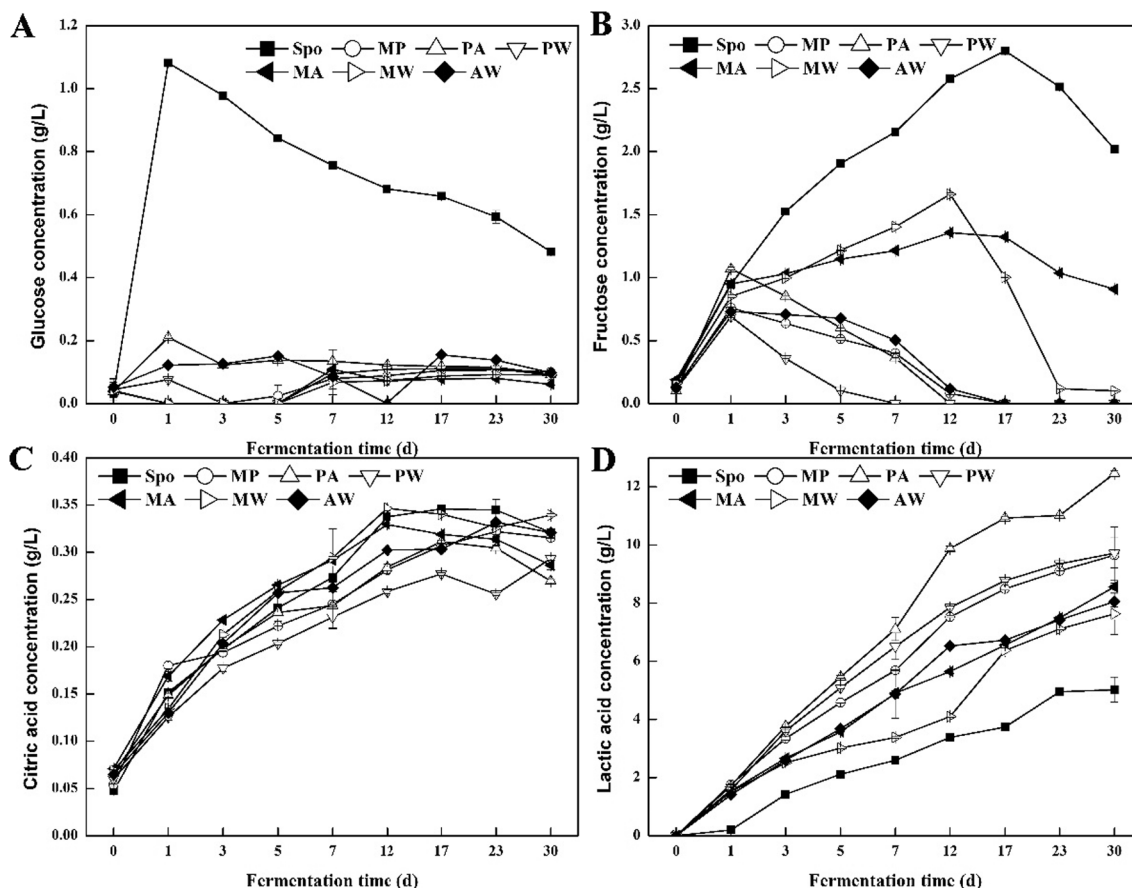


Fig. 2. Changes in glucose (A), fructose (B), citric acid (C) and lactic acid (D) concentrations of northeast sauerkraut during spontaneous (Spo) and different mix-cultured (MP, MA, MW, PA, PW and AW) fermentation.

from the cells of LAB that had grown to different physiological states. Secondly, qPCR method provided additional information for plate counting by detecting viable but non-culturable cells and dead cells.

3.2. Analysis of pH value

A low pH value not only influences the flavor of fermented food, but also ensures the safety of food by inhibiting the growth of spoilage and pathogenic microorganisms (Zhang et al., 2020). Among all samples, the pH value sharply decreased, then gradually decreased and finally tended to stabilize until the fermentation finished (Fig. 1). Throughout the fermentation process, the pH values of mix-cultured samples were obviously lower with respect to that of Spo samples. The mix-culture fermentation required only 1–3 days to reach a pH value below 4.0, while the Spo fermentation required 12 days. At the end of fermentation, the lowest pH value was found in the PA fermented sauerkraut, which might be explained by the homofermentative property of *L. plantarum* and *L. paracasei*. The result suggested that mix-culture fermentation enabled the brine acidified quickly, which reduced the possible risk of Enterobacteriaceae spoilage and reduced the lag phase of LAB, thereby shorten the total time of the fermentation process.

3.3. Analysis of non-volatiles determined by HPLC

Glucose and fructose are detected as major free sugars and play important roles as carbon sources for microbial metabolism during the fermentation of vegetables (Jung et al., 2012). At the beginning of fermentation, low contents of glucose (0.034–0.052 g/L) and fructose (0.10–0.19 g/L) were detected in all samples. As the fermentation progressed, the change of glucose concentration significantly differed in

different mix-cultured samples (Fig. 2A). During the initial fermentation of Spo, PA, PW and AW samples, the concentration of glucose increased, and the maximum levels were detected at day 1, 1, 1 and 5, respectively. While in other three groups (MP, MA and MW), no glucose was detected during the first 5 days of fermentation, then showed an upward trend from day 5 to 23, and subsequently decreased until the end of fermentation. Interestingly, this phenomenon was only found in the mix-culture fermentation involving *Leu. mesenteroides*, which could be explained that *Leu. mesenteroides* as heterofermentative LAB played an important role during the early stage of fermentation. At the end of fermentation, the glucose in all mix-cultured samples was almost completely exhausted, ranging from 0.06 to 0.10 g/L. Regarding the Spo fermentation, there was a remaining amount of glucose (0.48 g/L) at the end of fermentation, which was significantly ($p < 0.05$) higher than that in all mix-cultured samples (Supplementary Table S3). This result was consistent with the higher pH value in Spo samples than that in mix-cultured samples (Fig. 1), which might be related to the insufficient fermentation in Spo samples. The residual carbohydrates may lead to secondary fermentation by yeast and affect the stability of final products. Similar result was discovered during the fermentation of carrot by Wouters, Grosu-Tudor, Zamfir, and Vuyst (2013), who reported that secondary fermentation resulted in the tissue softening due to the pectinolytic activity and production of off-flavor through lipolytic and saccharolytic activities. Thus, a low concentration of glucose in sauerkraut could be in favor of the quality of final products.

The preferred use of fructose as electron acceptor has been observed in most heterofermentative LAB. In all samples, the concentration of fructose initially increased, followed by a decrease, while the peak time varied depending on the type of mixed cultures added (Fig. 2B). The maximum of fructose concentration was detected at day 17 in Spo

Table 1

FAAs concentrations (mg/L) in northeast sauerkraut by spontaneous (Spo) and mix-cultured (MP, MA, MW, PA, PW, AW) fermentation.

FAAs (mg/L)	1 d	30 d						
		Spo	MP	MA	MW	PA	PW	AW
Asp	10.86 ± 0.26	32.09 ± 1.10 ^d	74.69 ± 8.31 ^{bc}	110.78 ± 1.43 ^a	84.39 ± 1.37 ^{abc}	75.36 ± 5.48 ^{bc}	95.86 ± 7.54 ^{ab}	63.25 ± 2.50 ^c
Glu	346.58 ± 11.51	657.52 ± 31.61 ^c	1214.42 ± 43.74 ^{ab}	1470.99 ± 112.83 ^a	1345.95 ± 62.84 ^a	1463.78 ± 52.53 ^a	905.77 ± 9.19 ^{bc}	773.88 ± 12.88 ^c
Val	3.25 ± 0.21	23.53 ± 3.25 ^{ab}	17.16 ± 0.27 ^{bc}	25.15 ± 0.51 ^a	17.46 ± 0.40 ^{abc}	21.63 ± 1.53 ^{abc}	15.44 ± 0.20 ^c	15.79 ± 0.50 ^{bc}
Ile	1.67 ± 0.05	15.51 ± 1.35 ^a	11.34 ± 0.94 ^{ab}	14.24 ± 0.95 ^{ab}	9.46 ± 0.57 ^b	13.13 ± 1.12 ^{ab}	9.14 ± 0.56 ^b	10.54 ± 0.50 ^{ab}
Leu	1.53 ± 0.12	23.94 ± 2.40 ^a	15.06 ± 0.70 ^{bc}	20.13 ± 0.77 ^{ab}	13.73 ± 0.52 ^{bc}	19.19 ± 1.30 ^{ab}	12.63 ± 0.38 ^c	11.36 ± 0.50 ^c
Ala	35.24 ± 0.95	87.81 ± 3.54 ^c	134.08 ± 2.10 ^b	176.36 ± 5.57 ^a	126.52 ± 0.49 ^b	189.06 ± 1.19 ^a	120.09 ± 1.88 ^b	88.02 ± 1.00 ^c
Pro	5.57 ± 0.51	31.63 ± 0.87 ^{abc}	35.67 ± 4.70 ^{ab}	40.00 ± 0.45 ^a	26.05 ± 0.60 ^{bc}	39.90 ± 0.35 ^a	26.15 ± 0.56 ^{bc}	21.63 ± 0.50 ^c
Thr	20.86 ± 0.57	63.71 ± 1.53 ^a	33.86 ± 0.24 ^d	47.07 ± 0.50 ^c	7.64 ± 0.22 ^e	67.18 ± 1.04 ^a	55.50 ± 1.48 ^b	45.92 ± 0.90 ^c
Ser	32.31 ± 0.53	95.37 ± 1.82 ^c	102.97 ± 1.78 ^{bc}	140.79 ± 1.04 ^a	111.70 ± 4.17 ^b	138.21 ± 1.62 ^a	110.45 ± 2.33 ^b	96.13 ± 0.17 ^c
Gly	2.69 ± 0.28	21.22 ± 1.63 ^{bc}	21.57 ± 0.67 ^{bc}	27.37 ± 0.47 ^a	16.97 ± 0.87 ^{cd}	27.65 ± 0.37 ^a	17.84 ± 0.50 ^{bcd}	14.37 ± 0.47 ^d
Lys	0.87 ± 0.07	18.80 ± 1.70 ^a	10.49 ± 0.19 ^{cd}	14.05 ± 0.41 ^{bc}	9.44 ± 0.28 ^d	17.45 ± 0.13 ^{ab}	10.43 ± 0.25 ^{cd}	7.13 ± 0.38 ^d
Phe	1.71 ± 0.14	16.19 ± 0.67 ^a	7.11 ± 0.11 ^{cd}	15.61 ± 0.19 ^a	8.62 ± 0.59 ^{bc}	10.13 ± 0.29 ^b	4.96 ± 0.09 ^d	8.44 ± 0.50 ^{bc}
Tyr	0.98 ± 0.04	11.05 ± 0.40 ^a	3.77 ± 0.12 ^{de}	9.14 ± 0.52 ^b	4.69 ± 0.06 ^{de}	5.43 ± 0.45 ^{cd}	3.25 ± 0.09 ^e	6.03 ± 0.29 ^c
Cys	0.65 ± 0.07	5.68 ± 2.56 ^a	0.99 ± 0.20 ^a	4.17 ± 0.23 ^a	1.16 ± 0.02 ^a	1.33 ± 0.19 ^a	1.43 ± 0.17 ^a	3.30 ± 0.23 ^a
Met	0.63 ± 0.05	5.24 ± 0.16 ^a	0.03 ± 0.01 ^e	0.04 ± 0.01 ^e	3.39 ± 0.09 ^b	0.02 ± 0.00 ^e	1.53 ± 0.13 ^d	2.08 ± 0.11 ^c
His	2.34 ± 0.28	12.66 ± 0.28 ^a	12.73 ± 1.95 ^a	15.06 ± 0.37 ^a	15.36 ± 5.13 ^a	13.08 ± 1.64 ^a	12.11 ± 3.39 ^a	8.94 ± 0.49 ^a
Arg	0.78 ± 0.07	23.50 ± 4.07 ^{bc}	50.84 ± 5.33 ^a	53.97 ± 1.79 ^a	11.59 ± 2.15 ^{cd}	37.95 ± 3.13 ^{ab}	31.02 ± 1.18 ^b	6.11 ± 0.33 ^d
GABA	4.18 ± 0.17	35.08 ± 3.48 ^{bc}	69.88 ± 0.51 ^a	35.25 ± 4.64 ^{bc}	51.76 ± 2.52 ^b	47.28 ± 4.87 ^b	23.39 ± 1.43 ^{cd}	16.62 ± 1.06 ^d

Data are the mean ± standard deviation. Values marked with different letters in the same column are significantly different ($p < 0.05$).

Spo, spontaneous fermentation; MP, inoculated with mixed culture of *Leu. mesenteroides* and *L. plantarum*; MA, inoculated with mixed culture of *Leu. mesenteroides* and *W. cibaria*; PA, inoculated with mixed culture of *L. plantarum* and *L. paracasei*; PW, inoculated with mixed culture of *L. plantarum* and *W. cibaria*; AW, inoculated with mixed culture of *L. paracasei* and *W. cibaria*.

samples, at day 1 in four mix-cultured groups (MP, PA, PW and AW), and at day 12 in two mix-cultured groups (MA and MW). Fructose, which diffused from cabbage into brine, was completely exhausted by four mixed cultures (MP, PA, PW and AW), of which the most efficient consumption was observed in PW samples. The preference for reducing sugars depended on the type of LAB strains, as demonstrated by the changes in glucose and fructose contents during fermentation.

Citric acid is found in many substrates used for food fermentation such as fruits, vegetables and milk. The degradation of citric acid by microorganisms leads to the formation of some metabolites, such as diacetyl, acetoin, butanediol and acetaldehyde, which have contributions to the flavor quality of final products. Among all samples, citric acid was elevated during the early stage of fermentation and then decreased until the fermentation finished (Fig. 2C). At the end of fermentation, the PA fermented sauerkraut had the lowest concentration of citric acid ($p < 0.05$, Supplementary Table S3), followed by MA. A probable explanation for the result was that *L. paracasei* had a high capacity for utilization of citric acid, according to a previous study by Chan et al. (2019). The degradation of carbohydrates, major components of cabbage, contributes to the formation of numerous organic acids, which could improve the flavor properties and enhance the safety of products by inhibiting the growth of spoilage microorganisms (Lee et al., 2020). In addition, these organic acids are important secondary carbon sources for the proliferation of microorganisms and intermediates of a variety of biochemical processes during fermentation (Battelli et al., 2019). The concentration of lactic acid significantly increased with increasing fermentation time, regardless of spontaneous or mix-culture fermentation (Fig. 2D). In particular, this increase in lactic acid concentration was more marked in the mix-cultured samples. As shown in Supplementary Table S3, the lactic acid concentrations in all mix-cultured sauerkraut at day 30 were significantly higher than that in Spo sauerkraut ($p < 0.05$). At the end of fermentation, among all mix-cultured samples, the maximum and minimum level of lactic acid were detected in PA (12.46 g/L) and MW (7.63 g/L) fermented sauerkraut, respectively. Interestingly, higher yield of lactic acid was obtained from the final samples fermented with mixed cultures containing *L. plantarum* (MP, PA and PW), which was significantly greater than that of a previous study regarding the fermentation of suan cai with *L. curvatus* and *Leu. mesenteroides* (Yang et al., 2016). This result might be caused by that the ability to produce lactic acid by heterofermentative LAB was poor than that by homofermentative LAB. High lactic acid production testified to

the effectiveness of inoculation with homofermentative LAB strains. These results indicated that the concentration of lactic acid produced by LAB depended on the type of strains used for fermentation and the type of lactic acid fermentation.

3.4. FAAs analysis

LAB are able to break down protein to FAAs that improve the flavor and nutritional value of northeast sauerkraut (Wu et al., 2015). FAAs not only have their own flavors, but also can be involved in flavor biosynthesis as direct precursors and produce various aroma metabolites, such as acids, alcohols, esters and carbonyls in fermented foods.

In this study, eighteen FAAs were detected, and their contents varied in different sauerkraut samples (Table 1). The total concentration of FAAs was approximately 472.69 mg/L at the beginning of fermentation in all samples, and increased by almost 3- to 5-fold in mix-cultured samples while only 2-fold in Spo samples. Glutamic acid (Glu) were the most abundant FAAs in all samples, followed by aspartic acid (Asp), alanine (Ala), serine (Ser), glycine (Gly) and proline (Pro). A similar result had also been reported in a previous study regarding the fermentation of kimchi (Wu et al., 2015).

The content of umami-tasting FAAs, Glu and Asp, were 1–2 times higher in mix-cultured samples than that in Spo samples, of which the highest level was detected in MA samples. The result was consistent with the E-tongue result (Fig. 5). In addition, the contents of Asp and Glu obtained in this study were far higher than that in a previous study on traditional northeast sauerkraut (Wu et al., 2015).

Ser, providing a sweet taste, could be subsequently converted into acetic acid, 2,3-butanedione and acetoin through the deamination reaction (Wang, Sun, Lassabliere, Yu, & Liu, 2019). According to the result of HS-SPME/GC-MS, the contents of acetic acid and acetoin exhibited a significant difference ($p < 0.05$) between Spo and mix-culture fermentation, which indicated that inoculation with mixed cultures might alter the flavor of sauerkraut by regulating the amino acid metabolism.

The concentrations of branched-chain amino acids (valine-Val, leucine-Leu and isoleucine-Ile), which were considered to be important precursors of flavor compounds (aldehydes, alcohols and esters), were significantly ($p < 0.05$) higher in Spo samples than that in all mix-cultured samples. The result was agreed with the report of Li, Tang, He, Hu, and Zheng (2019), who investigated the influence of *L. plantarum* co-fermented with *Streptococcus thermophilus* on the

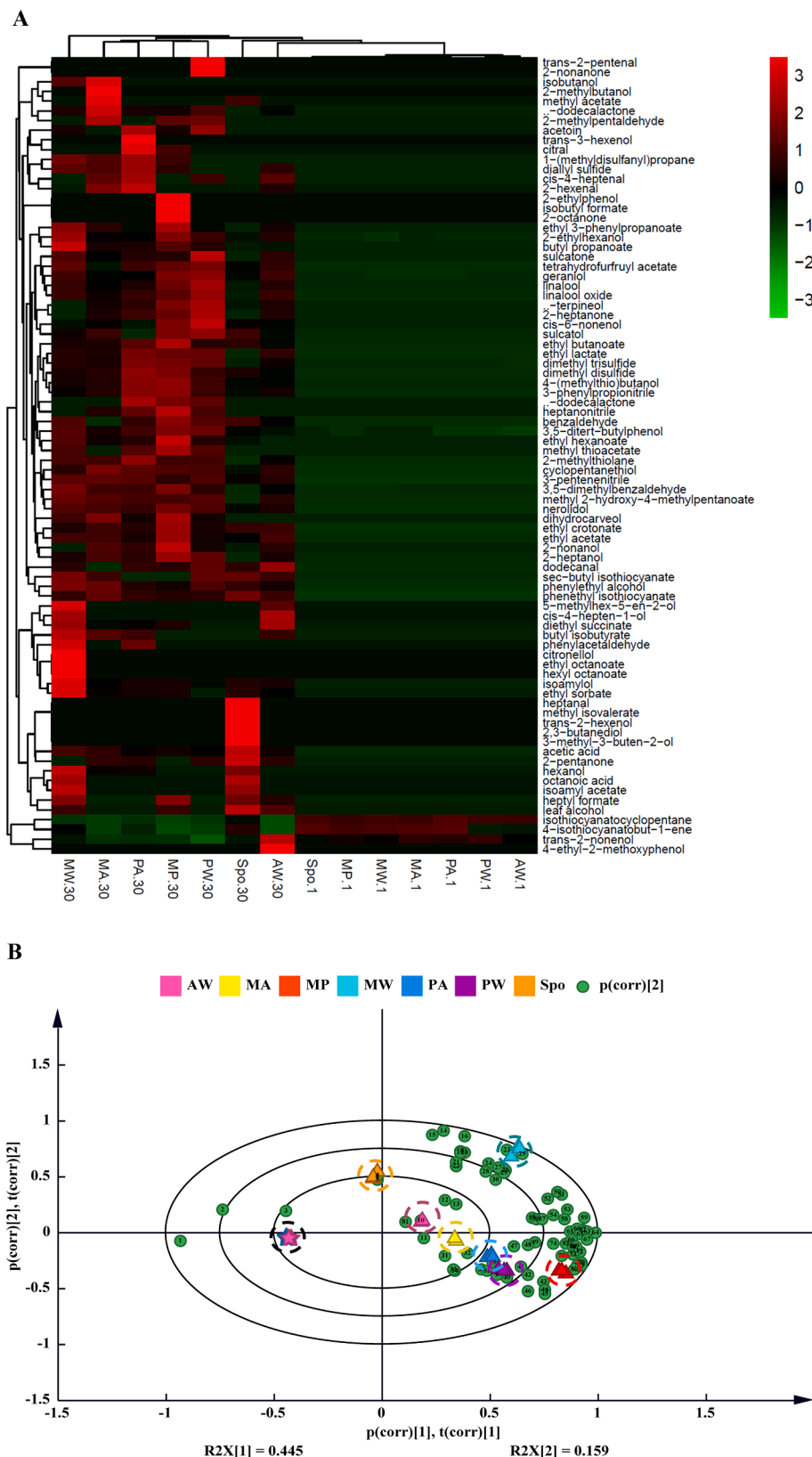


Fig. 3. Hierarchical clustering analysis (A) and biplot (score plots combined with loading plots) (B) of the volatile profiles of sauerkraut by spontaneous (Spo) and different mix-cultured (MP, MA, MW, PA, PW and AW) fermentation at days 1 and 30. (Spo., MP., MA., MW., PA., PW., AW.) 1 and 30 represents sauerkraut samples at day 1 and 30, respectively. The black dotted area represents all samples at day 1. Orange, red, yellow, light blue, navy blue, purple and pink dotted areas represent sauerkraut fermented by Spo and different mix-cultured (MP, MA, MW, PA, PW and AW) fermentation, respectively. The green circle represents all volatile compounds detected in this study, and the numbers (from 1 to 82) in circles represent volatile compound names as shown in Supplementary Table S2. (For interpretation of the references to color in this figure legend, the reader is referred to the web version of this article.)

proteolysis profile of fermented milk. Aromatic FAAs (phenylalanine-Phe and tyrosine-Tyr) are involved in the generation of some aromatic volatiles contributing to flavors like rose and flowers (Park & Kim, 2019). In addition, Phe and Tyr are critical for the lactic acid production by LAB (Toe et al., 2019). This

might be the reason why the MP and PW mix-cultured sauerkraut had significant ($p < 0.05$) lower contents of aromatic FAAs, higher content of lactic acid, and higher contents of aromatic volatiles (phenylethyl alcohol and ethyl 3-phenylpropanoate).

Sulfur-containing volatiles come from the degradation of sulfur-

containing amino acids (methionine-Met and cysteine-Cys), and contribute to flavors as boiled cabbage, potatoes and garlic in many fermented foods (Park & Kim, 2019). Compared to the Spo sauerkraut, the mix-cultured sauerkraut, especially PA and MP inoculated samples, had significant ($p < 0.05$) lower content of sulfur-containing FAAs. This result was consistent with the result of sulfide volatiles detected by HS-SPME/GC-MS.

Higher content of arginine (Arg) was produced in samples mix-cultured with *L. plantarum*, which concurred with the result of pH value (Fig. 1). A probable explanation of this result was that Arg played a major role in pH homeostasis and stationary phase survival of LAB (Ganzle, 2015).

GABA is produced by the decarboxylation of Glu catalyzed by the glutamate decarboxylase. Although the content is generally low in plants and animals, the application of GABA is wide and versatile as it has numerous physiological functions in animals and humans. According to Ly, Mayrhofer, Yogeswara, Nguyen, and Domig (2019), GABA was biosynthesized by *L. plantarum* and was used in fermented foods as an active component, which could be used to explain the higher contents detected in MP and PA samples. In turn, the PW fermented samples had lower content of GABA, which probably implied that the accumulation of GABA was inhibited when *L. plantarum* and *W. cibaria* were mixed together.

During sauerkraut fermentation, proteolysis occurs because of microbial enzymes and endogenous enzymes, leading to an increase in the contents of FAAs. The FAAs contents of sauerkraut fermented with mixed cultures were obviously higher than that in Spo sauerkraut, which could be explained by the increase of LAB population by inoculating mixed cultures, resulting in higher production of microbial enzymes for proteolysis (Zhang et al., 2020). These results indicated that mix-culture fermentation could improve the flavor of northeast sauerkraut by changing the composition of FAAs.

3.5. Volatilome profile analysis

Flavor is one of the most important characteristics that determines the quality of fermented products and acceptance of consumers. Hierarchical cluster analysis was used as a preliminary method to assess if the volatilome profile associated to each sample could drive the clustering of samples according to their Euclidean distance. The color scale represented the abundance of volatile compounds, with red indicating high abundance and green indicating low abundance, which highlighted differences between different samples. According to the flavor clustering result, 82 volatile compounds were attributed to 11 classes, including 2 organic acids, 17 alcohols, 19 esters, 9 terpenes, 2 lactones, 9 aldehydes, 6 ketones, 8 sulfides, 4 ITCs, 3 polyphenols and 3 nitriles (Fig. 3A). All samples were clustered into five clusters according to the different stages of fermentation and types of mixed culture. Cluster 1 was composed of all samples at day 1, showing the lowest types and levels of volatiles. Cluster 2, 3, 5 were composed of the AW-30 d, Spo-30 d and MW-30 d samples, respectively. Among all samples at day 30, AW samples showed few differences from samples at day 1. Cluster 4 showed a group of samples (MA-30 d, PA-30 d, MP-30 d and PW-30 d) whose volatile contents were higher than that of other clusters. All samples showed a high aromatic potential after 30 days of fermentation. According to the color scale, it was observed that northeast sauerkraut fermented with different mixed cultures exhibited different flavor characteristics. These results were similar to that achieved in the biplot analysis (Fig. 3B).

The contribution of volatile compound to the comprehensive flavor rested with the ratio of its actual concentration in the matrix to its odor threshold, which was called OAV. Generally speaking, the composition was considered to make a practical contribution when its OAV greater than 1. Nevertheless, individual volatile with OAV between 0.2 and 1 as background information might impact the odor by potential synergistic interaction (Wei et al., 2021). There were 45 volatiles with the OAV more than 1 that played an important role in the odor of sauerkraut

(Supplementary Table S2).

3.5.1. Organic acids and alcohols

In this study, only two acids were detected (acetic acid and octanoic acid), of which octanoic acid was only detected in Spo and MW samples at day 30, especially in Spo samples. Octanoic acid could contribute to an unpleasant odor (rancid and musty aroma), indicating that spontaneous fermentation might result in poor flavor of sauerkraut. Among all samples, except for Spo (OAV > 1), the MW samples had the highest concentration of acetic acid, which was similar to a previous study that found that *Leu. kimchii* and *W. cibaria* led to the highest production of acetic acid (Rizzello et al., 2018). A probable explanation for this result could be that *Leu. mesenteroides* and *W. cibaria* behaved as heterofermentative LAB during the fermentation.

The total content of alcohols was detected at the highest level in MP samples at day 30, which was mainly represented by 2-ethylhexanol, 2-nonanol (OAV = 122) and 2-heptanol (OAV = 6). These volatiles contributed unique flavor of sweet, floral and rose aroma according to Liu et al. (2019a). 2,3-butanediol (OAV = 78) was detected only in Spo samples, which was linked to yeast metabolism. It is noteworthy that a high occurrence of yeast would be likely to cause an undesirable fermentation. Therefore, it was suggested that the inhibition of yeast growth might be necessary to maintain good quality of sauerkraut (Li et al., 2017).

3.5.2. Esters

Esters are an important group of sensory-active compounds and mainly formed by esterification of acids with alcohols, as the source of fruity and floral aromas in finished products. In this study, total content of esters in mix-cultured samples was significantly ($p < 0.05$) higher (from 2- to 4-fold) than that in Spo samples, especially ethyl lactate, ethyl acetate (OAV: 0 - 3236), ethyl 3-phenylpropanoate (OAV: 0 - 3414) and methyl 2-hydroxy-4-methylpentanoate. Ethyl lactate was related to fruity and buttery flavor, with mixed cultures containing *L. plantarum* showing higher production. Correspondingly, higher production of ethyl lactate might account for the higher production of lactic acid in PA, PW and MP samples, as it was well known that ethyl lactate was formed by the reaction of lactic acid with ethanol. Ethyl 3-phenylpropanoate, which could be used in the preparation of flavors and fragrances and could also be used as a food flavoring agent, was detected only in sauerkraut samples fermented with mixed cultures.

3.5.3. Aldehydes and ketones

Aldehydes are very important compounds in fruits and vegetables, which are mainly produced by amino acid metabolism and fatty acid oxidation. They contribute to characteristic fragrances and flavors, show antimicrobial activity, and protect the plants from pathogens (Jampaphaeng et al., 2018). Total content of aldehydes in all mix-cultured samples was significantly ($p < 0.05$) higher than that in Spo samples, suggesting that the amino acid metabolism and lipid oxidation were more active in mix-culture fermentation. 2-hexenal (apple-like odor, OAV: 8 - 27) was detected only in samples fermented with mixed cultures containing *L. paracasei* (MA, PA and AW), which suggested that *L. paracasei* was responsible for the production of 2-hexenal.

Methyl ketones were detected in higher level in sauerkraut samples inoculated with mixed cultures containing *L. plantarum* (PW, PA and MP), especially acetoin (OAV: 54 - 189), 2-heptanone (OAV: 3 - 7), 2-nonanone (OAV: 0 - 72) and 2-octanone (OAV: 0 - 22). This result concurred with a previous finding by Liu, Li, Yang, Yi, Zhang, and He (2019b) who concluded that ketones were mainly produced by homofermentative LAB. The presence of various methyl ketones is beneficial for the sensory attribute of sauerkraut, which are associated with floral, fruity and creamy notes (Tian, Sun, Yu, Ai, & Chen, 2020).

3.5.4. Terpenes and lactones

Terpenes confer distinct odors to foods, with low thresholds, and are

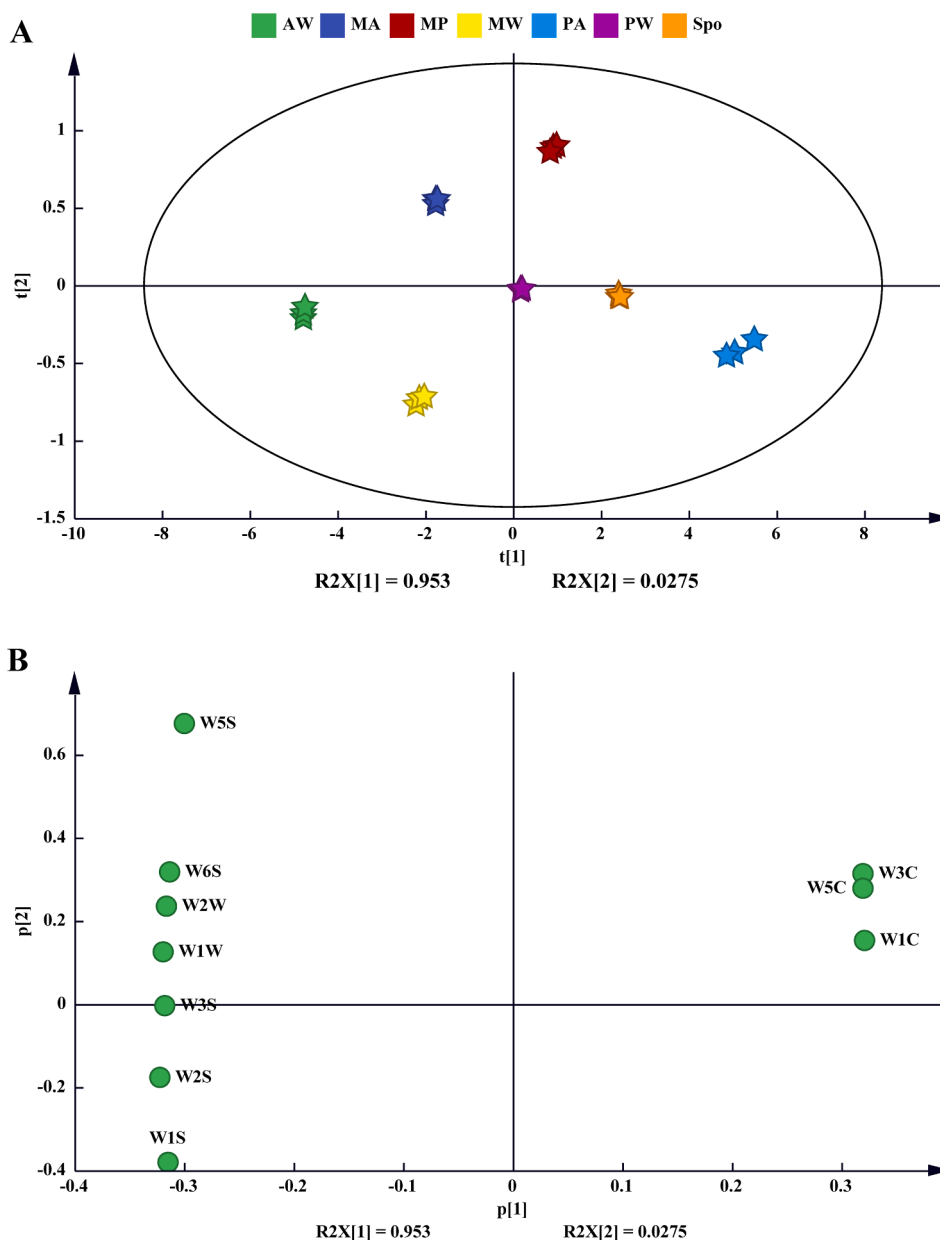


Fig. 4. Principal component analysis (PCA) of E-nose data of northeast sauerkraut by spontaneous (Spo) and different mix-cultured (MP, MA, MW, PA, PW and AW) fermentation at day 30. (A) score plot investigated the differences in flavor properties among different sauerkraut samples. (B) loading plot identified the ten sensors responsible for the separation in score plot.

usually used in perfume synthesis (v). Eight sterols with OAV > 1, including geraniol, linalool, α -terpineol, nerolidol, linalool oxide, citral, leaf alcohol and citronellol, have unique fragrances and contribute greatly to the flavor of sauerkraut (Tackenberg, Marmann, Thommes, Schuchmann, & Kleinebudde, 2014). Sauerkraut fermented with MP had the highest level of terpenes, followed by PW fermented sauerkraut, suggesting that the generation of terpenes was enhanced when *L. plantarum* was mixed with the heterofermentative LAB.

Lactones are formed from unsaturated fatty acids, and significantly contribute to the aroma of fermented foods, as fruity and floral notes (Park & Kim, 2019). A particularly interesting finding in this study was that no lactone was detected in Spo samples at day 30, which concurred with a previous finding that LAB contributed to the formation of lactones in fermented vegetables (Lee, Lim, Chang, Hurh, & Kim, 2018). δ -dodecalactone was only detected in sauerkraut fermented with mixed cultures containing *L. plantarum* (MP, PA and PW), which indicated that δ -dodecalactone was a metabolite of *L. plantarum* during fermentation,

although the underlying mechanism remained unclear.

3.5.5. Polyphenols

Polyphenols could be produced from Tyr by LAB, which might help to explain the highest concentration of Tyr and the lowest concentration of polyphenols in Spo samples at day 30 (Battelli et al., 2019). Polyphenols had been reported to be closely related to the antioxidant activity of fermented food (Zhang et al., 2019b). The highest concentration of polyphenols (OAV = 35) was detected in MP fermented sauerkraut, suggesting that the antioxidant activity of sauerkraut could be strengthened by inoculating with *L. plantarum* and *Leu. mesenteroides*.

3.5.6. ITCs, nitriles and sulfides

Previous study demonstrated that the breakdown products of glucosinolates, such as isothiocyanates (ITCs) and nitriles, provided many members of the *Brassica* genus with characteristic pungent and sulfurous flavors (Xu et al., 2020). ITCs (OAV: 50–900) were detected at the

highest concentration at day 0, reaching 90% of all volatile compounds. As the fermentation process continued, the contents of ITCs rapidly decreased and was significantly ($p < 0.05$) lower in mix-cultured samples (ranging from 19.32 to 38.72 ng/L) than that in Spo samples (65.53 ng/L) at the end of fermentation, which was in line with the higher levels of nitriles in mix-cultured samples. These results demonstrated that inoculation with mixed cultures could make the fermentation more effective.

Sulfides are known to be the most important volatile compounds that determine the flavor of sauerkraut, which are associated with cooked cabbage and green onion aroma (Lee et al., 2020). In this study, dimethyl disulfide (OAV: 15 - 59), 4-(methylthio) butanol (OAV: 442 - 2081), dimethyl trisulfide (OAV: 89 - 1275) and methyl thioacetate (OAV: 0 - 214) presented extremely high OAVs. These sulfides were found in higher levels in the sauerkraut samples mix-cultured with MP, PA and PW, coupled with the lower levels of sulfur-containing amino acids (Cys and Met), which verified that LAB were able to produce sulfides through the degradation of sulfur-containing amino acids. Additionally, this result was agreed with a previous study that the contents of sulfides produced by *L. plantarum* were higher than that by *Leu. mesenteroides* (Yun et al., 2020a; 2020b).

3.6. Principal component analysis (PCA) of volatile compounds

PCA is one of the most widely used multivariate and unsupervised clustering techniques, which does not require any knowledge of a dataset and reduces the dimensionality of multivariate data while preserving most of the variance therein (Park et al., 2010). To further understand and visualize the differences in volatilome profile of each fermentation trail, PCA was conducted based on the data of HS-SPME/GC-MS. The PCA biplot explained about 60.40% of total variability in the dataset, with PC1 as the primary axis explaining 44.50% of entire dataset and PC2 explaining 15.90% of total variability (Fig. 3B). The PCA biplot clearly distinguished the seven groups subjected to different treatments, which indicated that the volatilome profile of sauerkraut was significantly affected by the identity of inoculated mixed cultures. All samples at day 0 (the third quadrant) and Spo samples at day 30 (the second quadrant) were located on the negative PC1, whereas all mix-cultured samples at day 30 were located on the positive PC1. At the beginning of fermentation, all samples were related to ITCs, 2-ethylhexanol, 3,5-dimethylbenzaldehyde and 3,5-ditert-butylphenol. At the end of fermentation, the Spo fermentation was distinguished from six mix-cultured groups on PC1, and the former was distinguished by the higher content of ITCs. As for the six mix-cultured groups, MW and AW fermented sauerkraut lie on the first quadrant, while the other four groups (MA, PA, PW and MP) situated in the fourth quadrant. Specifically, the sauerkraut mix-cultured with MP was characterized by a greater number of flavor compounds including alcohols (2-nonanol and 2-heptanol), esters (ethyl crotonate, ethyl butanoate, ethyl lactate, ethyl hexanoate, ethyl 3-phenylpropanoate and ethyl acetate), terpenes (geraniol, nerolidol and dihydrocarveol), polyphenols and nitriles. Lactones, isobutanol, methyl acetate and 2-methylpentanaldehyde were the most abundant in the MA mix-cultured sauerkraut. MW fermented sauerkraut was featured by relatively high contents of acetic acid, phenylacetaldehyde, citronellol, esters (hexyl octanoate, ethyl octanoate, ethyl sorbate and isoamyl acetate) and alcohols (hexanol, isoamylol and phenylethyl alcohol). The sauerkraut mix-cultured with PA was mainly signified by having higher levels of ethyl lactate and sulfides (dimethyl disulfide and dimethyl trisulfide). Cis-6-nonen-1-ol, tetrahydrofurfuryl acetate, linalool, *trans*-2-pentenal and ketones (acetoin, 2-heptanone and 2-nonanone) were representative compounds in PW mix-cultured sauerkraut and might be the potential biomarkers. Volatile compounds, such as diethyl succinate, dodecanal and 4-ethyl-2-methoxyphenol, were well described as the sauerkraut fermented with AW. These results indicated that northeast sauerkraut with different flavor characteristics could be made according to the type of starter cultures

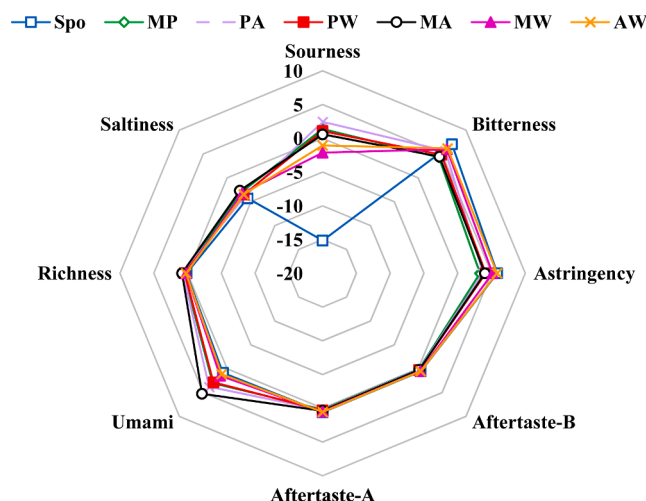


Fig. 5. Radar chart of E-tongue data of northeast sauerkraut by spontaneous (Spo) and different mix-cultured (MP, MA, MW, PA, PW and AW) fermentation at day 30.

used.

3.7. E-nose analysis

E-nose has been widely used in the research of fermentation process monitoring, as a quality assurance method due to its rapid and accurate characteristics. This study also performed PCA on the E-nose data to analyze the volatile characteristics of spontaneous and mix-cultured sauerkraut.

The dataset was divided into two principal components, which accounted for 98.05% of the total variance. As displayed in Fig. 4A, all samples were largely accumulated into seven groups in the score plot of PCA. MP fermented samples fell in the first quadrant, samples fermented with MA were situated in the second quadrant, two mix-cultured groups (AW and MW) were located in the third quadrant, and three treatments (Spo, PW and PA) were positioned in the fourth quadrant. The result demonstrated that these sensors could more effectively discriminate sauerkraut samples fermented with different mixed cultures, indicating that the type of mixed cultures used exhibited obvious effects on the flavor of sauerkraut. The loading analysis would help to identify the sensors responsible for distribution and discrimination of the samples in current score plot file (Fig. 4B). Considering that the loading parameter values of sensors were positively correlated with their contributions to the total resolution of system, sensors W1C (sensitive to aromatic constituents and benzene), W3C (sensitive to aroma and ammonia) and W5C (sensitive to short-chain alkane aromatic components) potentially contributed further to the samples mix-cultured with MP. The increased response values of aromatic compounds in the analysis of E-nose were consistent with the results of HS-SPME/GC-MS.

3.8. E-tongue analysis

Sourness and saltiness, as important sensory evaluation indicators in sauerkraut samples, were significantly different among different sauerkraut samples, followed by umami and bitterness (Yun et al., 2020a; 2020b). As shown in Fig. 5, the PA mix-cultured sauerkraut showed the strongest aroma intensity of sourness, while that in Spo samples had the lowest value, which was in line with the results of pH value (Fig. 1). As shown in Supplementary Table S4, the mix-cultured sauerkraut yielded significantly ($p < 0.05$) higher umami and lower bitterness values, especially MP and MA. This could be due to the suppression effect of umami on bitterness (Ismail, Hwang, & Joo, 2020). Additionally, the high acidity might inhibit the bitterness and further give sauerkraut a

Table 2

Sensory evaluation of northeast sauerkraut at day 30 by spontaneous (Spo) and mix-cultured (MP, MA, MW, PA, PW, AW) fermentation.

Attributes Samples	Spo	MP	MA	MW	PA	PW	AW
Color	1.20 ± 0.54 ^e	8.47 ± 0.72 ^a	8.73 ± 0.44 ^a	2.27 ± 1.18 ^d	6.20 ± 0.91 ^b	3.67 ± 1.53 ^c	1.33 ± 0.60 ^{de}
Crispness	1.13 ± 0.34 ^e	8.47 ± 0.62 ^a	7.87 ± 0.81 ^{ab}	2.93 ± 0.68 ^d	6.93 ± 0.44 ^c	7.20 ± 0.54 ^{bc}	1.67 ± 0.79 ^e
Sourness	1.00 ± 0.00 ^e	8.40 ± 0.49 ^a	5.60 ± 0.61 ^c	4.73 ± 0.10 ^d	7.67 ± 0.60 ^{ab}	6.93 ± 0.93 ^b	5.07 ± 0.93 ^{cd}
Flavor	1.13 ± 0.34 ^f	8.60 ± 0.49 ^a	6.93 ± 0.57 ^c	2.87 ± 0.62 ^e	7.33 ± 0.47 ^{bc}	7.60 ± 0.61 ^b	3.73 ± 0.78 ^d
Taste	1.27 ± 0.57 ^d	8.53 ± 0.50 ^a	7.13 ± 0.50 ^b	3.07 ± 0.57 ^c	7.60 ± 0.61 ^b	7.47 ± 0.50 ^b	3.60 ± 0.71 ^c
Overall acceptability	1.07 ± 0.25 ^d	8.73 ± 0.44 ^a	7.87 ± 0.62 ^b	2.80 ± 0.40 ^c	7.73 ± 0.68 ^b	7.53 ± 0.72 ^b	3.13 ± 0.50 ^c

Data are the mean ± standard deviation. Values marked with different letters in the same column are significantly different ($p < 0.05$).

Spo, spontaneous fermentation; MP, inoculated with mixed culture of *Leu. mesenteroides* and *L. plantarum*; MA, inoculated with mixed culture of *Leu. mesenteroides* and *L. paracasei*; MW, inoculated with mixed culture of *Leu. mesenteroides* and *W. cibaria*; PA, inoculated with mixed culture of *L. plantarum* and *L. paracasei*; PW, inoculated with mixed culture of *L. plantarum* and *W. cibaria*; AW, inoculated with mixed culture of *L. paracasei* and *W. cibaria*.

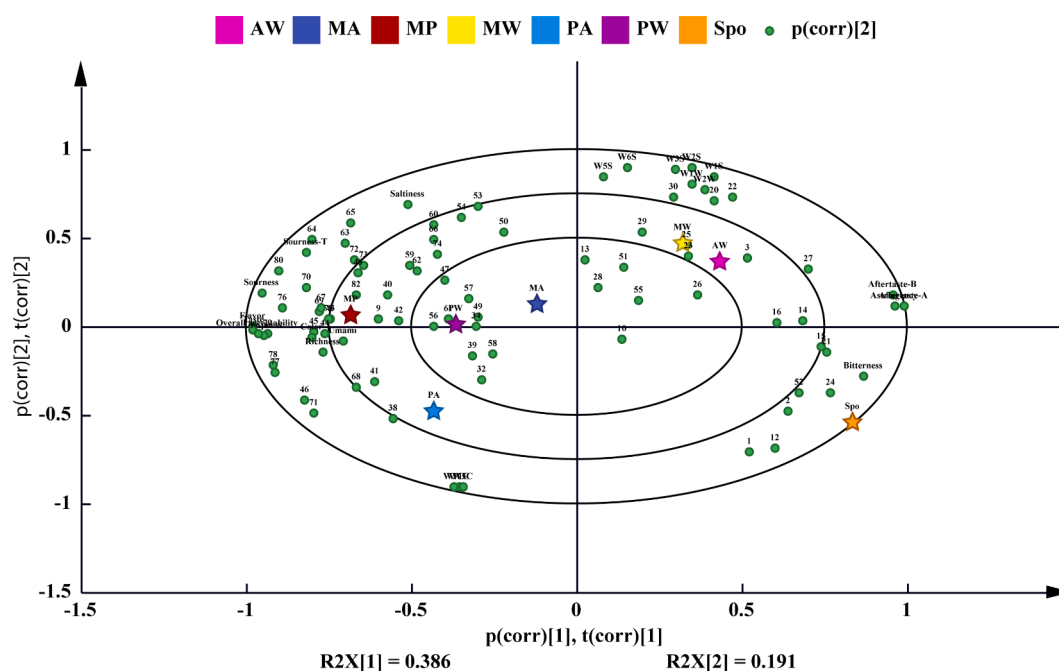


Fig. 6. Biplot (score plots combined with loading plots) based on the data of HS-SPME/GC-MS, E-nose, E-tongue and sensory evaluation for northeast sauerkraut by spontaneous (Spo) and different mix-cultured (MP, MA, MW, PA, PW and AW) fermentation at day 30. Five-pointed stars in orange, red, navy blue, yellow, light blue, purple and pink represent sauerkraut fermented by spontaneous (Spo) and different mixed cultures (MP, MA, MW, PA, PW and AW) fermentation at day 30. The numbers (from 1 to 82) next to green circles represent volatile compound names as shown in Supplementary Table S2. (For interpretation of the references to color in this figure legend, the reader is referred to the web version of this article.)

palatable taste, which concurred with a previous finding by [Chen et al. \(2019\)](#). The result indicated that mixed cultures improved the flavor of raw materials (including taste and aroma) through their metabolism. Among all mix-cultured samples, the MP fermented sauerkraut had the lowest values of bitterness, astringency, aftertaste-A and aftertaste-B, and significantly higher umami and richness values ($p < 0.05$, Supplementary Table S4), which suggested that the northeast sauerkraut fermented with the mixed culture of MP might have better flavor characteristics.

3.9. Sensory evaluation

As presented in [Table 2](#), the sensory evaluation showed that the Spo sauerkraut exhibited significant ($p < 0.05$) difference in the six attributes compared to the mix-cultured samples. Sauerkraut mix-cultured with MP received the highest scores in the taste and flavor, while Spo sauerkraut obtained the lowest scores. These results were consistent with the results of the E-tongue and E-nose, respectively. The off-flavor of sauerkraut might be caused by the propagation of film yeast and aerobic bacteria. In the case of sauerkraut fermented with mixed

cultures, microorganisms causing the deterioration were suppressed by the starter cultures. Altogether, the overall acceptability score of MP mix-cultured sauerkraut was higher than that of other samples, which indicated that the northeast sauerkraut fermented with a mixed culture of MP was more favored by panelists. Multivariate statistical analysis of the comprehensive sensory characteristics was presented in a biplot ([Fig. 6](#)), which was performed by combining the data of HS-SPME/GC-MS, E-nose, E-tongue and sensory evaluation. Clear discrimination was obtained from the biplot, which indicated that northeast sauerkraut fermented with different mixed cultures could be distinguished by their sensory characteristics. As indicated in [Fig. 6](#), Spo fermented sauerkraut was featured by higher levels of acetic acid and ITCs (isothiocyanatocyclopentane, 4-isothiocyanatobut-1-ene and phenethyl isothiocyanate), which correlated well with the bitterness. MW and AW fermented sauerkraut were situated in the first quadrant, which were closely related to seven E-nose sensors (W5S, W6S, W1S, W1W, W2S, W2W and W3S). The result was in good agreement with the result of HS-SPME/GC-MS that MW and AW fermented sauerkraut were characterized by relatively high contents of alcohols and aldehydes, especially trans-2-nonenol, hexanol, isoamylol, phenylethyl alcohol, dodecanol

and phenylacetaldehyde. It was noteworthy that most of the volatile compounds were significantly associated with the MP fermented sauerkraut, such as esters (ethyl lactate, tetrahydrofurfuryl acetate, ethyl hexanoate, ethyl 3-phenylpropanoate and ethyl acetate), terpenes (geraniol, linalool, nerolidol and dihydrocarveol) and 3,5-ditert-butylphenol. These compounds were found to be close to several aspects of E-tongue (umami and richness) and sensory evaluation (crispness, taste, flavor, color and overall acceptability), which was highly in keeping with the results of E-tongue and sensory evaluation.

4. Conclusion

The results of this study indicated that the application of mix-culture fermentation and the type of mixed cultures had significant effects on the quality of northeast sauerkraut. Mix-culture fermentation increased the population of LAB but decreased the undesirable microorganisms compared with the spontaneous fermentation. Based on the results of HS-SPME/GC-MS, E-nose, E-tongue and sensory evaluation, northeast sauerkraut fermented with MP showed the best quality. MP inoculation enhanced the contents of desirable compounds, such as lactic acid, FAAs, esters, terpenes and polyphenols. It was indicated that MP was considered as the most promising mixed culture to accelerate and standardize the process, reduce the growth of spoilage microorganisms and improve the aroma of final products. It is clear that the interactions between *Leu. mesenteroides* and *L. plantarum* are the most important factors in producing the distinctive flavor of northeast sauerkraut. So, further studies are needed to reveal the metabolic activity and interactions of microorganisms in mix-culture fermentation.

CRedit authorship contribution statement

Wenzhong Hu: Conceptualization, Funding acquisition, Investigation, Project administration, Supervision, Validation, Writing - original draft, Writing - review & editing. **Xiaozhe Yang:** Data curation, Formal analysis, Writing - original draft, Writing - review & editing. **Yaru Ji:** Writing - review & editing. **Yuge Guan:** Writing - review & editing.

Declaration of Competing Interest

The authors declare that they have no known competing financial interests or personal relationships that could have appeared to influence the work reported in this paper.

Acknowledgement

This study was supported by 'Thirteenth Five-Year Plan' for National key research and development program (Grant No. 2016YFD0400903), National Natural Science Foundation (Grant No. 31471923), and 'Twelfth Five-Year Plan' for National Science and Technology Support Program (Grant No. 2012BAD38B05).

Appendix A. Supplementary material

Supplementary data to this article can be found online at <https://doi.org/10.1016/j.foodres.2021.110605>.

References

Battelli, G., Scano, P., Albano, C., Cagliani, L. R., Brasca, M., & Consonni, R. (2019). Modifications of the volatile and nonvolatile metabolome of goat cheese due to adjunct of non-starter lactic acid bacteria. *LWT - Food Science and Technology*, *116*, Article 108576. <https://doi.org/10.1016/j.lwt.2019.108576>.

Chan, M. Z. A., Chua, J. Y., Toh, M., & Liu, S. Q. (2019). Survival of probiotic strain *Lactobacillus paracasei* L26 during co-fermentation with *S. cerevisiae* for the development of a novel beer beverage. *Food Microbiology*, *82*, 541-550. <https://doi.org/10.1016/j.fm.2019.04.001>.

Chen, A., Luo, W., Peng, Y., Niu, K., Liu, X., Shen, G., ... Li, S. (2019). Quality and microbial flora changes of radish paocai during multiple fermentation rounds. *Food Control*, *106*, Article 106733. <https://doi.org/10.1016/j.foodcont.2019.106733>.

Choi, Y. J., Yong, S., Lee, M. J., Park, S. J., Yun, Y. R., Park, S. H., & Lee, M. A. (2019). Changes in volatile and non-volatile compounds of model kimchi through fermentation by lactic acid bacteria. *LWT - Food science and technology*, *105*, 118-126. <http://doi.org/10.1016/j.lwt.2019.02.001>.

Fittipaldi, M., Nocker, A., & Codony, F. (2012). Progress in understanding preferential detection of live cells using viability dyes in combination with DNA amplification. *Journal of Microbiological Methods*, *91*, 276-289. <https://doi.org/10.1016/j.mimet.2012.08.007>.

Ganzle, M. G. (2015). Lactic metabolism revisited: Metabolism of lactic acid bacteria in food fermentations and food spoilage. *Current Opinion in Food science*, *2*, 106-117. <https://doi.org/10.1016/j.cofs.2015.03.001>.

Hossain, M. I., Mizan, M. F. R., Ashrafudoulla, M., Nahar, S., Joo, H. J., Jahid, I. K., ... Ha, S. D. (2020). Inhibitory effects of probiotic potential lactic acid bacteria isolated from kimchi against *Listeria monocytogenes* biofilm on lettuce, stainless-steel surfaces, and MEBC™ biofilm device. *LWT - Food Science and Technology*, *118*, Article 108864. <https://doi.org/10.1016/j.lwt.2019.108864>.

Ismail, I., Hwang, Y. H., & Joo, S. T. (2020). Low-temperature and long-time heating regimes on non-volatile compound and taste traits of beef assessed by the electronic tongue system. *Food Chemistry*, *320*, Article 126656. <https://doi.org/10.1016/j.foodchem.2020.126656>.

Jung, J. Y., Lee, S. H., Lee, H. J., Seo, H. Y., Park, W. S., & Jeon, C. O. (2012). Effects of *Leuconostoc mesenteroides* starter cultures on microbial communities and metabolites during kimchi fermentation. *International Journal of Food Microbiology*, *153*, 378-387. <https://doi.org/10.1016/j.ijfoodmicro.2011.11.030>.

Jampaphaeng, K., Ferrocino, I., Giordano, M., Rantsiou, K., Maneerat, S., & Cocolin, L. (2018). Microbiota dynamics and volatile profile during stink bean fermentation (Sataw-Dong) with *Lactobacillus plantarum* KJ03 as a starter culture. *Food Microbiology*, *76*, 91-102. <https://doi.org/10.1016/j.fm.2018.04.012>.

Ly, D., Mayrhofer, S., Yogeswara, I. B. A., Nguyen, T. H., & Domig, K. J. (2019). Identification, classification and screening for γ -Amino-butyric acid production in lactic acid bacteria from Cambodian fermented foods. *Biomolecules*, *9*, Article 768. <https://doi.org/10.3390/biom9120768>.

Liu, S., Yang, L., Zhou, Y., He, S., Li, J., Sun, H., ... Xu, S. (2019). Effect of mixed moulds starters on volatile flavor compounds in rice wine. *LWT - Food Science and Technology*, *112*, Article 108215. <https://doi.org/10.1016/j.lwt.2019.05.113>.

Liu, T., Li, Y., Yang, Y., Yi, H., Zhang, L., & He, G. (2019b). The influence of different lactic acid bacteria in sourdough flavor and a deep insight into sourdough fermentation through RNA sequencing. *Food Chemistry*, *307*, Article 125529. <https://doi.org/10.1016/j.foodchem.2019.125529>.

Li, Q., Kang, J., Ma, Z., Li, X., Liu, L., & Hui, X. (2017). Microbial succession and metabolite changes during traditional serofluid dish fermentation. *LWT - Food Science and Technology*, *84*, 771-779. <https://doi.org/10.1016/j.lwt.2017.06.051>.

Li, S., Tang, S., He, Q., Hu, J., & Zheng, J. (2019). Changes in proteolysis in fermented milk produced by *Streptococcus thermophilus* in co-culture with *Lactobacillus plantarum* or *Bifidobacterium animalis* subsp. *lactis* during refrigerated storage. *Molecules*, *24*, Article 3699. <https://doi.org/10.3390/molecules24203699>.

Lee, J. J., Choi, Y. J., Lee, M. J., Park, S. J., Oh, S. J., Yun, Y. R., ... Lee, M. A. (2020). Effects of combining two lactic acid bacteria as a starter culture on model kimchi fermentation. *Food Research International*, *136*, Article 109591. <https://doi.org/10.1016/j.foodres.2020.109591>.

Lee, S. M., Lim, H. J., Chang, J. W., Hurh, B. S., & Kim, Y. S. (2018). Investigation on the formations of volatile compounds, fatty acids, and γ -lactones in white and brown rice during fermentation. *Food Chemistry*, *269*, 347-354. <https://doi.org/10.1016/j.foodchem.2018.07.037>.

Liang, H., He, Z., Wang, X., Song, G., Chen, H., Lin, X., ... Li, S. (2020). Effects of salt concentration on microbial diversity and volatile compounds during suancai fermentation. *Food Microbiology*, *91*, Article 103537. <https://doi.org/10.1016/j.fm.2020.103537>.

Liang, H., Yin, L., Zhang, Y., Chang, C., & Zhang, W. (2018). Dynamics and diversity of a microbial community during the fermentation of industrialized Qingcai paocai, a traditional Chinese fermented vegetable food, as assessed by Illumina Miseq sequencing, DGGE and qPCR assay. *Annals of Microbiology*, *68*, 111-122. <https://doi.org/10.1007/s13213-017-1321-z>.

Minervini, F., Missaoui, J., Celano, G., Calasso, M., Achour, L., Saidane, D., ... De Angelis, M. (2019). Use of autochthonous *Lactobacilli* to increase the safety of Zgougou. *Microorganisms*, *8*, Article 29. <https://doi.org/10.3390/microorganisms8010029>.

Özcan, E., Seven, M., Şirin, B., Çakır, T., Nikerel, E., Teusink, B., & Öner, E. T. (2020). Dynamic co-culture metabolic models reveal the fermentation dynamics, metabolic capacities and interplays of cheese starter cultures. *Biotechnology and Bioengineering*, *2*, 1-15. <https://doi.org/10.1002/bit.27565>.

Park, M. K., & Kim, Y. S. (2019). Distinctive formation of volatile compounds in fermented rice inoculated by different molds, yeasts, and lactic acid bacteria. *Molecules*, *24*, Article 2123. <https://doi.org/10.3390/molecules24112123>.

Park, M. K., Cho, I. H., Lee, S., Choi, H. K., Kwon, D. Y., & Kim, Y. S. (2010). Metabolite profiling of Cheonggukjang, a fermented soybean paste, during fermentation by gas chromatography-mass spectrometry and principal component analysis. *Food Chemistry*, *122*, 1313-1319. <https://doi.org/10.1016/j.foodchem.2010.03.095>.

Park, S. E., Seo, S. H., Kim, E. J., Byun, S., Na, C. S., & Son, H. S. (2019). Changes of microbial community and metabolite in kimchi inoculated with different microbial community starters. *Food Chemistry*, *274*, 558-565. <https://doi.org/10.1016/j.foodchem.2018.09.032>.

- Rizzello, C. G., Coda, R., Wang, Y., Verni, M., Kajala, L., Katina, K., & Laitila, A. (2018). Characterization of indigenous *Pediococcus pentosaceus*, *Leuconostoc kimchii*, *Weissella cibaria* and *Weissella confusa* for faba bean bioprocessing. *International Journal of Food Microbiology*, 302, 24–34. <https://doi.org/10.1016/j.ijfoodmicro.2018.08.014>.
- Soni, R., Jain, N. K., Shah, V., Soni, J., Suthar, D., & Gohel, P. (2020). Development of probiotic yogurt: Effect of strain combination on nutritional, rheological, organoleptic and probiotic properties. *Journal of Food Science and Technology*, 57, 2038–2050. <https://doi.org/10.1007/s13197-020-04238-3>.
- Toe, C. J., Foo, H. L., Loh, T. C., Mohamad, R., Rahim, R. A., & Idrus, Z. (2019). Extracellular proteolytic activity and amino acid production by lactic acid bacteria isolated from Malaysian foods. *International Journal of Molecular Sciences*, 20, Article 1777. <https://doi.org/10.3390/ijms20071777>.
- Tian, H., Sun, X., Yu, H., Ai, L., & Chen, C. (2020). Characterization of the key aroma compounds in Yunnan goat milk cake using a sensory-directed flavor analysis. *Journal of Food Science*, 85, 3981–3997. <https://doi.org/10.1111/1750-3841.15490>.
- Tackenberg, M. W., Marmann, A., Thommes, M., Schuchmann, H. P., & Kleinebudde, P. (2014). Orange terpenes, carvacrol and α -tocopherol encapsulated in maltodextrin and sucrose matrices via batch mixing. *Journal of Food Engineering*, 135, 44–52. <https://doi.org/10.1016/j.jfoodeng.2014.03.010>.
- Vaccalluzzo, A., Pino, A., Russo, N., De Angelis, M., Caggia, C., & Randazzo, C. L. (2020). FoodOmics as a new frontier to reveal microbial community and metabolic processes occurring on table olives fermentation. *Food Microbiology*, 92, Article 103606. <https://doi.org/10.1016/j.fm.2020.103606>.
- Wouters, D., Grosu-Tudor, S., Zamfir, M., & Vuyst, L. D. (2013). Applicability of *Lactobacillus plantarum* IMDO788 as a starter culture to control vegetable fermentations. *Journal of the Science of Food and Agriculture*, 93, 3352–3361. <https://doi.org/10.1002/jsfa.6184>.
- Wu, R., Yu, M., Liu, X., Meng, L., Wang, Q., Xue, Y., ... Yue, X. (2015). Changes in flavour and microbial diversity during natural fermentation of suan-cai, a traditional food made in Northeast China. *International Journal of Food Microbiology*, 211, 23–31. <https://doi.org/10.1016/j.ijfoodmicro.2015.06.028>.
- Wang, C., Sun, J., Lassabliere, B., Yu, B., & Liu, S. (2019). Coffee flavour modification through controlled fermentation of green coffee beans by *Lactococcus lactis* subsp. cremoris. *LWT - Food Science and Technology*, 120, Article 108930. <https://doi.org/10.1016/j.lwt.2019.108930>.
- Wang, C., Zhang, X., Gao, Y., Han, Y., & Wu, X. (2021). Path analysis of non-enzymatic browning in Dongbei Suancai during storage caused by different fermentation conditions. *Food Chemistry*, 335, Article 127620. <https://doi.org/10.1016/j.foodchem.2020.127620>.
- Wei, S., Xiao, X., Wei, L., Li, L., Li, G., Liu, F., ... Zhong, Y. (2021). Development and comprehensive HS-SPME/GC-MS analysis optimization, comparison, and evaluation of different cabbage cultivars (*Brassica oleracea* L. var. capitata L.) volatile components. *Food Chemistry*, 340, Article 128166. <https://doi.org/10.1016/j.foodchem.2020.128166>.
- Xu, Z., He, H., Zhang, S., & Kong, J. (2017). Effects of inoculants *Lactobacillus brevis* and *Lactobacillus parafarraginis* on the fermentation characteristics and microbial communities of corn stover silage. *Scientific Reports*, 7, Article 13614. <https://doi.org/10.1038/s41598-017-14052-1>.
- Xu, X., Bi, S., Lao, F., Chen, F., Liao, X., & Wu, J. (2020). Comprehensive investigation on volatile and non-volatile metabolites in broccoli juices fermented by animal- and plant-derived *Pediococcus pentosaceus*. *Food Chemistry*, 341, Article 128118. <https://doi.org/10.1016/j.foodchem.2020.128118>.
- Yang, H., Hao, W., Gao, L., Jia, H., Zhang, Y., Cui, Z., & Li, Y. (2016). Effects of *Lactobacillus curvatus* and *Leuconostoc mesenteroides* on suan cai fermentation in Northeast China. *Journal of Microbiology & Biotechnology*, 26, 2148–2158. <https://doi.org/10.4014/jmb.1607.07010>.
- Yun, L., Mao, B., Cui, S., Tang, X., Zhang, H., Zhao, J., & Chen, W. (2020a). Gas chromatography–mass spectrometry-based metabolomics analysis of metabolites in commercial and inoculated pickles. *Journal of the Science of Food and Agriculture*, 10757. <https://doi.org/10.1002/jsfa.10757>.
- Yang, X., Hu, W., Xiu, Z., Jiang, A., Yang, X., Saren, G., ... Feng, K. (2020). Comparison of northeast sauerkraut fermentation between single lactic acid bacteria strains and traditional fermentation. *Food Research International*, 137, Article 109553. <https://doi.org/10.1016/j.foodres.2020.109553>.
- Yi, C., Zhu, H., Tong, L., Zhou, S., Yang, R., & Niu, M. (2019). Volatile profiles of fresh rice noodles fermented with pure and mixed cultures. *Food Research International*, 119, 152–160. <https://doi.org/10.1016/j.foodres.2019.01.044>.
- Yun, L., Mao, B., Cui, S., Tang, X., Zhang, H., Zhao, J., & Chen, W. (2020b). Gas chromatography–mass spectrometry-based metabolomics analysis of metabolites in commercial and inoculated pickles. *Journal of the Science of Food and Agriculture*, 101, 1436–1446. <https://doi.org/10.1002/jsfa.10757>.
- Zhang, P., Zhang, P., Wu, J., Tao, D., & Wu, R. (2019). Effects of *Leuconostoc mesenteroides* on physicochemical and microbial succession characterization of soybean paste. *Da-jiang LWT - Food Science and Technology*, 115, Article 108028. <https://doi.org/10.1016/j.lwt.2019.04.029>.
- Zhang, Y., Hu, P., Xie, Y., & Wang, X. (2020). Co-fermentation with *Lactobacillus curvatus* LAB26 and *Pediococcus pentosaceus* SWU73571 for improving quality and safety of sour meat. *Meat Science*, 170, Article 108240. <https://doi.org/10.1016/j.meatsci.2020.108240>.
- Zhang, X., Wang, P., Xu, D., Wang, W., & Zhao, Y. (2019). Aroma patterns of Beijing rice vinegar and their potential biomarker for traditional Chinese cereal vinegars. *Food Research International*, 119, 398–410. <https://doi.org/10.1016/j.foodres.2019.02.008>.



The *p*-Anisaldehyde/ β -cyclodextrin inclusion complexes as fumigation agent for control of postharvest decay and quality of strawberry

Ying Lin^b, Ran Huang^{c,d}, Xiuxiu Sun^e, Xi Yu^a, Ying Xiao^a, Ling Wang^a, Wenzhong Hu^{b,**}, Tian Zhong^{a,*}

^a Faculty of Medicine, Macau University of Science and Technology, Avenida Wai Long, Taipa, Macau, China

^b School of Pharmacy and Food Science, Zuhai College of Science and Technology, Zuhai, Guangdong, China

^c Academy for Engineering and Technology, Fudan University, Shanghai, China

^d Department of Materials Technology and Engineering, Research Institute of Zhejiang University-Taizhou, Taizhou, Zhejiang, China

^e United States Horticultural Research Laboratory, USDA-ARS, Fort Pierce, Florida, United States

ARTICLE INFO

Keywords:

Essential oil
Cyclodextrin
Inclusion complexes
Encapsulation
Fumigation agent
Colony morphology
Postharvest decay
Incidence
Antifungal activity
Fruit quality
Sensory
Strawberry

ABSTRACT

In order to evaluate the potential of developed β -cyclodextrin (β -CD)/*p*-Anisaldehyde (PAA) inclusion complexes as a fumigation agent for the postharvest decay control in strawberry, both *in vitro* and *in vivo* tests were conducted. According to the colony morphology analysis on PDA media, inclusion complexes showed activity on inhibiting the mycelial growth of the fungi including *Rhizopus stolonifer*, *Aspergillus niger* and *Penicillium*. The effect of inclusion complexes on controlling postharvest decay in fresh strawberry was also confirmed by *in vivo* test, in which the inclusion complexes-treated fruit displayed significantly lower incidence and severity than control, β -CD-treated and free PAA-treated fruit. Moreover, evaluations of fruit qualities including color, weight loss, firmness and TSS, as well as the sensory indexes including appearance, color, texture and flavor were carried out in turn, showing there was no significant difference between inclusion complexes-treated fruit and the other groups.

1. Introduction

Strawberry is a unique fruit with vivid appearance and rich bioactive compounds including polyphenolic compounds, flavonoids, anthocyanins, vitamins, pectin and organic acids, etc. (Aday, Buyukcan, & Caner, 2013; Kallio, Hakala, Pelkkikangas, & Lapveteläinen, 2000; Tulipani et al., 2011). However, due to the absence of peel and low cell-wall strength, mechanical injury and fungal pathogen infection are the two primary causes to induce the postharvest decay and spoilage of strawberry, which reduce its quality and commercial value (Basu, Nguyen, Betts, & Lyons, 2014; Jesmin et al., 2016; Jiang et al., 2019). In addition, the high respiration and metabolic rates of fresh strawberry significantly accelerate the decay progress and aggravate the spoilage severity (Caner, Aday, & Demir, 2008; Sousa-Gallagher, Mahajan, & Mezdad, 2013). It is reported that strawberry is prone to microbial infection with a storage life of 1–2 days at room temperature without proper

preservative measures (Cao, Hu, & Pang, 2010; Hashmi, East, Palmer, & Heyes, 2013; Neri et al., 2015). Major threatening fungi that reduce the postharvest storage life of strawberry include *Botrytis*, *Rhizopus*, *Aspergillus*, *Penicillium* and *Gilbertella* (Bautista-Baños, García-Domínguez, Barrera-Necha, Reyes-Chilpa, & Wilson, 2003; Bhaskara; Reddy, Angers, Gosselin, & Arul, 1998; Palmer, Mansouripour, Blauer, & Holmes, 2019; Zhang et al., 2020).

Presently, various preservation measures such as pre-cooling, cold-chain transportation, modified atmosphere packaging (MAP) or ethylene absorption (Almenar et al., 2007; Picón, Martínez-Jávega, Cuquerella, Del Río, & Navarro, 1993) and a series of chemical agents are commonly employed for fruit storage and preservation (Pan et al., 2014; Vanti, Leshem, & Masaphy, 2021). However, most of the above-mentioned methods require expensive cost in equipment and investment or produce harmful chemical residues in fruit (Bose, Howlader, Wang, & Yin, 2021). Therefore, a low-cost, non-toxic,

* Corresponding author.

** Corresponding author.

E-mail addresses: hwz@dlnu.edu.cn (W. Hu), tzhong@must.edu.mo (T. Zhong).

pollution-free antimicrobial manufactured by natural active compounds and biodegradable materials is maybe a potential alternative for food preservation.

Essential oils (EOs) are natural and volatile liquids derived from plants. They were generally recognized as safe (GRAS) by the US Food and Drug Administration (FDA) and considered as good chemical antimicrobial additive alternatives in food field due to their broad antimicrobial properties (Food & Administration, 1997). Moreover, EOs was reported may not only inhibit a variety of pathogens, but also not easily cause the resistance of pathogens (Wang et al., 2017). However, the application of EOs were quite limited by their natures including low water solubility, low thermal and chemical stability (Köse, Tekin, & Marques, 2010). Additionally, the treatment with EOs affects the sensory acceptability, due to the strong odor-flavor that can be transmitted from the oil to the food product (Ayala-Zavala, Del-Toro-Sánchez, Alvarez-Parrilla, & González-Aguilar, 2008). High concentrations of EO even induces serious surface harming when contact fruit directly (Chen et al., 2020).

In order to overcome these drawbacks, one effective and widely used solution is to encapsulate the EO components as guest molecules into cyclodextrins to form inclusion complexes. Former researches have reported that encapsulation in cyclodextrin improved the stability (García-Sotelo et al., 2019), water solubility (Barbieri et al., 2018; Siva, Li, Cui, Meenatchi, & Lin, 2020) and bioavailability (Suvarna, Gujar, & Murahari, 2017) of EOs, and ensured the sustained- or controlled-release of the guest active substances (Chen & Liu, 2016; Yin et al., 2021). The *p*-Anisaldehyde (PAA), which is a major compound of the essential oil extracted from the seeds of *Pimpinella anisum* (Shreaz et al., 2011), exhibits efficient antimicrobial activities against most foodborne bacteria (*Candida Bacillus subtilis*, *Pseudomonas aeruginosa*, and *Fusarium oxysporum*, *Listeria monocytogenes* and *Staphylococcus aureus*), yeasts (*Candida*) and mold strains (*Aspergillus niger*) in many previous researches (Okamoto, Narayama, Katsuo, Shigematsu, & Yanase, 2002; Shi et al., 2017). But to our knowledge, this is the first report on encapsulating PAA into cyclodextrins for food application. In this study, PAA/ β -CD inclusion complexes were used as a fumigation antimicrobial agent for extending the storage life of fresh strawberry. The aims of this study are to (i) determine the *in vitro* antifungal activity of the inclusion complexes against the fungi isolated from local strawberries; (ii) investigate the effects of the inclusion complexes as a fumigation agent on postharvest decay control in fresh strawberries; and (iii) evaluate the effects of this agent on fruit qualities during storage and verify that the influences are acceptable to consumers.

2. Materials and methods

2.1. Fruit and pathogens

Strawberry fruit (*Fragaria ananassa* Duch.) were harvested from a local orchard in Zhuhai, China. Fruit selected for the experiments were uniform in size, shape, maturity, and without any physical injuries or disease symptoms. Strains of postharvest fungi including *Rhizopus stolonifer*, *Aspergillus niger* and *Penicillium* were isolated from the harvested diseased strawberry and identified by morphological characterization. Cultures of the microorganisms were maintained on potato dextrose agar (PDA) media.

2.2. Colony morphology analysis

Assessment of the antifungal activity of the inclusion complexes was carried out using the poisoned food technique on fungus-inoculated PDA media as described by the previous research (2013). For different treatments, molten PDA were previously incorporated with 121.0 mg of β -CD, 11.5 mg of pure PAA and 121.0 mg of inclusion complexes (encapsulating approximately 11.5 mg of PAA), respectively. After solidifying, all the PDAs including the control ones (without additives)

were inoculated by agar plugs (6 mm in diameter) with mycelia which were cut from the edge of the fungal colony of the pre-prepared cultured PDAs. Then the inoculated media were incubated at 25 °C for up to 6 days for observation. Both of the morphological images and diameters of the fungal colony were recorded daily by an automatic colony counts analyzer (DW-V, Xunshu, China).

2.3. Decay assessment

The *in vivo* antifungal activity of the inclusion complexes was evaluated by investigating the incidence and severity of the fungi-caused postharvest decay in fruit. For each treatment, 60 strawberries were randomly divided into 3 replicates. And the 20 fruit of each replicate were distribute to five 0.75-L sealed containers with 4 strawberries each. Semipermeable sachets (3 × 3 cm) containing 1.0 g of β -CD, 0.1 g of PAA and 1.0 g of inclusion complexes (encapsulated 0.1 g of PAA) were fixed in the center of the container for different treatments, respectively. No sachets were set in the control group. All the containers were placed at room temperature (25 °C) for the fungi incubation. During storage, both incidence and severity were evaluated daily until day 8. Severity was evaluated by a scale composed of five degrees (0 = absence of symptoms; 1 = 1–25% of injured area; 2 = 26–50%; 3 = 51–75% and 4 = 76–100%). The incidence and severity were calculated by equations (1) and (2), respectively (Zhang, Howell, Starr, & Wheeler, 1996):

$$\text{Incidence (\%)} = \frac{n_1 + n_2 + n_3 + n_4}{n} \times 100 \quad (1)$$

$$\text{Severity (\%)} = \frac{1n_1 + 2n_2 + 3n_3 + 4n_4}{4n} \times 100 \quad (2)$$

where n_1 – n_4 are numbers of fruit in categories 1 to 4 of the disease scale and n is the total number assessed in each replicate.

2.4. Quality evaluation

For the fruit quality assessment, a quantity of 384 strawberries was randomly divided into four groups, for different treatments (control, β -CD, PAA and inclusion complexes), respectively. For each treatment, the 96 fruit were arranged into twenty-four 0.75-L sealed containers with 4 each. The sachets containing corresponding fumigation agents (consistent with the above *in vivo* test) were fixed in the center of the container except control group. Twelve fruit without any decay were selected and analyzed for each treatment. The skin color was evaluated using a CR-10 plus colorimeter (Konica Minolta, Osaka, Japan) by measuring the L^* and a^* parameters in three zones around the equator of each fruit. The weight loss was determined by weighing each fruit daily during the storage and expressed as a percentage of weight lost compared to the initial weight. Firmness of these fruit was measured using a texture analyzer fitted with a 6-mm-diameter cylinder probe (Baosheng Technology, China). The fruit was pressed at the equatorial area with 1 N of trigger force and 6 mm of loading displacement. The pre-test, test, and post-test speeds of the probe were 10, 1, and 10 mm s^{-1} , respectively. The crushed fruit from the firmness test were used for TSS analysis. Every 4 fruit from each treatment were homogenized together as a new replicate. Then, the homogenates were centrifuged at 4000 g for 10 min, and the supernatant was collected and measured using a PAL-1 pocket refractometer (Atago, Japan) and expressed as percent.

2.5. Sensory analysis

The sensory analysis was developed following the standard ISO 11035:1994. Strawberries with different treatments for the test were stored at room temperature (25 °C) for up to 3 days. Ten fruit without any decay lesions from each treatment were picked out and cut into small pieces, and then scored by 10 random untrained sensory assessors

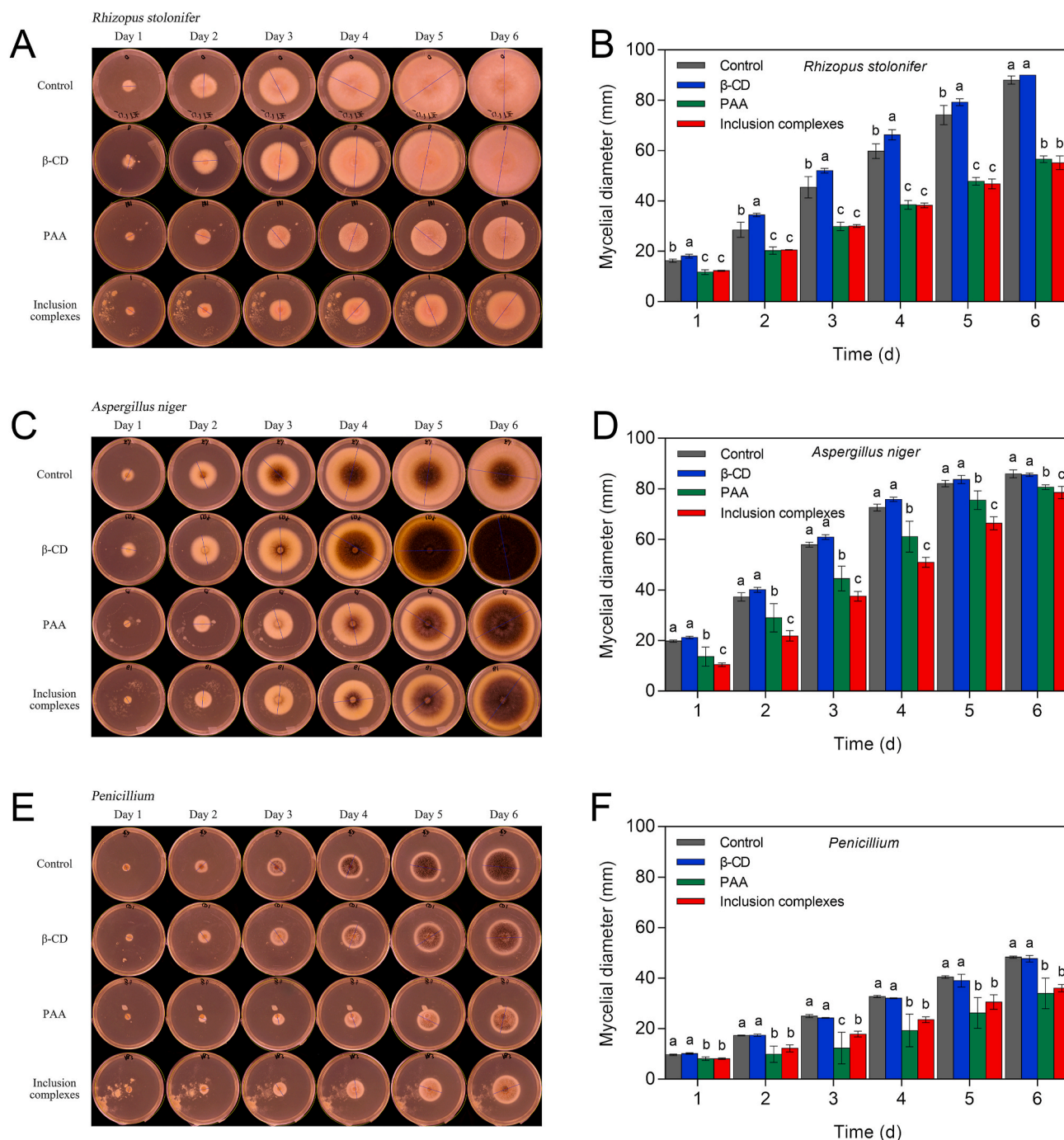


Fig. 1. Colony images (A) and diameters (B) of *Rhizopus stolonifer*, colony images (C) and diameters (D) of *Aspergillus niger*, and colony images (E) and diameters (F) of *Penicillium* on 90-mm PDA media over time at 25 °C. Different letters a-c above the columns indicate significant differences among the treatments for each time interval based on Duncan’s multiple range test ($p < 0.05$).

each day. A sensory quality scoring criteria was developed according to the reported method with modifications (Peralta-Ruiz et al., 2020), in which the acceptance of indexes including appearance, color, flavor and texture were rated on 10-point scales.

2.6. Statistical analysis

Data were analyzed using SPSS version 17.0 software (Experian QAS, Boston, MA) one-way analysis of variance (ANOVA). When significant differences ($p < 0.05$) were found, the treatment means were compared using Duncan’s multiple range test ($p < 0.05$).

3. Results

3.1. Colony morphology analysis

Both colony morphology images and diameters of *R. stolonifer*, *A. niger*, and *Penicillium* on PDA media during the 6-day storage were showed in Fig. 1. Generally, all the three fungi exhibited a gradually increase in colony diameter for all the treatments over time. However, for each time point, both PAA and inclusion complexes groups showed significantly lower diameters than those of control and β -CD groups in the three fungal colonies ($p < 0.05$). The colonies of *R. stolonifer* and

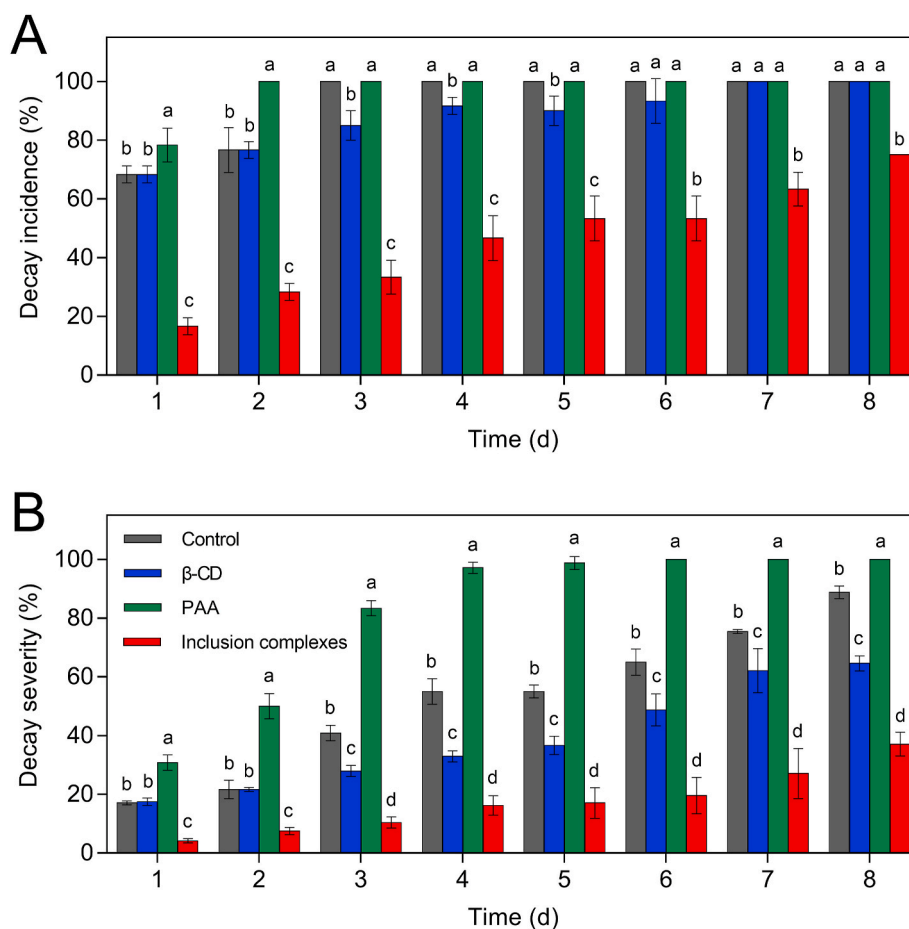


Fig. 2. Effects of different treatments on incidence (A) and severity (B) of the postharvest decay in fresh strawberry during storage at room temperature (25 °C). Different letters a-d above the columns indicate significant differences among the treatments based on Duncan’s multiple range test ($p < 0.05$).

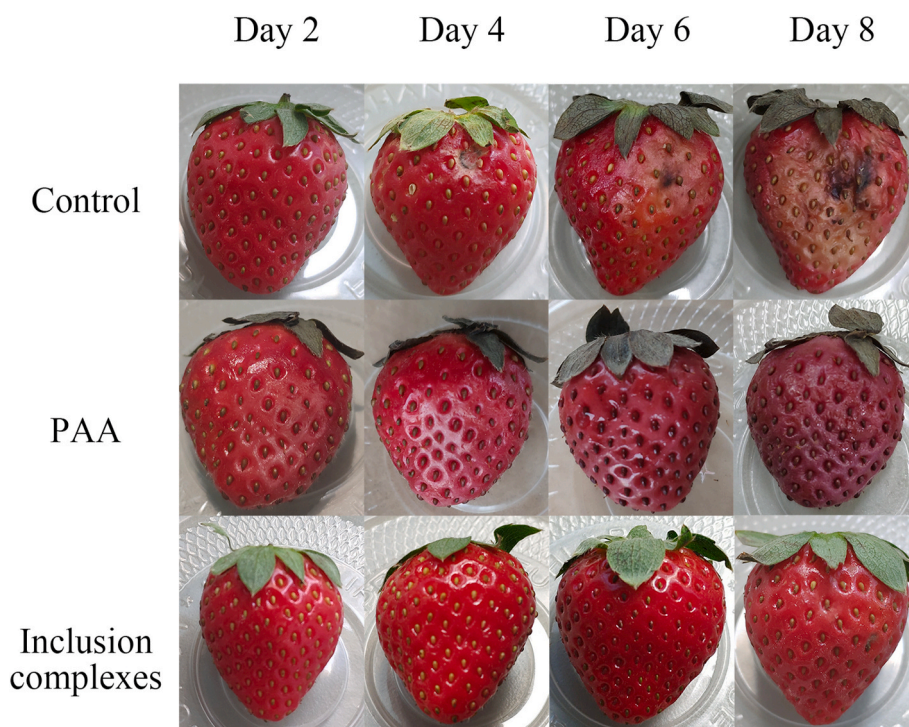


Fig. 3. Images of strawberry appearance at 25 °C over time.

Table 1

Effects of different treatments on color parameters (L^* and a^*) of strawberries after 8 days of storage at 25 °C.

Treatment	L^*	a^*
Initial	37.02 ± 2.73 ^a	38.92 ± 1.54 ^a
Control	36.60 ± 1.55 ^a	38.32 ± 1.45 ^{ab}
β-CD	35.48 ± 2.11 ^a	37.41 ± 2.31 ^b
PAA	31.40 ± 1.97 ^b	22.38 ± 1.08 ^c
Inclusion complexes	36.48 ± 2.95 ^a	37.54 ± 1.76 ^{ab}

Different superscript letters ^{a-c} within a column indicate significant differences among the treatments based on Duncan's multiple range test ($p < 0.05$).

Penicillium from PAA and inclusion complexes treated PDAs (Fig. 1A and B) showed no difference with each other in diameter ($p < 0.05$), only except the data of *Penicillium* at the third day. According to Fig. 1C and D, colony diameter of inclusion complexes group was lower than that of PAA group for each day ($p < 0.05$). An interesting phenomenon is that β-CD group exhibited even larger *R. stolonifer* colonies than control until the fifth day ($p < 0.05$).

3.2. Decay assessment

Both incidence (Fig. 2A) and severity (Fig. 2B) of the postharvest decay on fresh strawberry were investigated daily during the 8-day storage. The fruit treated with free PAA reached 100% in decay incidence by the second day and also showed the highest severity among the treatments throughout the storage period. In contrast, the fruit treated by inclusion complexes presented the lowest values in both incidence and severity at each interval. By the end of the storage (day 8), incidence of the inclusion complexes-treated group was 75%, while those of all other three groups reached to 100%. For severity, the inclusion complexes-treated group also presented the lowest value of 37.08%, while the severity for groups of control, β-CD and PAA were 88.75, 64.58 and 100%, respectively. As exhibited in Fig. 3, the PAA treated fruit showed obviously atrophy and browning in appearance during storage, and they were all classified as rotten fruit when investigation.

3.3. Fruit quality

The changes of fruit color during storage were evaluated by measuring lightness (L^*) and redness (a^*) and the results were shown in Table 1. Compared with the initial data, only PAA-treated fruit showed significant decrease in both L^* and a^* values after storage ($p < 0.05$). Although some changes were not statistically significant ($p > 0.05$), all the weight loss of the strawberries exhibited slightly uptrends during the storage over time (Fig. 4A). The data of PAA-treated fruit showed the largest variation among the treatments from day 5–8. For firmness, PAA-treated fruit demonstrated the lowest value in firmness after storage ($p < 0.05$). The other three treatments including inclusion complexes-treated fruit did not show significant changes in firmness comparing with the initial value. TSS of all treatments decreased after storage in this study (Fig. 4C). No difference was observed between the inclusion complexes-treated fruit and the control ones.

3.4. Sensory analysis

In order to evaluate the effects of the inclusion complexes on sensory quality, a sensory panel was carried out in which the acceptability was studied in terms of appearance, color, flavor and texture of the fruit. The results of the detail parameters for the first 3 days was shown in Fig. 5A. The inclusion complexes-treated fruit received scores for the four parameters not lower than those of control samples during the first two days, and also showed a general acceptability that was no worse than any other groups for each day (Fig. 5B). The only inadequate performance of the inclusion complexes group is its color score, which was slightly lower than that of control in the third day (Fig. 5A). However,

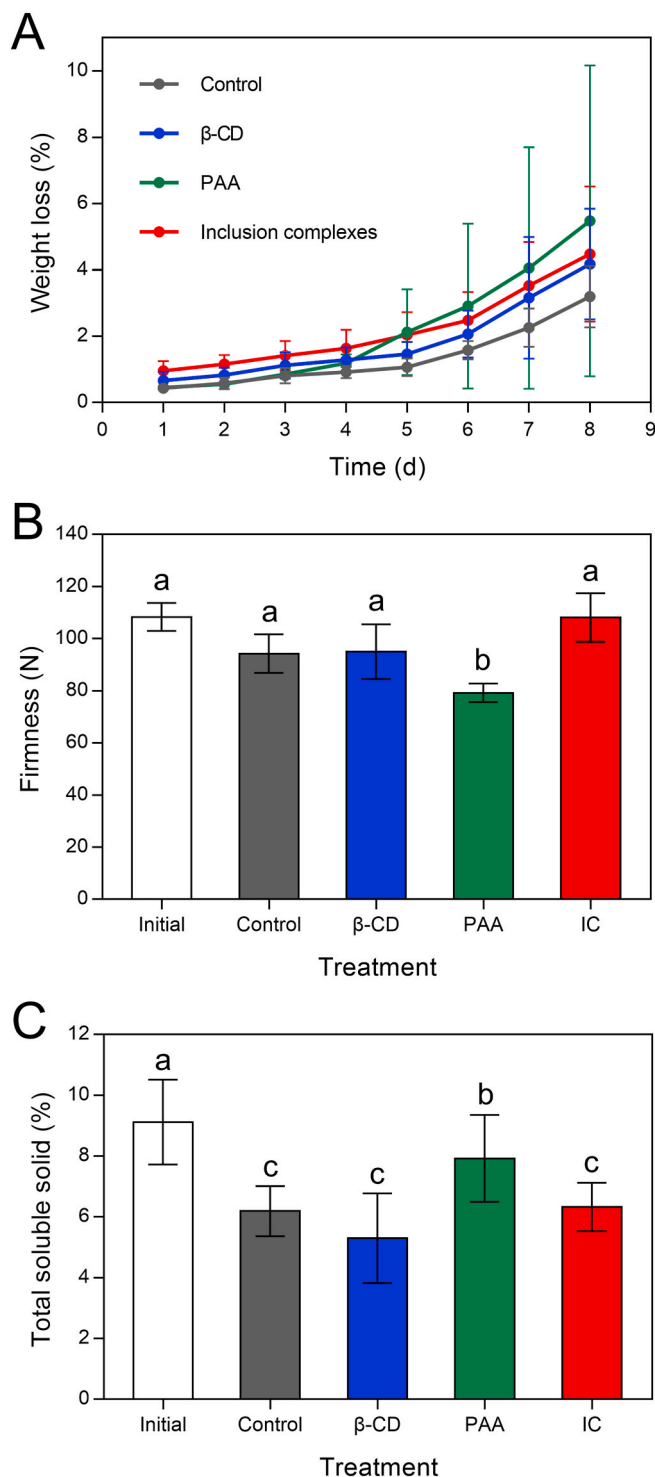


Fig. 4. Effects of different treatments on weight loss (A), firmness (B) and total soluble solid (C) of the strawberry after 8 days of storage at 25 °C. IC: inclusion complexes. Different letters a-c above the columns indicate significant differences among the treatments based on Duncan's multiple range test ($p < 0.05$).

the PAA-treated fruit received lower scores for flavor and texture at the second day, and for color, flavor and texture at the third day. For the general acceptability, PAA-treated group was the only one which got a significant lower score than the other three groups at day 2 and 3 (Fig. 5B).

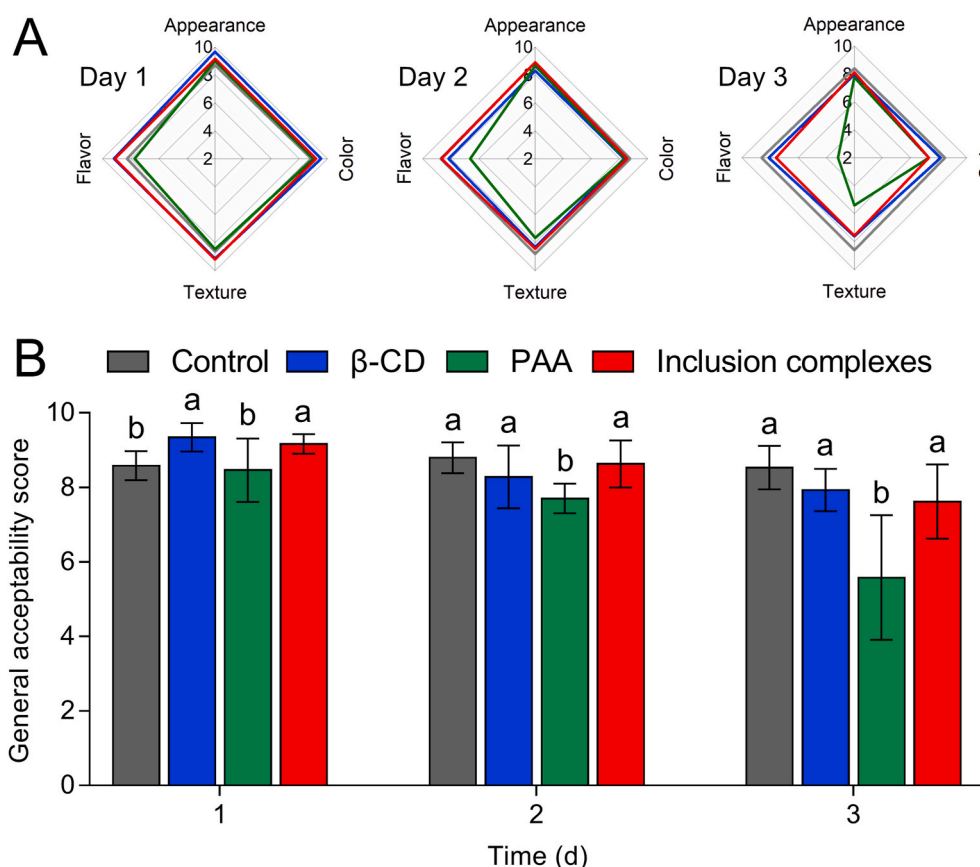


Fig. 5. Sensory characteristics scales (A) and general acceptability scores (B) of the strawberry for different treatments in the first three days. Different letters a and b above the columns indicate significant differences among the treatments based on Duncan's multiple range test ($p < 0.05$).

4. Discussion

It was reported that PAA exerts its antifungal effect by decreasing NADPH routed through up-regulation of putative aryl-alcohol dehydrogenases (Shreaz et al., 2011). In the current study, PAA demonstrated its efficient antifungal activity against *R. stolonifer*, *A. niger*, and *Penicillium* on PDA media in both free and encapsulated forms. The two forms of PAA presented almost the same activity on control the mycelial growth of *R. stolonifer* and *Penicillium* at most investigation time points, and the mycelia of *A. niger* treated by the inclusion form of PAA presented even smaller colony diameters than those of free PAA treated group, indicating a better *in vitro* antifungal activity of the EO's inclusion form than free form towards *A. niger*. Differing from pure PAA, the active compounds start to diffuse at a relatively low rate from its carrier material to reach the target microorganism, acting as a slow-release agent that maintains an effective inhibitory concentration over a long period of time. A similar research reported that the EO-loaded microcapsules demonstrated an initial quick release followed by a slow release in the *in vitro* release profiles, which effectively delayed the volatilization of EO and extended its antifungal activity (Li et al., 2018). Besides, the phenomenon that β -CD group exhibited larger *R. stolonifer* colonies than control for most days was probably due to that the fungal growth could benefit from the supplement of β -CD as a carbon source in PDA media (De Mot & Verachert, 1986).

For the consuming purpose, any abnormalities in appearance, flavor, or texture can be regarded as a loss of freshness. Thus, the fruit with atrophy and browning in PAA treated group were all classified as decayed when investigation. The pure essential oil extract was reported to have seriously burn effect on the fruit surface, due to its strong volatility and chemical activity. The initial burst of the compounds could induce a local accumulation of concentration, which caused the damage

in surface cells of fruit (Chen et al., 2020). The injury lesions provide a 'green channel' for the microorganism, insect pests or any other polluters, from which the pathogens could easily pass the barrier of fruit peel or surface and accelerate the decay development in the fruit tissue (Knoche, 2015). And the excessive concentration of the compounds in the initial stage could affect the acceptability of the food products in flavor, some researches has showed that the pungent odor of essential oils left on food could cause the disgust of consumers (Ayala-Zavala et al., 2008). In addition, due to the strong volatility and initial burst, the free PAA could not provide a long-term protection for the fruit, this may lead to a late-stage outbreak or flourish of decay during postharvest storage. In contrast, the good performance of inclusion complex *in vivo* tests confirmed the *in vitro* antifungal activity evaluated above. Additionally, its better stability and long-term releasing property indicated its great potential for the postharvest decay control as a sustained-release fumigation agent.

External color of the fresh fruit is one of the most important factors that might determine consumer acceptance of the product (Del-Valle, Hernández-Muñoz, Guarda, & Galotto, 2005; Yang, Wu, Ng, & Wang, 2017). The significant decrease in L^* and a^* of PAA-treated fruit reflected the loss of lightness and saturation of the surface color, respectively (Peretto et al., 2014), which was consistent with the visual appearance changes of strawberry in Fig. 3. Weight loss of fruit is mainly caused by water vapor transpiration (Valero et al., 2013; Zhang, Chen, Lai, Wang, & Yang, 2018). Water from the tissue of fruit runs off through the surface, especially through the openings including stomata, wound openings, blossom and stem scars (Knoche, 2015). According to the results of decay evaluation above, the fumigation using free PAA induced serious damage and decay in fruit, which might cause a higher water loss than the other treatments. Fruit softening is one of the main undesirable changes during storage. The water loss leads to the

reduction of turgor pressure, and finally results in loss of firmness (Saladié et al., 2007), which was confirmed by the firmness data (Fig. 4B) in this study. Another vital reason of softening at the biochemical level is the cell wall polysaccharide solubilisation and depolymerisation during the storage (Zhang, Zhao, Lai, Chen, & Yang, 2018). As one of the major cell wall polysaccharides, pectin plays an essential role in maintaining fruit texture. The side-chain conformation of the type I rhamnogalacturonan (RG-I) region of pectin also appears to be closely related to the firmness of fruit (Yang, 2014). The total soluble solid (TSS) content is an important quality index to examine fruit quality during postharvest storage. TSS is related to fruit ripening, and a higher amount of soluble solids can also contribute to the flavor of fruit, especially sweetness (Zhang et al., 2019). According to the previous research, TSS decreases gradually after harvest because the physiological activities (metabolisms and respiration) of fresh fruit are maintained basing on the consuming of sugars (Aday et al., 2013). Exactly, TSS also showed a consistent reduction after storage for all treatments in this study (Fig. 4C), and the treatment of inclusion complexes had no influence on the change of TSS of strawberries during storage.

When EO was directly applied on fruit, meat or vegetable, sensory characteristics and fungal infectivity of fresh product could be tremendously influenced by exposure of EO, which was resulted from the extremely low flavor threshold and the highly water insolubility of EO (Kalemba & Kunicka, 2003). According to the results of sensory panel, the free PAA treatment affected the fruit sensory indexes and general acceptability significantly, but the inclusion complexes did not show any flavor transfers or surface damage on fruit. That could be attributed to the sustained-release effect of the encapsulation, which avoided the excessive local accumulation by the initial burst of free PAA. Similar results were obtained in *Carica papaya* fruit, where fruit was treated with chitosan-*Ruta graveolens* L. essential oil (Peralta-Ruiz et al., 2020).

5. Conclusions

In this study, β -CD-based inclusion complexes encapsulating PAA were employed as a fumigation agent to control the postharvest decay in strawberry. The *in vitro* antifungal activity of inclusion complexes was proved by fungal colony analysis of *R. stolonifer*, *A. niger* and *Penicillium* on PDA media. *In vivo* test on the fresh strawberry also confirmed the efficient activity of inclusion complexes on postharvest decay control. The fumigation of inclusion complexes significantly depressed the decay incidence and severity to 75% and 37.08%, respectively. As a potential fumigation agent, the inclusion complexes also maintained the fruit quality parameters including color, firmness, and TSS, as well as the sensory indexes for acceptability during the storage, no significant differences were found between the inclusion complexes-treated and control fruit.

CRedit authorship contribution statement

Ying Lin: Data curation, Writing – original draft. **Ran Huang:** Funding acquisition. **Xiuxiu Sun:** Methodology. **Xi Yu:** Investigation. **Ying Xiao:** Conceptualization. **Ling Wang:** Investigation. **Wenzhong Hu:** Supervision. **Tian Zhong:** Conceptualization, Writing - review & editing, Supervision.

Declaration of competing interest

The authors declare that they have no known competing financial interests or personal relationships that could have appeared to influence the work reported in this paper.

Acknowledgements

This research was funded by Taizhou Municipal Science and Technology Program (Grant number: 2017CLS01).

References

- Aday, M. S., Buyukan, M. B., & Caner, C. (2013). Maintaining the quality of strawberries by combined effect of aqueous chlorine dioxide with modified atmosphere packaging. *Journal of Food Processing and Preservation*, 37(5), 568–581.
- Almenar, E., Del-Valle, V., Hernández-Muñoz, P., Lagarón, J. M., Catalá, R., & Gavara, R. (2007). Equilibrium modified atmosphere packaging of wild strawberries. *Journal of the Science of Food and Agriculture*, 87(10), 1931–1939.
- Ayala-Zavala, J. F., Del-Toro-Sánchez, L., Alvarez-Parrilla, E., & González-Aguilar, G. A. (2008). High relative humidity in-package of fresh-cut fruits and vegetables: Advantage or disadvantage considering microbiological problems and antimicrobial delivering systems? *Journal of Food Science*, 73(4), R41–R47.
- Barbieri, N., Sanchez-Contreras, A., Canto, A., Cauich-Rodríguez, J. V., Vargas-Coronado, R., & Calvo-Irabién, L. M. (2018). Effect of cyclodextrins and Mexican oregano (*Lippia graveolens* Kunth) chemotypes on the microencapsulation of essential oil. *Industrial Crops and Products*, 121, 114–123.
- Basu, A., Nguyen, A., Betts, N. M., & Lyons, T. J. (2014). Strawberry as a functional food: An evidence-based review. *Critical Reviews in Food Science and Nutrition*, 54(6), 790–806.
- Bautista-Baños, S., Garcia-Dominguez, E., Barrera-Necha, L. L., Reyes-Chilpa, R., & Wilson, C. L. (2003). Seasonal evaluation of the postharvest fungicidal activity of powders and extracts of huamuchil (*pithecellobium dulce*): Action against botrytis cinerea, *Penicillium digitatum* and *Rhizopus stolonifer* of strawberry fruit. *Postharvest Biology and Technology*, 29(1), 81–92.
- Bose, S. K., Howlader, P., Wang, W., & Yin, H. (2021). Oligosaccharide is a promising natural preservative for improving postharvest preservation of fruit: A review. *Food Chemistry*, 341, 128178.
- Caner, C., Aday, M. S., & Demir, M. (2008). Extending the quality of fresh strawberries by equilibrium modified atmosphere packaging. *European Food Research and Technology*, 227(6), 1575–1583.
- Cao, S., Hu, Z., & Pang, B. (2010). Optimization of postharvest ultrasonic treatment of strawberry fruit. *Postharvest Biology and Technology*, 55(3), 150–153.
- Chen, P., Ference, C., Sun, X., Lin, Y., Tan, L., & Zhong, T. (2020). Antimicrobial efficacy of liposome-encapsulated citral and its effect on the shelf life of shatangju Mandarin. *Journal of Food Protection*, 83(8), 1315–1322.
- Chen, G., & Liu, B. (2016). Cellulose sulfate based film with slow-release antimicrobial properties prepared by incorporation of mustard essential oil and β -cyclodextrin. *Food Hydrocolloids*, 55, 100–107.
- De Mot, R., & Verachert, H. (1986). Enhanced production of extracellular α -amylase and glucoamylase by amyolytic yeasts using β -cyclodextrin as carbon source. *Applied Microbiology and Biotechnology*, 24(6), 459–462.
- Del-Valle, V., Hernández-Muñoz, P., Guarda, A., & Galotto, M. J. (2005). Development of a cactus-mucilage edible coating (*Opuntia ficus indica*) and its application to extend strawberry (*Fragaria ananassa*) shelf-life. *Food Chemistry*, 91(4), 751–756.
- Food, U., & Administration, D. (1997). Substances generally recognized as safe, proposed rule. *Federal Register*, 62(74), 18937–18964.
- García-Sotelo, D., Silva-Espinoza, B., Perez-Tello, M., Olivas, I., Alvarez-Parrilla, E., González-Aguilar, G. A., et al. (2019). Antimicrobial activity and thermal stability of rosemary essential oil: β -cyclodextrin capsules applied in tomato juice. *Lebensmittel-Wissenschaft & Technologie*, 111, 837–845.
- Hashmi, M. S., East, A. R., Palmer, J. S., & Heyes, J. A. (2013). Hypobaric treatment stimulates defence-related enzymes in strawberry. *Postharvest Biology and Technology*, 85, 77–82.
- Jesmin, S., Jubayer, A.-A., Eusuf, S., Kamal, A. H. M., Islam, J. M. M., Ferdoush, F., et al. (2016). Gamma radiation treated chitosan solution for strawberry preservation: Physico-chemical properties and sensory evaluation. *International Letters of Natural Sciences*, 60, 30–37.
- Jiang, Y., Yu, L., Hu, Y., Zhu, Z., Zhuang, C., Zhao, Y., et al. (2019). Electrostatic spraying of chitosan coating with different deacetylation degree for strawberry preservation. *International Journal of Biological Macromolecules*, 139, 1232–1238.
- Kalemba, D., & Kunicka, A. (2003). Antibacterial and antifungal properties of essential oils. *Current Medicinal Chemistry*, 10(10), 813–829.
- Kallio, H., Hakala, M., Pelkkikangas, A. M., & Lapveteläinen, A. (2000). Sugars and acids of strawberry varieties. *European Food Research and Technology*, 212(1), 81–85.
- Knoche, M. (2015). Barriers, mechanism, factors, and potential role in cracking. In Y. Kanayama, & A. Kochetov (Eds.), *Water uptake through the surface of fleshy soft fruit Abiotic stress biology in horticultural plants* (pp. 147–166). Tokyo: Springer (Japan).
- Köse, M. D., Tekin, B. N., & Bayraktar, O. (2021). Simultaneous isolation and selective encapsulation of volatile compounds from essential oil during electrospraying of β -Cyclodextrin. *Carbohydrate Polymers*, 258, 117673.
- Li, N., Zhang, Z.-J., Li, X.-J., Li, H.-Z., Cui, L.-X., & He, D.-L. (2018). Microcapsules biologically prepared using *Perilla frutescens* (L.) Britt. essential oil and their use for extension of fruit shelf life. *Journal of the Science of Food and Agriculture*, 98(3), 1033–1041.
- Marques, H. M. C. (2010). A review on cyclodextrin encapsulation of essential oils and volatiles. *Flavour and Fragrance Journal*, 25(5), 313–326.
- Neri, F., Cappellin, L., Spadoni, A., Cameldi, I., Algarra Alarcon, A., Aprea, E., et al. (2015). Role of strawberry volatile organic compounds in the development of Botrytis cinerea infection. *Plant Pathology*, 64(3), 709–717.
- Okamoto, K., Narayama, S., Katsuo, A., Shigematsu, I., & Yanase, H. (2002). Biosynthesis of p-anisaldehyde by the white-rot basidiomycete *Pleurotus ostreatus*. *Journal of Bioscience and Bioengineering*, 93(2), 207–210.
- Palmer, M. G., Mansourpour, S., Blauer, K. A., & Holmes, G. J. (2019). First report of *Aspergillus tubingensis* causing strawberry fruit rot in California. *Plant Disease*, 103(11).

- Pan, X., Zhu, B., Zhu, H., Chen, Y., Tian, H., Luo, Y., et al. (2014). iTRAQ protein profile Analysis of tomato green-ripe mutant reveals new aspects critical for fruit ripening. *Journal of Proteome Research*, 13(4), 1979–1993.
- Peralta-Ruiz, Y., Grande Tovar, C., Sinning-Mangonez, A., Bermont, D., Pérez Cordero, A., Paparella, A., et al. (2020). Colletotrichum gloesporioides inhibition using chitosan-Ruta graveolens L essential oil coatings: Studies in vitro and in situ on Carica papaya fruit. *International Journal of Food Microbiology*, 326, 108649.
- Peretto, G., Du, W.-X., Avena-Bustillos, R. J., Sarreal, S. B. L., Hua, S. S. T., Sambo, P., et al. (2014). Increasing strawberry shelf-life with carvacrol and methyl cinnamate antimicrobial vapors released from edible films. *Postharvest Biology and Technology*, 89, 11–18.
- Picón, A., Martínez-Jávega, J. M., Cuquerella, J., Del Río, M. A., & Navarro, P. (1993). Effects of precooling, packaging film, modified atmosphere and ethylene absorber on the quality of refrigerated Chandler and Douglas strawberries. *Food Chemistry*, 48(2), 189–193.
- Reddy, B. V. M., Angers, P., Gosselin, A., & Arul, J. (1998). Characterization and use of essential oil from Thymus vulgaris against Botrytis cinerea and Rhizopus stolonifer in strawberry fruits. *Phytochemistry*, 47(8), 1515–1520.
- Saladié, M., Matas, A. J., Isaacson, T., Jenks, M. A., Goodwin, S. M., Niklas, K. J., et al. (2007). A reevaluation of the key factors that influence tomato fruit softening and integrity. *Plant Physiology*, 144(2), 1012–1028.
- Shi, C., Zhao, X., Meng, R., Liu, Z., Zhang, G., & Guo, N. (2017). Synergistic antimicrobial effects of nisin and p-Anisaldehyde on Staphylococcus aureus in pasteurized milk. *Lebensmittel-Wissenschaft & Technologie*, 84, 222–230.
- Shreaz, S., Bhatia, R., Khan, N., Muralidhar, S., Basir, S. F., Manzoor, N., et al. (2011). Exposure of Candida to p-anisaldehyde inhibits its growth and ergosterol biosynthesis. *Journal of General and Applied Microbiology*, 57(3), 129–136.
- Siva, S., Li, C., Cui, H., Meenatchi, V., & Lin, L. (2020). Encapsulation of essential oil components with methyl- β -cyclodextrin using ultrasonication: Solubility, characterization, DPPH and antibacterial assay. *Ultrasonics Sonochemistry*, 64, 104997.
- Sousa-Gallagher, M. J., Mahajan, P. V., & Mezdad, T. (2013). Engineering packaging design accounting for transpiration rate: Model development and validation with strawberries. *Journal of Food Engineering*, 119(2), 370–376.
- Suvarna, V., Gujar, P., & Murahari, M. (2017). Complexation of phytochemicals with cyclodextrin derivatives – an insight. *Biomedicine & Pharmacotherapy*, 88, 1122–1144.
- Tulipani, S., Marzban, G., Herndl, A., Laimer, M., Mezzetti, B., & Battino, M. (2011). Influence of environmental and genetic factors on health-related compounds in strawberry. *Food Chemistry*, 124(3), 906–913.
- Valero, D., Díaz-Mula, H. M., Zapata, P. J., Guillén, F., Martínez-Romero, D., Castillo, S., et al. (2013). Effects of alginate edible coating on preserving fruit quality in four plum cultivars during postharvest storage. *Postharvest Biology and Technology*, 77, 1–6.
- Vanti, G. L., Leshem, Y., & Masaphy, S. (2021). Resistance response enhancement and reduction of Botrytis cinerea infection in strawberry fruit by Morchella conica mycelial extract. *Postharvest Biology and Technology*, 175, 111470.
- Wang, F., Wei, F., Song, C., Jiang, B., Tian, S., Yi, J., et al. (2017). Dodartia orientalis L. essential oil exerts antibacterial activity by mechanisms of disrupting cell structure and resisting biofilm. *Industrial Crops and Products*, 109, 358–366.
- Yang, H. (2014). *Atomic force microscopy (AFM): Principles, modes of operation and limitations: Nova Science Publishers* (Incorporated).
- Yang, H., Wu, Q., Ng, L. Y., & Wang, S. (2017). Effects of vacuum impregnation with calcium lactate and pectin methylesterase on quality attributes and chelate-soluble pectin morphology of fresh-cut papayas. *Food and Bioprocess Technology*, 10(5), 901–913.
- Yin, H., Wang, C., Yue, J., Deng, Y., Jiao, S., Zhao, Y., et al. (2021). Optimization and characterization of 1,8-cineole/hydroxypropyl- β -cyclodextrin inclusion complex and study of its release kinetics. *Food Hydrocolloids*, 110, 106159.
- Zhang, L., Chen, F., Lai, S., Wang, H., & Yang, H. (2018). Impact of soybean protein isolate-chitosan edible coating on the softening of apricot fruit during storage. *Lebensmittel-Wissenschaft & Technologie*, 96, 604–611.
- Zhang, J., Howell, C., Starr, J., & Wheeler, M. (1996). Frequency of isolation and the pathogenicity of Fusarium species associated with roots of healthy cotton seedlings. *Mycological Research*, 100(6), 747–752.
- Zhang, J., Kou, J., Ozbudak, E., Zhong, T., Pan, T., Bai, J., et al. (2020). First report of Gilbertella persicaria causing postharvest soft rot of strawberry fruit in Florida. *Plant Disease*, 104(10), 2736.
- Zhang, L., Wang, P., Chen, F., Lai, S., Yu, H., & Yang, H. (2019). Effects of calcium and pectin methylesterase on quality attributes and pectin morphology of jujube fruit under vacuum impregnation during storage. *Food Chemistry*, 289, 40–48.

SPECIAL GUEST EDITOR SECTION

Dynamic Analysis of Nucleosides and Carbohydrates during Developmental Stages of *Cordyceps militaris* in Silkworm (*Bombyxmori*)

LAN-YING WANG

University of Macau, Institute of Chinese Medical Sciences, State Key Laboratory of Quality Research in Chinese Medicine, Macau, China; University of Jilin, College of Zhuhai, Department of Chemistry and Pharmacy, Zhuhai 519000, China

XIAO LIANG

Bino Beijing Limited, Beijing, China

JING ZHAO¹, YING WANG, and SHAO-PING LI

University of Macau, Institute of Chinese Medical Sciences, State Key Laboratory of Quality Research in Chinese Medicine, Macau, China

Background: Cultured *Cordyceps militaris* is very popular. **Objective:** To gain dynamic insight into activity markers in fruiting body of *Cordyceps militaris* (*C. militaris*) in *Bombyxmori* (*B. mori*), also named silkworm. **Methods:** The development stages of samples at 3, 9, 12, 19, 27, and 33 days after inoculation (DAI) were collected. HPLC coupled with diode array detection and evaporative light-scattering detection method (HPLC–DAD–ELSD) was used to determine eight makers, including six nucleosides and two carbohydrates from the samples. **Results:** *C. militaris* cultured 33 DAI with fifth star silkworm larva could accumulate higher levels of cordycepin (13.43 mg/g) than the highest reported cordycepin (8.57 g/L). The contents of cordycepin, adenosine, and trehalose were gradually increased with the formation of *C. militaris* fruiting bodies on silkworm larva, while mannitol was decreased. The change of guanosine was similar to uracil. **Conclusions:** Results suggested that mannitol could be accumulated in a short period during mycelium growth and could metabolize and transform into energy store and trehalose during fruit body formation. The inosine in the insect was completely utilized and transformed. The synergistic formation of cordycepin and adenosine or differences in metabolized pathways are a great possibility according to the same trend. **Highlights:** This research offered some reference to further find a certain regularity or metabolic mechanism.

of insects (family: Hepialidae). For centuries, the combination of dead insect and fungus has been used as famous traditional Chinese medicine. It is very difficult to realize large-scale cultivation of natural *C. sinensis* stromata. However, cultured *C. militaris* has made significant progress. It infects and grows on a wide range of insects, mainly lepidopteron larva and pupa such as *Bombyxpthyocampa*, *Bombyx. caja*, *Bombyxrubi*, or others (1). The survey records show that *C. militaris* or its extraction have a broad range of applications, such as anti-inflammatory, antioxidant (2), antiageing, anticancer, antitumor, antileukemic, antimetastatic, immunomodulatory, antibacterial, antiviral, antifungal, antiprotozoal, antifibrotic, steroidogenic, hypoglycaemic, hypolipidaemic, antiangiogenetic, antidiabetic, anti-HIV, antimalarial, antifatigue, neuroprotective, insecticidal, larvicidal, liver-protective, reno-protective, prosexual, and pneumo-protective properties (3).

Many techniques, including storage or stock culture, preculture, solid culture in substrate (husked rice, saw dusk), and liquid culture (shaking, submerged, surface liquid, and continuous/repeated batch culture) have been developed (3). The stromata of *C. militaris* can be easily cultivated in different substrates. Therefore, *C. militaris* is considered a model organism with which study cultured *Cordyceps* species (4). Some laboratories have carried out a lot of work, including genome-wide transcriptome and proteome analysis on artificially cultivated *C. militaris* (5). In a previous report, *C. militaris* was found to be sexually heterothallic, as fruiting can occur without an opposite mating-type partner. It was believed that fruiting involves induction of the Zn2Cys 6-type transcription factors, and MAPK pathway and the PKA pathway are not activated according the transcriptional profiling (6). During asexual and sexual development, genes involved in cell or energy metabolism and stress responses, as well as those associated with cell wall structures, were upregulated (7).

At the same time, it is very important ensure the safety and efficacy of *Cordyceps* and its products. Presently, multiple markers such as nucleosides (8), ergosterol, mannitol, and polysaccharides are being used for their quality control (9). The markers and analytical methods for quality control of *Cordyceps* have been discussed and reviewed (9, 10). Many works on the qualitative and quantitative determination of nucleosides and their bases in *Cordyceps* have been reported. Several methods including capillary electrophoresis (11–14),

Cordyceps is a composite consisting of the stromata of the fungus, *Cordyceps sinensis* (Berk.) Sacc. (family: Hypocreaceae), parasitized on the larva of some species

Guest edited as a special report on “Facing the Challenge for Quality Control of Chinese Medicines” by Jing Zhao, Shuangcheng Ma, and Shaoping Li

This research was supported by grants from the Science and Technology Development Fund of Macao (059/2011/A3) and the University of Macau (MYRG140 and MYRG2014-00041) to Shao-Ping Li.

¹Corresponding author’s e-mail: zhaojing.cpu@163.com

DOI: <https://doi.org/10.5740/jaoacint.18-0309>

capillary electrochromatography (15), HPLC with diode array detection (DAD; 16–21), UPLC (22), and GC–MS (23, 24), have been used for nucleosides analysis. Each technique has its specific characteristics. HPLC is a commonly used technique for separation and analysis of nucleosides in *Cordyceps*. Evaporative light-scattering detector (ELSD) response does not depend on the optical characteristics of the analytes, which eliminates the problems associated with refractive index detector. ELSD can be easily connected in series with DAD for simultaneous determination of different types of compounds. According to our published work, the HPLC–DAD–ELSD method has been successfully applied to simultaneously quantify 12 components, including carbohydrate, myriocin, nucleosides, and nucleobases, in different natural and cultured *Cordyceps* (20).

In the present study, the HPLC–DAD–ELSD method was used for further qualitative and quantitative analyses of markers of *C. militaris*. It would be more precise and accurate to simultaneously analyze the development stages of samples of cultured *C. militaris*. Their contents in different stages of samples of *C. militaris* were compared, which had not been reported before. Through this research, a reliable rule to illustrate the complicated metabolic relationship between *C. militaris* and the host silkworm could be found.

Materials and Methods

Chemicals and Reagents

Bacto Yeast Extract was purchased from Becton, Dickinson and Co. (Franklin Lakes, NJ), and KH_2PO_4 (AR grade) and $\text{MgSO}_4 \cdot 7\text{H}_2\text{O}$ (AR grade) were purchased from Tianjin Damao Chemical Factory, China. Uracil, cordycepin, adenosine, uridine, inosine, guanosine, and D-(1)-trehalose hydrate were purchased from Sigma (St. Louis, MO), and D-mannitol was purchased from MBCHEM (Shanghai, China). ACN for HPLC analysis was purchased from Merck (Darmstadt, Germany). Deionized water was prepared using a Millipore Milli-Q Plus system (Millipore, Bedford, MA). Reagents not mentioned here were from standard sources.

Microorganism

C. militaris strain was provided by Shaoping Li (University of Macau, Macao, China). The stock was stored in a potato dextrose agar tube slant at 4°C. The fungal strains were transferred to the plate incubated at 25°C for 7 days. Then, for spawn production, the potato glucose medium consisted of 200 g potato supernatant, 20 g glucose, 4.5 g yeast extract, 5 g KH_2PO_4 , 2.5 g NH_4NO_3 , 2.5 g $\text{MgSO}_4 \cdot 7\text{H}_2\text{O}$, and 0.1 g CaCl_2 per liter solution. The seed culture medium was poured into 500 mL flasks and autoclaved at 121°C for 30 min. After cooling, each flask was inoculated with the mycelia discs (5 mm) of *C. militaris* on the plate and incubated at 25°C on a rotary shaker (150 rpm) for 5 days.

Cultured Fruit Body of *C. militaris* on Rice Medium

Rice medium was composed of 35 mL potato glucose liquid medium and 30 g rice mixed with 3 g silkworm pupae powder (per 300 mL bottle). The rice medium was sterilization

at 121°C for 1 h. After cooling, each bottle was inoculated with 6 mL liquid seed. The conditions of mycelium growth stage were 25°C in darkness. Then, the development of stromata was controlled at a lower temperature of 20°C in 12 h darkness and at a higher temperature of 25°C in 12 h light of 1000 lx. The mature fruit body was incubated for up to 60 days.

Fruit Body Formation on Silkworm

The fifth instar larvae of silkworm *B. mori* were purchased from Sericulture & Agri-Food Research Institute GAAS (Guangdong, China) and continued rearing with natural mulberry leaves. After 2 days, the fifth instar silkworm larvae were injected inoculation using 100 μL homogenized hyphal bodies and spawn of *C. militaris* (25). They were injected into each haemocoel of the head in the larvae of the silkworm. The injection volumes of a hyphal suspension contained 2×10^5 CFU. After infection, silkworm larvae were reared on mulberry leaves at 22–25°C and 40–90% humidity. As shown in Figure 1B, the developmental stages of the samples of *C. militaris* were collected for dynamic analysis. For description of the samples, refer to Table 1.

Sample Preparation

Sample preparation was performed using pressurized liquid extraction, which was done using a Dionex ASE 200 system (Dionex, Sunnyvale, CA) as reported before (20). In brief, powder of *C. militaris* developmental stages (0.2 g) was mixed with diatomaceous earth in a proportion 1:1 and placed into an 11 mL stainless steel extraction cell. The extraction was performed under optimized conditions. The extract was concentrated in a 50°C water bath using a rotary evaporator (BUCHI, Switzerland), then transferred into a 10 mL volumetric flask and diluted to the mark with 95% methanol. The extract should be diluted to an appropriate concentration when the analytics are beyond the

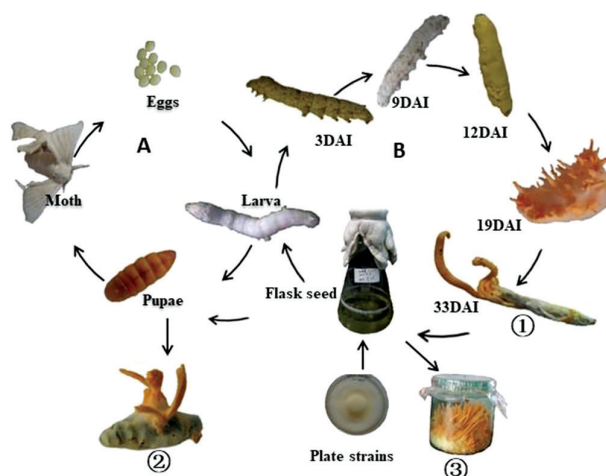


Figure 1. Model showing (A) the life cycle of silkworm and (B) the growth stages of *C. militaris* fruiting body. ①=Growth on silkworm larva of *C. militaris*. ②=Growth on silkworm pupa of *C. militaris*. ③=Growth on rice of *C. militaris*. DAI, days after inoculation.

Table 1. Contents of eight investigated compounds in cultured *C. militaris* extracted by pressurized liquid extraction

Sample ^a	Contents, mg/g							
	Uracil	Cordycepin	Uridine	Adenosine	Inosine	Guanosine	Mannitol	Trehalose
L5	0.027 ^b ± 0.0019	— ^c	0.337 ± 0.0295	0.876 ± 0.0145	0.186 ± 0.0224	0.269 ± 0.0326	0.891 ± 0.0833	17.332 ± 0.7839
3L	0.023 ± 0.0027	—	0.258 ± 0.0097	0.672 ± 0.0405	0.035 ± 0.0071	0.253 ± 0.0184	1.299 ± 0.0841	10.688 ± 0.5676
3D	0.034 ± 0.0029	—	0.503 ± 0.0260	1.372 ± 0.1424	—	0.328 ± 0.0213	0.904 ± 0.0302	11.14 ± 0.7823
PP	0.018 ± 0.0014	—	0.198 ± 0.0232	0.475 ± 0.0067	0.018 ± 0.0036	0.151 ± 0.0037	—	14.76 ± 0.6279
9W	0.015 ± 0.0014	4.853 ± 0.3400	0.166 ± 0.0151	1.045 ± 0.1477	—	0.060 ± 0.0085	10.130 ± 1.6411	4.11 ± 0.0812
12Y	0.016 ± 0.0012	6.962 ± 0.4041	0.209 ± 0.0202	2.519 ± 0.1449	—	0.082 ± 0.0024	8.900 ± 0.3082	9.47 ± 0.2483
19d	0.024 ± 0.0019	8.980 ± 0.4398	0.182 ± 0.0105	2.980 ± 0.1987	—	0.114 ± 0.0298	7.633 ± 0.0901	24.90 ± 2.5734
27d	0.019 ± 0.0014	10.014 ± 0.2743	0.162 ± 0.0029	2.990 ± 0.2612	—	0.104 ± 0.0092	9.161 ± 0.1738	18.95 ± 0.3921
33d	0.015 ± 0.0026	13.434 ± 0.8501	0.248 ± 0.0051	4.292 ± 0.1337	—	0.075 ± 0.0137	6.659 ± 0.3780	48.57 ± 0.7457
FB-S	0.03 ± 0.0029	4.260 ± 0.1316	0.662 ± 0.0340	0.558 ± 0.0345	—	0.275 ± 0.0174	7.15 ± 0.1288	165.85 ± 3.9197
SFM	0.046 ± 0.0114	1.829 ± 0.0297	0.394 ± 0.0128	0.390 ± 0.0171	—	0.213 ± 0.0288	102.854 ± 1.2191	32.96 ± 1.3649
FB-R	0.161 ± 0.0151	4.838 ± 0.0852	1.527 ± 0.0600	0.753 ± 0.0606	—	0.784 ± 0.0219	56.595 ± 21.1322	593.36 ± 12.2279
RS	0.03 ± 0.0027	2.510 ± 0.1137	0.21 ± 0.0223	0.086 ± 0.0093	—	0.093 ± 0.0139	12.91 ± 0.6028	28.91 ± 0.9198

^a L5, fifth instar silkworm larvae (normal); 3L, live silkworm 3 days after inoculation (DAI); 3D, dead silkworm 3 DAI (soft); 9W, prepupae (normal); PP, prepupae (stiff/white); 12Y, dead silkworm 12 DAI (stiff/yellow); 19d, fruiting body primordial of *C. militaris* 19 DAI; 27d, fruiting body in silkworm (length 1 cm) 27 DAI; 33d, fruiting body in silkworm (length 2 cm) 33 DAI; FB-S, fruiting body (cultured in silkworm); SFM, submerged fermented mycelium; FB-R, fruiting body (cultured on rice); RS, rice substrate (after cultured).

^b Average of three replicates.

^c — = Undetected.

linear ranges. After filtering through a 0.45 mm Econofilter (Agilent Technologies, Palo Alto, CA), 10 mL solution was injected into the HPLC system.

HPLC–DAD–ELSD Analysis

According to our published analysis, the HPLC–DAD–ELSD method was successfully applied to quantify eight components. All separations were performed on an Agilent Series 1100 liquid chromatography system, equipped with a vacuum degasser, a quaternary pump, an autosampler, a DAD, and an ELSD 2000ES (Alltech, Nicholasville, KY). A Prevail Carbohydrate ES column (250 mm × 4.6 mm id, 5 mm, Grace) was operated at 25°C. Solvents that constituted the mobile phase were ACN (A) and 5 mM ammonium acetate–0.1% acetic acid aqueous solution (B). The separation was achieved using gradient elution of 0–8 min, 5–10% B; 8–20 min, 10–12% B; 20–28 min, 12–20% B; 28–30 min, 20–25% B; 30–40 min, 25% B; 40–45 min, 25–50% B; and 45–50 min, 50% B. Then, 50% B was kept for 10 min to clean the column, and, finally, the reconditioning step of the column was 95% B isocratic for 35 min. The flow rate was 1 mL/min. The analysts for nucleosides were monitored at 254 nm, and ELSD was used for detection of mannitol and trehalose. The impact or position of ELSD was set off. The other parameters including mobilizing gas flow rate and drift tube temperature were optimized based on the S/N (20).

Data Processing and Multivariate Data Analysis

A data matrix was obtained containing retention times, accurate masses, and normalized peak intensities. The test was performed in triplicate. The resulting data were exported to Excel (Microsoft Office 2007). Hierarchical clustering analysis (HCA) was performed by SPSS 19.0 for windows (IBM, Armonk, NY). A method called the average linkage between groups was applied, and cosine distance was selected as measurement.

Biomarker Identification

Major metabolites were positively identified using standard compounds by comparing both the mass spectra and retention time.

Results and Discussion

Comparison of Nucleosides and Carbohydrates from *C. militaris* Cultured with Different Media or Substrates

Nucleosides and carbohydrates were extracted from fruiting bodies, mycelium or substrate of *C. militaris* cultured with silkworm larva, solid rice medium, and liquid medium. The developed HPLC–DAD–ELSD method was subsequently applied for simultaneous determination of six nucleosides (uracil, cordycepin, uridine, adenosine, inosine, guanosine) and two carbohydrates (mannitol and trehalose) in 13 samples of *C. militaris*. The typical chromatograms of the mixed standards (A) and 33 days after inoculation (DAI) *C. militaris* with dead silkworm larva are shown in Figure 2. According to the retention times, accurate mass numbers and normalized peak intensities of different chromatograms and the contents

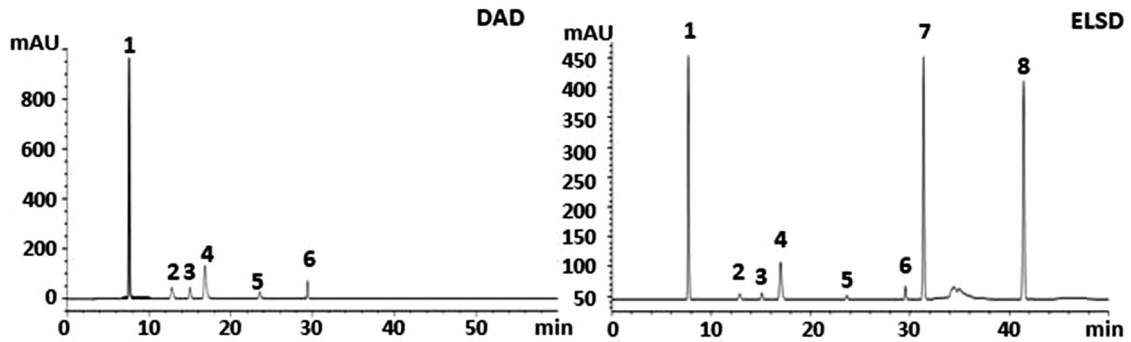
of the investigated compounds in *C. militaris* are summarized in Table 1. The results illustrated that their contents in different medium were greatly variant and suggested that these bioactive markers could be accumulated in a different culture medium.

Trehalose was the main solute in ascospores bioactive polysaccharides from this fungus. These carbohydrates were utilized by the fungus for adenosine triphosphate generation and amino acid biosynthesis, but they were also converted to storage compounds (e.g., glycogen, trehalose, and sugar alcohols) for the maintenance of a strong carbon sink (26). While the largest content of mycelium in liquid medium (submerged fermented mycelium; SFM) was mannitol (102.85 mg/g), trehalose had the highest contents compared with other tested compounds. The trehalose (165.85 mg/g) from *C. militaris* cultured fruiting body on silkworm were higher than the combination of *C. militaris* infected dead insect cultured 12 DAI on silkworm (12Y; 9.47 mg/g). Fruiting body in rice substrate (593.36 mg/g) was also higher than rice substrate (56.59 mg/g). In addition, the mannitol content of mycelium (SFM, 102.85 mg/g) was three-times that of trehalose (32.96 mg/g). It was very easy to find that the mannitol could be accumulated in the mycelium stage, whereas the trehalose was abundant in fruiting body stage. The result was consistent with that reported in the literature. It suggested that mannitol metabolism is enhanced in mycelia, and trehalose is upregulated in fruiting bodies of *Tuber melanosporum* (26).

Cordycepin was one of most important active ingredients of *C. militaris*. It exhibited significant therapeutic potential (27). The U.S. Food and Drug Administration granted orphan drug designation to cordycepin for the treatment of acute lymphocytic leukemia in patients who express the enzyme terminal deoxynucleotidyl transferase. Cordycepin as a nucleoside analog has known efficacy against viral infection. It was first a clinical stage development compound. Table 1 shows cordycepin content was more than other determined nucleosides. The contents of cordycepin (6.96 mg/g) and adenosine (2.52 mg/g) in 12 DAI infected fifth instar dead silkworms (12Y) were significantly higher than fruiting body cultured on silkworm. Cordycepin was similar with fruiting body in rice substrate (4.84 mg/g) and in silkworm larva (4.26 mg/g). However, cordycepin in rice substrate was less than fruit body cultured in rice substrate. It was easy to find the cordycepin in fruiting body, and solid substrates were more abundant than in mycelium from the liquid medium. In addition, it could be accumulated in a different substrate in the present study.

Adenosine was the bioactive ingredient and chief chemical marker of *C. militaris* that modulates many physiological processes. In the present study, the content of adenosine was approximately 0.09 to 4.29 mg/g. Adenosine in 12 DAI silkworms infected by *C. militaris* (12Y) was higher than other cultivation materials. Guanosine was determined to be in the range of approximately 0.028 to 0.780 mg/g. Uridine was approximately 0.209 to 1.530 mg/g, and uracil was approximately 0.016 to 0.160 mg/g. Guanosine, uridine, and uracil were highest in fruit body cultured in rice medium. The content of inosine was too low to be determined in *C. militaris* from different culture mediums, which is in accordance with the reported result (0.017 mg/g cultured *C. militaris*; 28).

A Mixed standards



B 33DAI FB+Silkworm

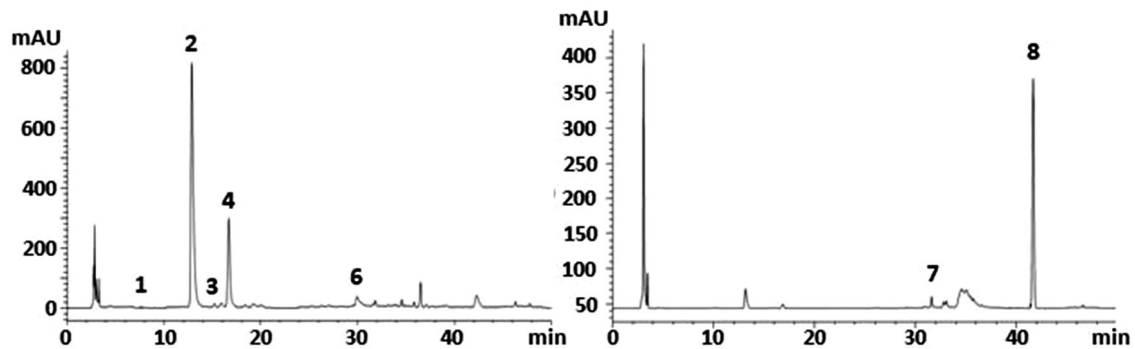


Figure 2. Typical HPLC–DAD–ELSD chromatograms of (A) the mixed standards and (B) 33 DAI *C. militaris* with dead silkworm larva. (1) Uracil, (2) cordycepin, (3) uridine, (4) adenosine, (5) inosine, (6) guanosine, (7) mannitol, (8) and trehalose. 3L, live silkworm 3 DAI; 3D, dead silkworm 3 DAI (soft); 33DAI FB+Silkworm, fruiting body in silkworm (length 2 cm) in 33 days after inoculation.

Dynamic Analysis of Nucleosides and Carbohydrates During Developmental Stages of *C. militaris* on Silkworm Larva

The variances of artificial *C. militaris* growth on silkworm larva and yield parameters were analyzed, and the results are summarized in Figure 3. Cordycepin, adenosine, trehalose, and mannitol were clearly increased during fruiting body growth of cultured *C. militaris* compared with both control groups. The content of cordycepin (Figure 3A) and adenosine (Figure 3C) from combination dead silkworm and fungus were significantly higher than fruiting body separation from *C. militaris* cultured on silkworm. However, guanosine (Figure 3B), uracil (Figure 3E), uridine (Figure 3F), and trehalose (Figure 3H) from a combination of dead silkworm and fungus were clearly lower than fruiting body. The cordycepin increased gradually with the growth of *C. militaris* from mycelium accumulation and fruiting body development, shown in Figure 3A. It was easy to discover that cordycepin could be enriched in silkworm because the mycelium infected it. There was a large difference between the content of the combination and fruiting body separated from it. The largest content of cordycepin 13.43 mg/g in *C. militaris* cultured with 33 days on silkworm was higher than the highest reported cordycepin content 8.57 g/L (29).

Figure 3C shows that the trends of adenosine were similar with cordycepin. Moreover, adenosine in health fifth instar larvae of silkworm was higher than prepupae (PP), but it was lower than the infected silkworm. Therefore, the results showed that cordycepin and adenosine could be accumulated in silkworm during the extended time of cultivation.

Figure 3D shows the inosine determined only in the uninfected silkworm (fifth instar silkworm, PP) and live silkworms (3 DAI). The content of inosine from fifth instar larvae of silkworm was the highest (0.19 mg/g). However, in dead silkworm infected by *C. militaris*, inosine was also not found or determined. The level of trehalose of PP declined from fifth instar larvae shown in Figure 3. The result that it played a role as the energy source was in accordance with the reference. All these stages accumulated the disaccharide trehalose. The levels of trehalose depended on the stage of growth and nutritional stage. Fruiting body was determined to accumulate much larger amounts of trehalose. In previous studies, during fruiting body formation, the importance of carbon metabolism in this complex morphogenesis had been suggested. Studies had been reported that some enzymes of amino acid and isoprenoid biosynthesis, the glyoxylate cycle, carbon and nitrogen metabolism, mitochondrial division, and cell wall synthesis were upregulated.

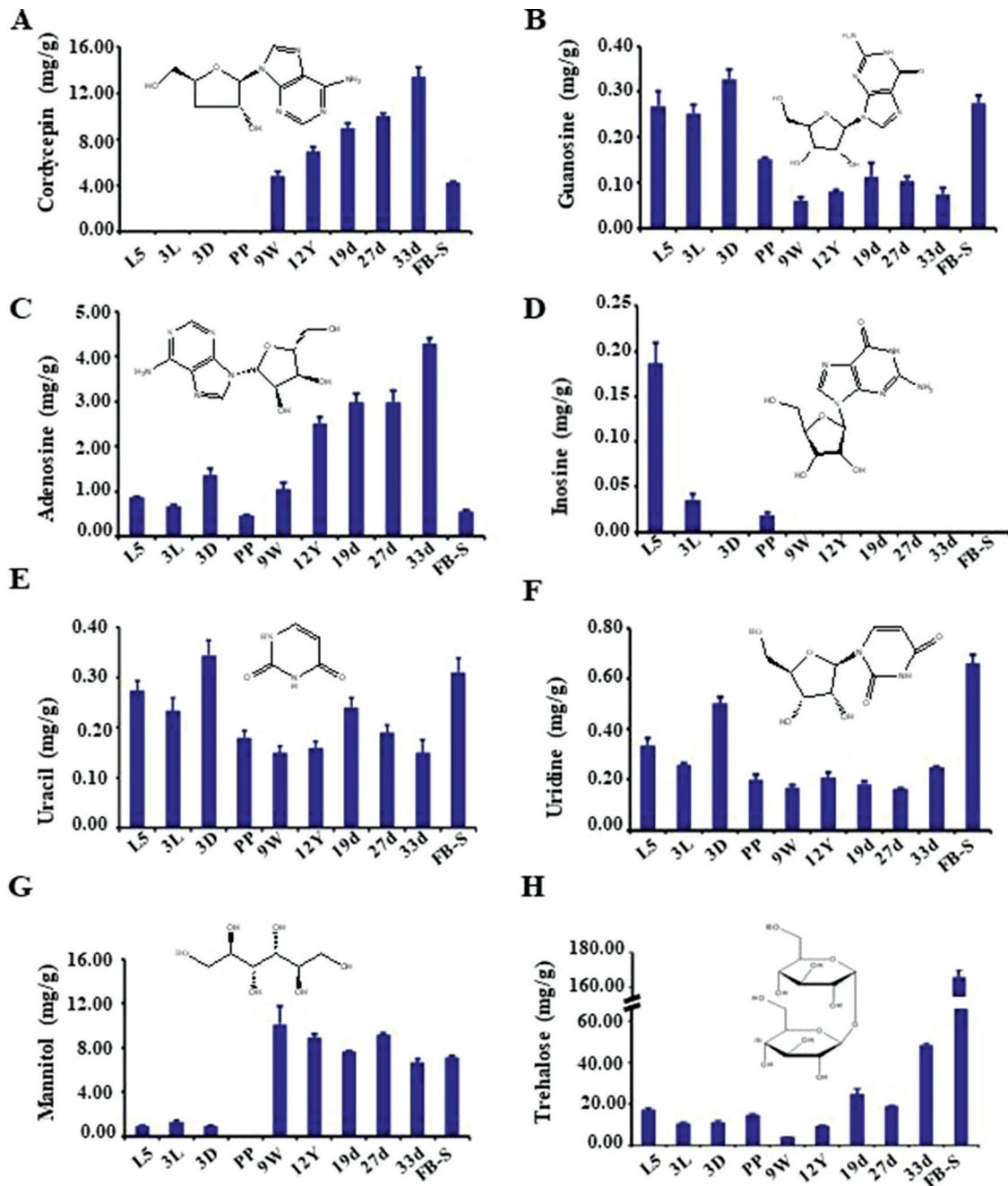


Figure 3. Chemical composition variation of the fruit body growth stages of *C. militaris* on silkworm larva. (A) Cordycepin, (B) guanosine, (C) adenosine, (D) inosine, (E) uracil, (F) uridine, (G) mannitol, and (H) trehalose. Samples are the same as shown in Table 1.

HCA of *C. militaris* Cultured in Different Conditions

HCA has been proven to be the most appropriate method to classify samples according to their characteristics. In the present work, HCA was implemented by SPSS 19.0 Software to evaluate the variation in the contents of nucleosides, mannitol, and trehalose among the growth stage samples of *C. militaris*. Between-group linkage was applied, and cosine distance was selected as a measurement (30). Dendrogram resulting from the contents of the eight analytes in the samples are shown in Figure 4. The results indicated that the samples, which the growth stage of fruiting body cultured in different substrates, were classified

in three clusters. Mycelium accumulation stage, fruit body formation stage, and fruit body maturation stage were clear. All the results demonstrate that the effect of cultivation condition was obvious for the contents of nucleosides, mannitol, and trehalose.

Furthermore, the transcriptomic analysis of developmental features of *Bombyx mori* wing disc during metamorphosis (31) and the genome-wide transcriptome and proteome analysis on different developmental stages of *C. militaris* (5) have been researched. In the next stages, the interaction of *Cordyceps* fungi and its host insect on the growth phases should be researched by transcriptome and proteome analysis to try to reveal the relationship. All these were very significant for the development of the health product.

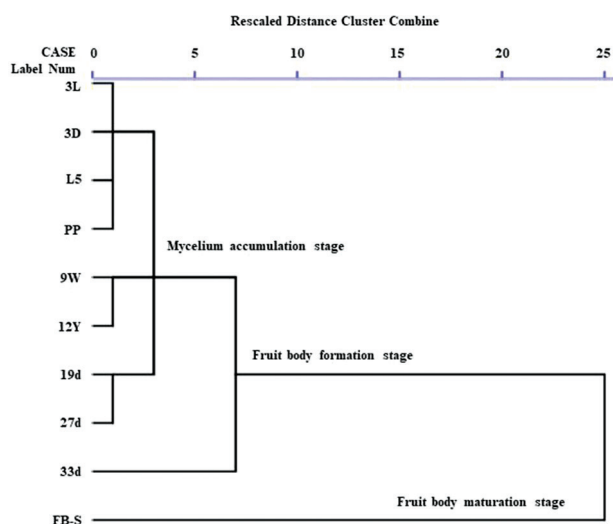


Figure 4. Dendrogram of hierarchical cluster analysis for *C. militaris* samples on the basis of contents of nucleosides, mannitol, and trehalose. Method: between-group linkage; measurement: cosine distance. Samples are the same as shown in Table 1.

Conclusions

In order to better analyze the trend of nucleosides and carbohydrate of *C. militaris* growing at different stages and in the different substrates, HPLC–DAD–ELSD was performed for these biomarkers. We can easily conclude that mannitol is mainly accumulated and stored during the final steps of fungal conidiophores development and then emerges. Trehalose underwent biotransformation and accumulated during the fruit body development. Cordycepin and adenosine were accumulated during the developmental stages of fruit body on silkworm larva. As we all know, the development of fruiting body needs stricter growth conditions. It has enabled life to survive, adapt, evolve, and flourish in diverse conditions. Therefore, the hyper production of cordycepin by solid culture on silkworm larvae offers a new idea. This is the first report of research that illustrates the relationship between the contents of nucleosides, nucleobases, mannitol, and trehalose and the development of fruiting body. It is very significant for further development of health products of *C. militaris*.

References

- (1) Shrestha, B., Zhang, W.M., Zhang, Y.J., & Liu, X.Z. (2012) *Mycol. Prog.* **11**, 599–614. doi:10.1007/s11557-012-0825-y
- (2) Li, S.P., Li, P., Dong, T.T.X., & Tsim, K.K.W. (2001) *Phytomedicine* **8**, 207–212. doi:10.1078/0944-7113-00030
- (3) Das, S.K., Masuda, M., Sakurai, A., & Sakakibara, M. (2010) *Fitoterapia* **81**, 961–968. doi:10.1016/j.fitote.2010.07.010
- (4) Shrestha, B., Kim, H.K., Sung, G.H., Spatafora, J.W., & Sung, J.M. (2004) *Biotechnol. Bioproc. E.* **9**, 440–446. doi:10.1007/bf02933483
- (5) Yin, Y.L., Yu, G.J., Chen, Y.J., Jiang, S., Wang, M., Jin, Y.X., Lan, X.Q., Liang, Y., & Sun, H. (2012) *PLOS One* **7**, e5185. doi:10.1371/journal.pone.0051853
- (6) Zheng, P., Xia, Y., Xiao, G., Xiong, C., Hu, X., Zhang, S., Zheng, H., Huang, Y., Zhou, Y., Wang, S., Zhao, G.P., Liu, X., St Leger, R.J., & Wang, C. (2011) *Genome Biol.* **12**, r116. doi:10.1186/gb-2011-12-11-r11
- (7) Xiong, C., Xia, Y., Zheng, P., Shi, S., & Wang, C. (2010) *Mycology* **1**, 25–66. doi:10.1080/21501201003674581
- (8) Xiao, J.H., & Xiong, Q. (2013) *Recent Pat. Biotechnol.* **7**, 153–166. doi:10.2174/18722105113079990008
- (9) Zhao, J., Xie, J., Wang, L.Y., & Li, S.P. (2013) *J. Pharm. Biomed. Anal.* **87**, 271–289. doi:10.1016/j.jpba.2013.04.025
- (10) Li, S.P., Yang, F.Q., & Tsim, K.K.W. (2006) *J. Pharm. Biomed. Anal.* **41**, 1571–1584. doi:10.1016/j.jpba.2006.01.046
- (11) Li, S.P., Li, P., Dong, T.T.X., & Tsim, K.K.W. (2001) *Electrophoresis* **22**, 144–150. doi:10.1002/1522-2683(200101)22:1<144::AID-ELPS144>3.0.CO;2-T
- (12) Gong, Y.X., Li, S.P., Li, P., Liu, J.J., & Wang, Y.T. (2004) *J. Chromatogr. A.* **1055**, 215–221. doi:10.1016/j.chroma.2004.09.015
- (13) Li, S.P., Song, Z., Dong, T.T.X., Ji, Z., Lo, C., Zhu, S., & Tsim, K.K.W. (2004) *Phytomedicine* **11**, 684–690. doi:10.1016/j.phymed.2003.07.011
- (14) Yang, F.Q., Ge, L.Y., Yong, J.W., Tan, S.N., & Li, S.P. (2009) *J. Pharm. Biomed. Anal.* **50**, 307–314. doi:10.1016/j.jpba.2009.04.027
- (15) Yang, F.Q., Li, S.P., Li, P., & Wang, Y.T. (2007) *Electrophoresis* **28**, 1681–1688. doi:10.1002/elps.200600416
- (16) Li, S.P., Li, P., Lai, C.M., Gong, Y.X., Kan, K.K.W., Dong, T.T.X., Tsim, K.K.W., & Wang, Y.T. (2004) *J. Chromatogr. A.* **1036**, 239–243. doi:10.1016/j.chroma.2004.02.080
- (17) Yu, L., Zhao, J., Li, S.P., Fan, H., Hong, M., Wang, Y.T., & Zhu, Q. (2006) *J. Sep. Sci.* **29**, 953–958. doi:10.1002/jssc.200600007
- (18) Yu, L., Zhao, J., Zhu, Q., & Li, S.P. (2007) *J. Pharm. Biomed. Anal.* **44**, 439–443. doi:10.1016/j.jpba.2007.01.003
- (19) Fan, H., Yang, F.Q., & Li, S.P. (2007) *J. Pharm. Biomed. Anal.* **45**, 141–144. doi:10.1016/j.jpba.2007.02.032
- (20) Wang, S., Yang, F.Q., Feng, K., Li, D.Q., Zhao, J., & Li, S.P. (2009) *J. Sep. Sci.* **32**, 4069–4076. doi:10.1002/jssc.200900570
- (21) Yang, F.Q., Li, D.Q., Feng, K., Hu, D.J., & Li, S.P. (2010) *J. Chromatogr. A.* **1217**, 5501–5510. doi:10.1016/j.chroma.2010.06.062
- (22) Yang, F.Q., Guan, J., & Li, S.P. (2007) *Talanta* **73**, 269–273. doi:10.1016/j.talanta.2007.03.034
- (23) Yang, F.Q., Feng, K., Zhao, J., & Li, S.P. (2009) *J. Pharm. Biomed. Anal.* **49**, 1172–1178. doi:10.1016/j.jpba.2009.02.025
- (24) Guan, J., Yang, F.Q., & Li, S.P. (2010) *Molecules* **15**, 4227–4241. doi:10.3390/molecules15064227
- (25) Hong, I.P., Kang, P.D., Kim, K.Y., Na, S.H., Lee, M.Y., Choi, Y.S., Kim, N.S., Kim, H.K., Lee, K.G., & Humber, R.A. (2010) *Mycobiology* **38**, 128–132. doi:10.4489/MYCO.2010.38.2.128
- (26) Ceccaroli, P., Buffalini, M., Saltarelli, R., Barbieri, E., Polidori, E., Ottonello, S., Kohler, A., Tisserant, E., Martin, F., & Stocchi, V. (2011) *New Phytol.* **189**, 751–764. doi:10.1111/j.1469-8137.2010.03520.x
- (27) Tuli, H.S., Sharma, A.K., Sandhu, S.S., & Kashyap, D. (2013) *Life Sci.* **93**, 863–869. doi:10.1016/j.lfs.2013.09.030
- (28) Yuan, J.P., Zhao, S.Y., Wang, J.H., Kuang, H.C., & Liu, X. (2008) *J. Agr. Food. Chem.* **56**, 809–815. doi:10.1021/jf0719205
- (29) Das, S.K., Masuda, M., Sakurai, A., & Sakakibara, M. (2009) *Afr. J. Biotechnol.* **8**, 3041–3047. doi:10.4314/ajb.v8i13.60983
- (30) Feng, K., Wang, S., Hu, D.J., Yang, F.Q., Wang, H.X., & Li, S.P. (2009) *J. Pharm. Biomed. Anal.* **50**, 522–526. doi:10.1016/j.jpba.2009.04.029
- (31) Ou, J., Deng, H.M., Zheng, S.C., Huang, L.H., & Feng, Q.L. (2014) *BMC Genomics* **15**, 820. doi:10.1186/1471-2164-15-820

RESEARCH ARTICLE

Phenylbutyl isoselenocyanate induces reactive oxygen species to inhibit androgen receptor and to initiate p53-mediated apoptosis in LNCaP prostate cancer cells

Wei Wu¹ | Deepkamal Karella¹ | Kartick Pramanik¹ | Shantu G. Amin^{1,2} |
Arun K. Sharma^{1,2} | Cheng Jiang¹ | Junxuan Lu^{1,2} 

¹ Department of Pharmacology, Pennsylvania State College of Medicine, Hershey, Pennsylvania

² Penn State Cancer Institute, Pennsylvania State College of Medicine, Hershey, Pennsylvania

Correspondence

Junxuan Lu, PhD, Department of Pharmacology and Penn State Cancer Institute, Penn State College of Medicine, Hershey, PA 17033.
Email: junxuanlu@pennstatehealth.psu.edu

Funding information

National Cancer Institute, Grant number: CA172169

Previous studies have established the in vivo bioavailability and efficacious dosages of phenylbutyl isoselenocyanate (ISC-4), a selenium-substituted isothiocyanate, against mouse xenograft models of human melanoma and colorectal cancer. To explore its potential attributes against prostate cancer, we treated human LNCaP prostate cancer cells with ISC-4 and examined their apoptosis responses, and interrogated the signaling mechanisms through pharmacological and siRNA knockdown approaches. Our results show that ISC-4 was more potent at inducing apoptosis than its sulfur analog phenylbutyl isothiocyanate (PBITC) without suppressing protein kinase AKT Ser⁴⁷³ phosphorylation. ISC-4 induced apoptosis in concentration- and time-dependent manners, and the apoptosis execution was attenuated by pre-incubation with a pan caspase inhibitor. ISC-4 decreased the abundance of androgen receptor (AR) and its best known target prostate specific antigen (PSA) without decreasing their steady state mRNA. ISC-4 upregulated the abundance of p53 protein and its Ser¹⁵-phosphorylation activation, and that of DNA double strand break marker Ser¹³⁹-p-H2A.X coincident with apoptotic exposure. Similar to the rapid induction of reactive oxygen species (ROS) by isothiocyanates, ISC-4 increased dihydroethidium-detectable signals in LNCaP cells. Pre-incubation with ROS scavenger N-acetyl-L-cysteine preserved AR and PSA abundance, markedly reduced ISC-4-induced apoptosis and attenuated p53 Ser¹⁵ phosphorylation, p21Cip1, and p-H2A.X. Furthermore, siRNA knockdown of p53 did not suppress ROS production, but decreased ISC-4-induced apoptosis. Knocking down p53-targets PUMA and Bax exerted greater protective effect on ISC-4-induced apoptosis than depleting p21Cip1. In summary, ISC-4 inhibited LNCaP cell growth and survival with ROS-mediated suppression of AR axis signaling and induction of p53-PUMA-Bax mitochondrial apoptosis.

KEYWORDS

apoptosis, isoselenocyanate, isothiocyanate, p53, prostate cancer

Abbreviations: AR, androgen receptor; Bax, Bcl 2-associated X protein; ISC, isoselenocyanate; ISC-4, phenylbutyl isoselenocyanate; ITC, isothiocyanate; NAC, N-Acetyl-L-cysteine; PBITC, phenylbutyl isothiocyanate; PEITC, phenethyl isothiocyanate; PCa, prostate cancer; PUMA, p53-upregulated modulator of apoptosis; ROS, Reactive oxygen species.

Current address of Wei Wu is Department of Chemistry and Pharmacology, Zhuhai College of Jilin University, Zhuhai, Guangdong, People's Republic of China, 519041.

Current address of Kartick Pramanik is Kentucky College of Osteopathic Medicine (KYCOM), University of Pikeville, Pikeville, KY 41501.

1 | INTRODUCTION

Prostate cancer (PCa) remains a top cause of cancer death in US men, second only to lung cancer. Androgens, functioning through androgen receptor (AR), are essential for the genesis, progression, and survival of PCa.¹ Androgen deprivation therapy (ADT) has remained the standard-of-care for metastatic PCa for decades with serious side effects on the patients' quality of life. Despite its initial efficacy to reduce tumor burden in the short-term, ADT is inevitably followed by the recurrence of castration-resistant prostate cancer (CRPC). Chemotherapy with docetaxel² or its derivative cabazitaxel in docetaxel resistant CRPC³ offers a survival benefit of a few months for CRPC patients with dose-limiting toxicities. The discovery of persistent AR signaling in CRPC led to development of "second generation" ADT drugs,⁴⁻⁵ such as androgen synthesis inhibitor abiraterone acetate (Zytiga)⁶⁻⁷ and AR antagonist enzalutamide/Xtandi.⁸⁻⁹ Each drug demonstrated an efficacy against chemotherapy-resistant CRPC with median survival benefit measured in months.^{6-8,10} However, nearly all CRPC patients inevitably develop acquired resistance to these novel ADT drugs.¹¹⁻¹² Autologous cell-based immunotherapy of CRPC such as the FDA-approved Provenge (Sipuleucel-T) remains highly personalized and expensive for the survival benefit (FDA website). In spite of rapid advances of checkpoint inhibitor monoclonal antibodies against a number of cancers of other organ sites, PCa remains rather unresponsive to these cutting edge immunotherapy modalities. Radiotherapy modalities for CRPC provide palliative pain relief at best. To effectively impact PCa morbidity and mortality, there remain clinically un-met needs to develop additional small molecular agents and drugs, especially for the chemoprevention or therapy of early stage PCa to block or delay the emergence of metastatic CRPC.

Isothiocyanates (ITCs), the naturally-occurring compounds stored as glucosinolates in plants and cruciferous vegetables,¹³⁻¹⁵ have been shown to be efficacious chemopreventive agents against animal carcinogenesis models both in the initiation (inhibit phase I and induce phase II enzymes) and the post-initiation (block cell-cycle progression and induce apoptosis in human cancer cells) stages for many organs sites. Some ITCs, especially phenethyl isothiocyanate (PEITC), have been studied extensively for the cell cycle and death effects¹⁶⁻²¹ as well as AR signaling²²⁻²³ in PCa cell lines and in animal models.²⁴⁻²⁵ Nearly a decade ago, a series of ITC analogs and their selenium-substituted isoselenocyanate (ISC) derivatives were designed and synthesized at our institution to further improve the anti-cancer efficacy and drug likeness.²⁶ Through extensive structure-activity relationship (SAR) studies, phenylbutyl isoselenocyanate (ISC-4, see Figure 1A for structure), demonstrated the most attractive drug-like attributes.²⁶ ISC-4 exhibits favorable LogP value (LogP 4.2) and molecular weight (MW 238) which satisfied Lipinski's Rule of Five.²⁷ Previous studies have established the *in vivo* bioavailability, and safe and efficacious dosages of ISC-4 in mouse xenograft models of melanoma²⁸⁻²⁹ and colorectal cancer³⁰ with an inhibition of protein kinase AKT (ie, AKT3 in melanoma and AKT1/2

in colorectal cancer) signaling as a putative mechanism of the anti-cancer action. Given its seleno-modification and improvement on drug likeness, we would hypothesize that ISC-4 could be a promising candidate for research and development (R&D) as a chemopreventive agent for PCa.

As an initial effort toward testing this hypothesis, we selected LNCaP cells, which possess wild-type p53 tumor suppressor protein,^{31,32} functional mutant AR,³³ and defective PTEN³⁴ (activated AKT-mTOR) as the target cells to examine their growth suppression and apoptosis responses to ISC-4 in cell culture. The rationale for choosing this cell line is several-fold: i) the wild type p53 is characteristic of precancerous prostatic lesions as well as localized prostate adenocarcinomas which mostly retain wild type p53 gene³⁵; ii) these cells are responsive to AR signaling for proliferation³³ as are most clinical prostate cancers with AR amplification or mutational activation³⁵; and iii) they have defective PTEN tumor suppressor,³⁴ therefore activated AKT-mTOR signaling, representing a prevalent oncogenic driver pathway in the human prostate adenocarcinomas. We selected ISC-4 exposure concentrations in the serum/plasma achievable range as demonstrated in an earlier pharmacokinetic (PK) experiment.³⁶

To provide insights into common versus unique mechanisms of action, we compared and contrasted ISC-4 and PBITC with a reference bioactive anti-cancer selenium compound, methylseleninic acid (MSeA).³⁷⁻³⁸ We have shown *in vivo* cancer growth inhibitory activities of MSeA in xenograft models³⁹ and in genetically-engineered mouse models of prostate carcinogenesis⁴⁰⁻⁴¹ with daily gavage dosing. In LNCaP cell culture model, MSeA exerted inhibitory impact on AR and its best characterized target prostate specific antigen (PSA)⁴² with minimal effect on p53 activation⁴³⁻⁴⁴ and without evident involvement of reactive oxygen species (ROS).⁴⁵ Given the pivotal significance of AR signaling in prostate epithelial survival, cancer genesis and progression, and the preservation of wild type p53 in early lesions and most localized PCa,³⁵ our findings indicate attractive cancer-intrinsic potential of ISC-4 for precision intervention and therapy of PCa.

2 | MATERIALS AND METHODS

2.1 | Chemicals and antibodies

ISC-4 was synthesized as previously described.²⁶ The purity of ISC-4 was higher than 97%. Stock solution was prepared at 10 mM in DMSO. MTT was purchased from Sigma-Aldrich (St. Louis, MO). PSA ELISA kits were purchased from Calbiotech (Spring Valley, CA). ROS and Annexin V kits were purchased from Pierce Biotechnology (Waltham, MA). Antibodies against Ser⁴⁷³-p-AKT, Ser¹⁵-p-p53, p21Cip1, PARP, c-PARP, Bax, PUMA, β -actin, and HRP-conjugated secondary antibodies were purchased from Cell Signaling Technology (Danvers, MA). Antibodies against p53 and AR were purchased from BD Pharmingen (San Jose, CA). Antibody against PSA was purchased from Dako (Glostrup, Denmark). Antibody against Ser¹³⁹-p-H2A.X was purchased from Abcam (Cambridge, MA).

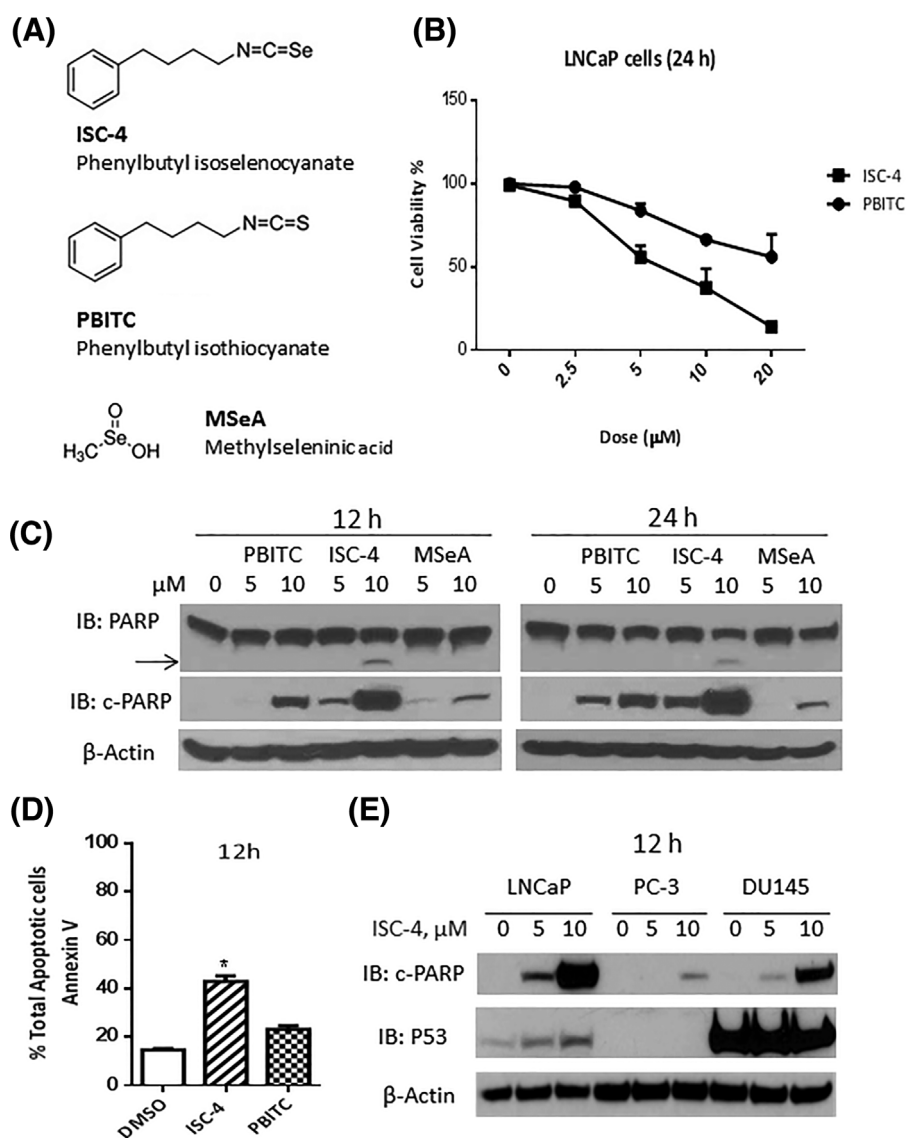


FIGURE 1 ISC-4 exerted stronger anti-proliferative and pro-apoptosis activities than sulfur-analog PBITC in LNCaP cells. A, The chemical structures of ISC-4 and PBITC and MSeA. B, The cell number/viability assessed by MTT assay. LNCaP cells were seeded into 96 well plates and treated with the indicated concentrations of ISC-4 and PBITC for 24 h. Error bar represents SD of triplicate determinations. C, Western blot detection of PARP cleavage as a marker for apoptotic caspase activation. LNCaP cells were seeded into 100 mm dishes and treated with 5 or 10 μM of ISC-4, PBITC, or MSeA for 12 and 24 h. Whole cell extracts were prepared. 30 μg portions of those extracts were resolved via Bolt 4-12% Bis-Tris Plus gel and probed with antibody specific for PARP (116kD; arrow pointed to 89 kD cleaved product) or the cleaved PARP (89 kD) only. The same blots were re-probed with β -actin antibody to verify protein loading. D, Cell death assessment by Annexin V binding assay. LNCaP cells were seeded into 6 well plates and treated with 10 μM of ISC-4 or PBITC for 12 h and the Annexin V binding was analyzed by Muse Cell Analyzer. Error bar represents SD of triplicate determinations. E, Apoptosis assessment by WB detection of cPARP in LNCaP versus PC-3 and DU145 cells after 12 h exposure to ISC-4 at indicated concentrations. Mutation of p53 in DU145 cells vastly increased protein stability

2.2 | Cell culture

LNCaP, PC-3, and DU145 prostate cancer cells were obtained from the American Type Culture Collection (ATCC, Manassas, VA). The LNCaP cells were cultured in RPMI 1640 Medium (Invitrogen, Carlsbad, CA) with 10% fetal bovine serum (Atlanta Biologicals, Flowery Branch, GA) without any antibiotics and maintained at 37°C with 5% CO₂ in humidified atmosphere. Authentication of the LNCaP cell lines was accomplished by next-gen DNA whole genome

sequencing (MacroGen Clinical Laboratory, Rockville, MD) and RNA sequencing (Penn State Hershey Genome Sciences Facility, Hershey, PA). In terms of p53 functional background, LNCaP PCa cells are p53-wild type, DU145 cells contain non-functional mutant p53 and PC3 cells are p53-null.^{31,32} DU145 cells were cultured in Minimum Essential Eagle's medium supplemented with 10% fetal bovine serum and 2 mM L-glutamine without antibiotics. PC-3 cells were cultured in F-12 K medium supplemented with 10% fetal bovine serum and 2 mM L-glutamine without antibiotics.

2.3 | Estimation of cell viability/number

The LNCaP cells were suspended at a density of 1.0×10^5 /mL and added to 96-well flat bottom microtiter plates at 100 μ L per well. Approximately 2 days after seeding, the cells were treated with concentrations of 0, 2.5, 5, 10, and 20 μ M of ISC-4 or PBITC to determine the percentage of metabolically viable cells. After incubation for 24 h, cell growth was measured by MTT assay. The percentage of cell viability ratio was calculated as follows: Cell viability ratio (%) = $(A_{490, \text{sample}} - A_{490, \text{blank}}) / (A_{490, \text{control}} - A_{490, \text{blank}}) * 100$.

2.4 | Annexin V assay

The LNCaP cells were seeded in six-well plate at 8×10^4 cells per well, for approximately 2 days, and were treated with indicated concentration(s) of ISC-4, PBITC or 0.1% DMSO. Annexin V & Dead Cell kits were used for measuring dead and dying cells in both floating and adherent cells with Muse Cell Analyzer (EMD Millipore, Billerica, MA), according to the manufacturer's protocol. Data were analyzed using Muse 1.4 software.

2.5 | Measurement of reactive oxygen species (ROS)

To assay intracellular ROS, LNCaP cells were seeded in 6-well plate at 8×10^4 cells per well for approximately 2 days and were treated with ISC-4 (5 and 10 μ M), or 0.1% DMSO for 6 h. Measurement of total ROS levels in LNCaP cells was performed by using the Muse Oxidative Stress Kit with Muse Cell Analyzer based on dihydroethidium (DHE) to react with superoxide anions to form DNA-binding fluorophore ethidium bromide which intercalates with DNA resulting in red fluorescence. The kit identifies two different cell populations of ROS (-) cells and ROS (+) cells, which were represented by the M1 and M2 peaks in the graph, respectively. Percentages of ROS (-) and ROS (+) cells were analyzed using Muse 1.4 software.

2.6 | Immunoblot analysis for proteins of interest

The LNCaP cells were plated in 100 mm dishes at 4.5×10^5 cells per dish, and after 2 days, treated with different concentrations of compounds. 200 μ L of the medium from each dish was collected for analysis of secreted PSA. Cells were harvested, washed with PBS once and whole-cell lysates were made in RIPA lysis buffer (ThermoFisher Scientific, Waltham, MA) containing protease inhibitor cocktail and phosphatase inhibitor cocktail (Sigma-Aldrich) at 4°C for 20 min. The resulting lysates were centrifuged at 16 000g at 4°C for 10 min to remove any insoluble debris. The protein concentrations were quantitated by a BCA Protein Assay Kit (ThermoFisher Scientific). Equal amounts of total proteins were separated by Bolt 4-12% Bis-Tris Plus gel (ThermoFisher Scientific), and after electrophoresis/SDS-PAGE, the resolved proteins were electro-transferred to a PVDF membrane (Bio-Rad, Hercules, CA). The membrane was blocked in 5% skimmed milk for 1 h at room temperature, incubated with indicated primary antibodies

at 4°C overnight and horseradish peroxidase (HRP)-conjugated secondary antibody for 1-4 h at room temperature. Immunoblots were developed using the enhanced chemiluminescent reagents (ThermoFisher Scientific).

2.7 | ELISA of secreted PSA

The amount of secreted PSA into medium was measured by using PSA ELISA kits (Calbiotech), according to manufacturer's instructions. Twenty five micro liter of standards and samples were pipetted into the holder with coated strips, and incubated with 100 μ L of anti-PSA conjugated reagents for 1 h. After removal of the liquid and three times wash by washing buffer, 100 μ L of TMB substrate was added and incubated for 15 min in room temperature, and then after adding 50 μ L of stop solution, absorbance was obtained on ELISA reader at 450 nm.

2.8 | Quantitative real-time PCR for mRNA detection

The LNCaP cells (1×10^6) were treated with DMSO (vehicle) and ISC-4 (5 and 10 μ M) for 1 and 3 h. Total RNA was isolated using Direct-Zol (Zymo Research, Irvine, CA). RNA quality and concentrations were determined using the Bioanalyzer 2100 (Agilent Technologies, Santa Clara, CA). First strand cDNA was produced from 1 μ g of total RNA using the standard High Capacity cDNA Reverse Transcription kit with RNase Inhibitors (ThermoFisher) protocol. The cDNA concentrations were quantified by absorbance using a NanoDrop-100 (ThermoFisher). Quantitative RT-PCR was performed using an ABI QuantStudio 12KFlex Sequence Detection System (ThermoFisher). Assays were prepared using 100 ng cDNA reaction product, 2X TaqMan Gene Expression Master Mix Master Mix and Assay-on-Demand primers and probes (900 nM unlabeled PCR primers; 250 nM FAM dye-labeled TaqMan MGB probe) (ThermoFisher) in a final reaction volume of 10 μ L. Quantitative RT-PCR conditions were 2 min at 50°C, 10 min at 95°C and 40 cycles of 15 s at 95°C and 1 min at 60°C. ABI SDS 2.2.2 software and the $2^{-\Delta\Delta C_t}$ analysis method⁴⁶ were used to quantitate relative amounts of product using GAPDH as endogenous control. Assays-on-Demand used for this analysis were: AR (Hs00171172_m1) KLK3 (PSA) (Hs02576345_m1) and GAPDH (Hs02786624_g1).

2.9 | Depletion of p53, p21Cip1, PUMA, or Bax by siRNA transfection

The p53 siRNA and negative control siRNA (scrambled RNA) were purchased from Santa Cruz Biotechnology (Santa Cruz, CA). The LNCaP cells were seeded in six-well plates at a density of 8×10^4 cells per well in 2 mL complete RPMI 1640 growth medium. Two days later, when cells reached 70-90% confluence, transfection was carried out with 50 nM of p53 siRNA or control siRNA using Lipofectamine 3000 transfection reagents (ThermoFisher Scientific) according to the manufacturer's instructions. After 36 h, the transfected cells were treated with 10 μ M of ISC-4 for 12 h.

Similarly, to knock down p21Cip1, PUMA, or Bax gene expression, siRNA against each molecular target was purchased from Cell Signaling. LNCaP cells (8×10^4 cells/well) were seeded for 2 days and then transfected with either scrambled or specific siRNA. After 2 days, cells were treated with 10 μ M of ISC-4 for 12 h and analyzed as above.

2.10 | Statistical analysis

All the presented data were confirmed in 2-3 independent experiments. Numerical values are expressed as mean \pm SD. Statistical analyses were carried out with GraphPad Prism 6 software (La Jolla, CA). Differences among groups were analyzed by one-way ANOVA. For comparison involving only two groups, the Student *t*-test was used. $P < 0.05$ was considered statistically significant.

3 | RESULTS

3.1 | Cell growth and death responses to ISC-4 compared to PBITC and MSeA

Exposure of LNCaP cells for 24 h to ISC-4 led to a strong concentration-dependent decrease of their numbers, estimated with MTT assay that detected cells capable of mitochondrial reductive metabolism, with an IC_{50} value of $\sim 5 \mu$ M (Figure 1B). ISC-4 was approximately fourfold more potent than its sulfur analog phenylbutyl isothiocyanate (PBITC, see Figure 1A for structure) possessing an estimated IC_{50} of $>20 \mu$ M in the same assay (Figure 1B). Under a phase contrast microscope, treated cells were observed to display typical apoptotic responses within a few hours of exposure to ISC-4, including rounding and detachment from culture vessel surface. The greater growth suppression effect of ISC-4 than PBITC was confirmed by immunoblotting for cleavage of PARP as a molecular indicator of caspase-mediated death execution (Figure 1C) and by Annexin V binding assay for phosphatidylserine that has translocated from the inner membrane leaflet to the surface of cells undergoing apoptosis (Figure 1D) (approximately fourfold net increase). The apoptotic induction effect of ISC-4 or PBITC was concentration-dependent as shown by PARP cleavage and was each more potent than MSeA (Figure 1C). Indeed, the ISC-4 apoptotic action was so rapid as to be detectable as early as 3 h (Supplementary Figure S1A). Pre-treatment of LNCaP cells with a pan-caspase inhibitor, z-VAD(OMe)-FMK, attenuated ISC-4-induced apoptotic PARP cleavage in an inhibitor concentration-dependent manner (Figure 2D). These results established the greater potency of ISC-4 than PBITC to inhibit the proliferation of LNCaP cells and to induce their demise through apoptosis that was largely preventable by inhibiting caspases.

The caspase-mediated apoptosis effect of ISC-4 (12 h exposure) in LNCaP cells was compared with PC-3 (P53-null, AR-null, high pAKT due to null Pten) and DU145 (mutant P53, AR-null, low pAKT due to wild type Pten) cells³² using cPARP as the readout with Western Blot detection (Figure 1E). The LNCaP cells showed the most sensitive apoptosis execution among the three cell lines tested, with PC-3 cells

being the least sensitive. Therefore, the rest of the study focused on using LNCaP cells.

3.2 | Lack of inhibition of AKT phosphorylation by ISC-4 in LNCaP cells

Given that earlier work had identified an inhibitory activity of ISC-4 on AKT3 signaling in melanoma cells²⁸ as well as AKT1/2 in colorectal cancer cells,³⁰ we examined whether AKT phosphorylation was decreased in ISC-4-exposed LNCaP cells by immunoblotting for Ser⁴⁷³-p-AKT. Exposure for 12 and 24 h to ISC-4 or PBITC did not result in any observable decrease of p-AKT band intensity (see Figure 2A for representative data). MSeA did not decrease p-AKT at 12 h, but decreased its band intensity by 24 h, showing a delayed effect as expected from our earlier studies.^{44,47} Because LNCaP cells are known not to express AKT3 protein,⁴⁸ we therefore ruled out the involvement of AKT1/2 inhibition by ISC-4 in our model. Subsequently, we examined other signaling pathways to account for the LNCaP-specific molecular and cellular responses to ISC-4.

3.3 | Impact of ISC-4 exposure on androgen receptor (AR) signaling axis

To determine whether ISC-4 affected AR signaling in LNCaP cells, we examined the protein level of AR and its best characterized transcriptional target PSA by immunoblotting the cellular extracts prepared from cells that had been exposed to increasing concentrations of ISC-4, PBITC, or MSeA for 12 and 24 h (Figure 2A). Both ISC-4 and PBITC exerted a strong and concentration-dependent suppression of AR at 12 and 24 h, whereas MSeA decreased AR more prominently at 24 h than at 12 h. By 12 h exposure, as little as 2.5 μ M ISC-4 decreased AR (Figure 2B) and the secretion of PSA into the medium (Supplementary Figure S1C) in a finer concentration-titration experiment. In time course experiments, the ISC-4-induced suppression of cellular AR and PSA preceded apoptotic PARP cleavage by a few hours (Figure 2C). ISC-4 treatment also decreased the secretion of PSA into culture medium at 3 h, the earliest time point sampled (Supplementary Figure S1D).

To further delineate the relationship between AR and PSA suppression by ISC-4 and its activation of the apoptotic caspases, we immunoblotted cellular AR and PSA in LNCaP cells that were co-treated with a pan caspase inhibitor and ISC-4 (Figure 2D). In spite of the much attenuated caspase-mediated apoptosis indicated by c-PARP in these cells, ISC-4 exposure maintained its strong suppression on AR and PSA proteins (Figure 2D). Detection of the steady state mRNA level by RT-qPCR for *AR* and *Klk3* (PSA) genes in LNCaP cells treated for 1 or 3 h did not reveal any decrease due to ISC-4 exposure (Figure 2E). These data and the time frame of AR and PSA changes in relation to cPARP (Figure 2C) therefore would be consistent with the suppression of AR and PSA through rapid post-transcriptional mechanism(s) related to hastened protein degradation and/or decreased protein synthesis and might contribute to the observed anti-proliferative and pro-apoptosis outcomes.

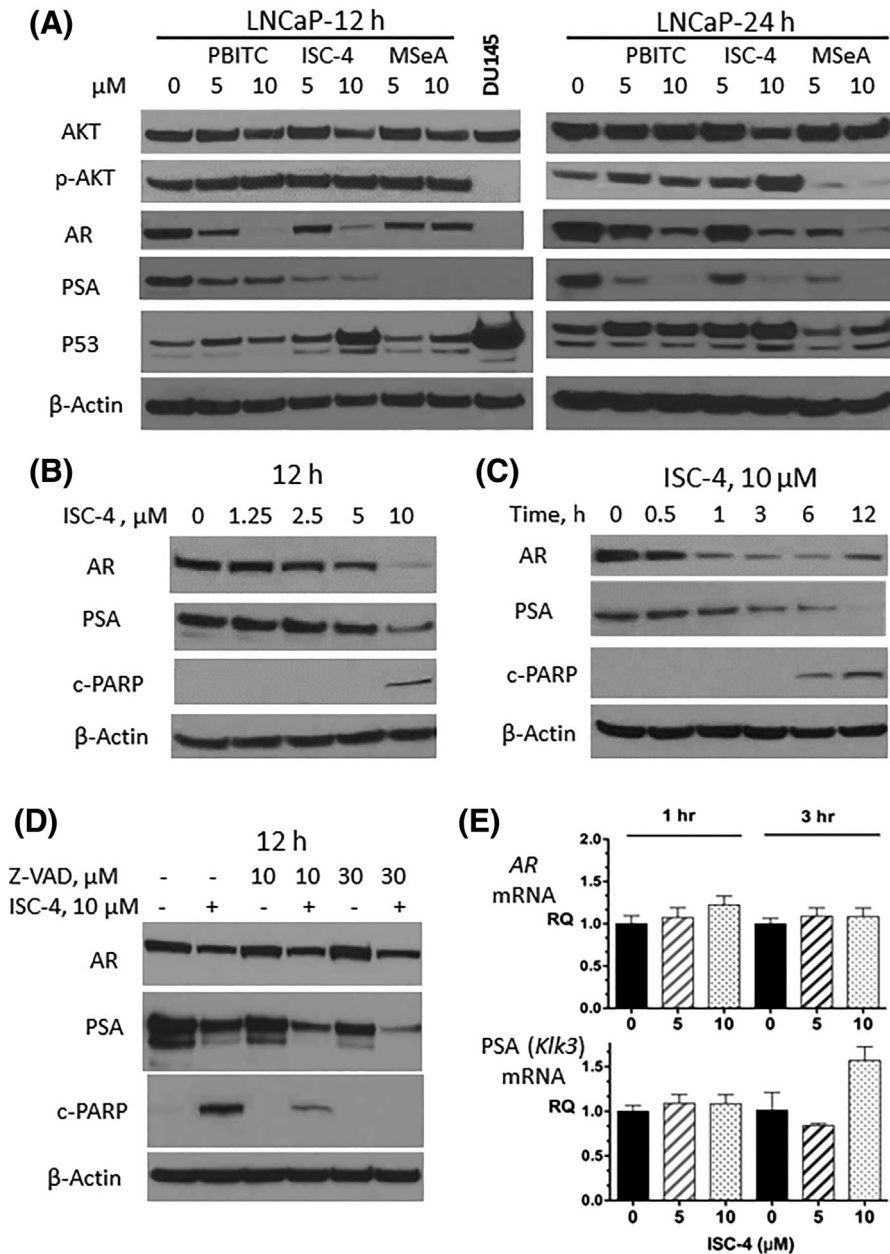


FIGURE 2 ISC-4 inhibited AR/PSA post-transcriptionally and independently of apoptosis. A, Western blot assessment of AKT phosphorylation, AR, PSA, and p53 abundance in LNCaP cells exposed to indicated concentrations of ISC-4, PBITC or MSeA. The AR-/PSA-null and Pten-wild type DU145 cell extract served as a negative control for AR and PSA and for pAKT, respectively. The mutant p53 protein in DU145 cells served as a "positive" size marker for p53. B, Western blot assessment of ISC-4 impact on AR and PSA in relation to cPARP in a concentration-titration experiment. LNCaP cells were treated with the indicated concentrations of ISC-4 for 12 h. C, Western blot assessment of ISC-4 impact on AR and PSA in relation to cPARP in a time course experiment. LNCaP cells were treated with 10 μ M of ISC-4 for 0.5–12 h. D, Western blot assessment of ISC-4 impact on AR and PSA and cPARP in presence of pan caspase inhibitor, Z-VAD(OMe)-FMK. LNCaP cells were pretreated for 1 h with or without Z-VAD (10 and 30 μ M), and then treated with 10 μ M of ISC-4 for 12 h. β -actin was detected as a loading control for WB. E, Real time PCR quantitation of steady state mRNA level for AR and PSA (*Klk3*) in LNCaP cells treated with 5 and 10 μ M of ISC-4 for 1 or 3 h. Relative quantitation (RQ) data were normalized to respective *GAPDH* mRNA. Error bar represents SD of triplicate PCR determinations

3.4 | Proximal mediator role of reactive oxygen species (ROS) in ISC-4-exposed cells

Because of the known induction of rapid ROS generation by ITCs in other prostate cancer cells^{18–19} and the previously reported in vitro

ROS generation by ISC-4 in a cell-free model,⁴⁹ we assessed the ability of ISC-4 to induce ROS in LNCaP cells. As shown in Figure 3A, ISC-4 exposure for 6 h increased the dihydroethidium (DHE)-reactive ROS in a concentration-dependent manner. Time course experiments indicated increased ROS as early as 2 h and peaked at

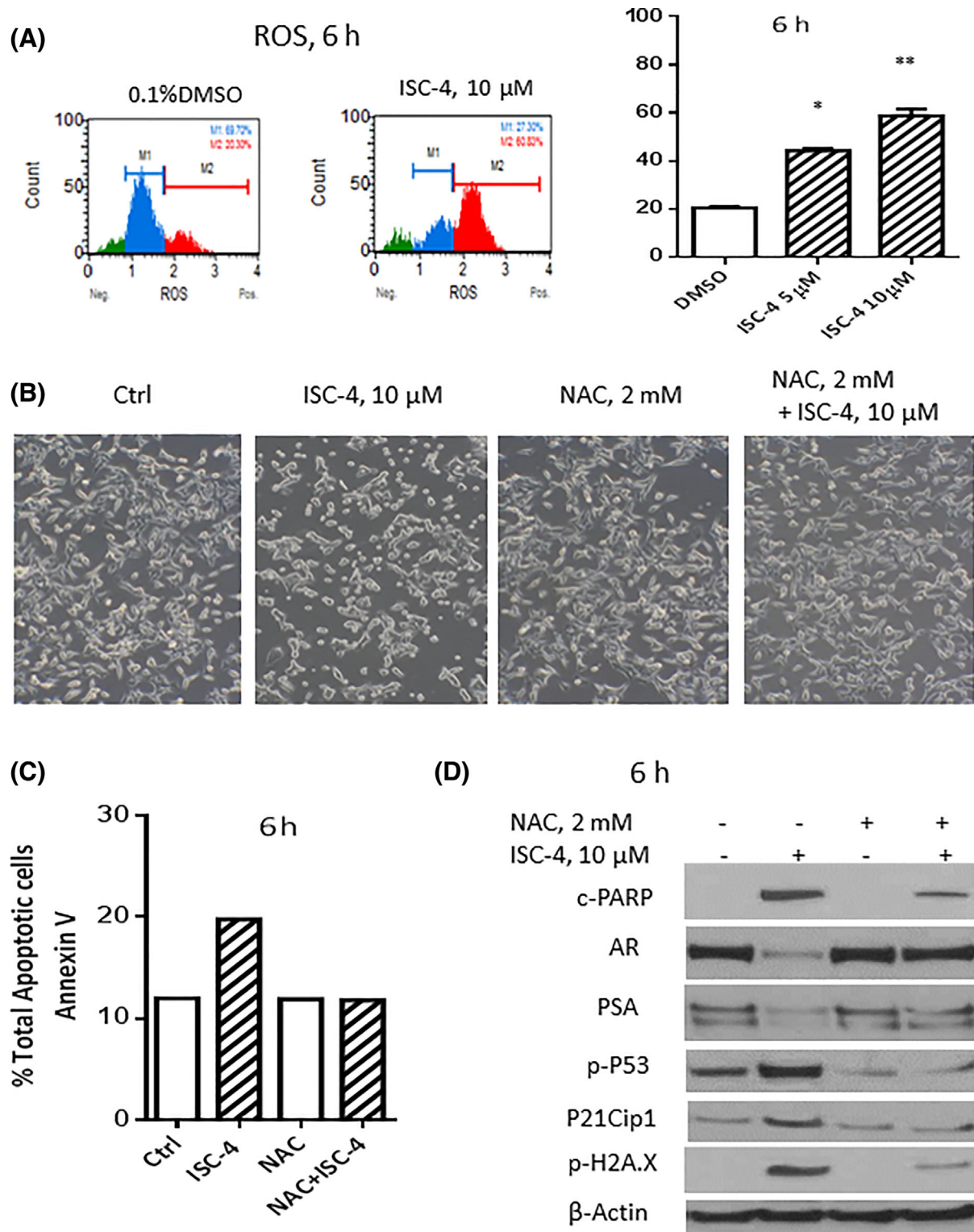


FIGURE 3 ISC-4 induced ROS to suppress AR/PSA and to initiate apoptosis in LNCaP cells. A, Detection of ROS by dihydroethidium (DHE) fluorescence. LNCaP cells were treated with 5 and 10 μ M of ISC-4 for 6 h. The cells were incubated with DHE and then analyzed by Muse Analyzer. Error bar represents SD of triplicate determinations. B, Photomicrograph of ISC-4 treated LNCaP cells with or without 2 h pre-treatment with 2 mM NAC. C, Impact of NAC on ISC-4 induced apoptosis assessed by Annexin V binding assay. D, Western blot assessment of NAC impact on ISC-4 effect on cPARP, AR and PSA and p53 axis. For B-D, LNCaP cells were pretreated with or without 2 mM of NAC and then treated with 10 μ M of ISC-4 for 6 h. Beside Annexin V binding assay, whole cell extracts were prepared and subjected to Western Blotting analysis using antibodies against c-PARP, AR, PSA, p-p53, p21Cip1, and p-H2A.X

6 h and subsided thereafter (Supplementary Figure S2). Pretreating LNCaP cells with ROS scavenger N-acetyl cysteine (NAC, 2 mM) significantly diminished the morphologic (Figure 3B), cell membrane biochemical (Figure 3C) (Annexin V binding), and nuclear molecular (Figure 3D) (c-PARP) manifestations of apoptosis in the ISC-4-exposed cells. Notably, NAC rescued the AR and PSA expression in ISC-4-exposed cells (Figure 3D). The data therefore supported intracellular ROS as the crucial primary mediator in discharging the anti-AR signaling and pro-apoptosis activities of ISC-4 in the LNCaP cells.

3.5 | p53 as a major nexus for apoptosis signaling induced by ISC-4

Because ROS and cellular oxidative stresses can trigger DNA damage and p53 plays a central role in DNA damage response (DDR), cell cycle arrest and apoptosis,⁵⁰ we immunoblotted for p53 in cells treated with ISC-4, PBITC or MSeA for 12 and 24 h (Figure 2A) and observed greater increases of p53 abundance by ISC-4 and PBITC than MSeA. For Ser¹⁵-p-p53 and the best known p53 transcriptional target p21Cip1⁵¹ as well as the DNA double strand break marker protein Ser¹³⁹-p-H2A.X (γ -H2A.X),⁵² NAC pre-treatment reversed the ISC-4-induced increase of each of these proteins of interest (Figure 3D, lane 4 vs lane 2).

To further probe possible cause-effect relationship between p-H2A.X (marking DNA double strand breaks) and p53 activation, we examined the concentration-dependency as well as temporal sequence of changes among these proteins. ISC-4 exposure increased the level of total p53 protein (Figures 2A and 4A) and Ser¹⁵-p-p53 at 5 and 10 μ M (Figure 4A; Supplementary Figures S1A and S1D). On the other hand, the level of Ser¹³⁹-p-H2A.X was only detected at the apoptotic concentration of 10 μ M ISC-4 (Figure 4A) (Supplementary Figure S1A). Temporally, ISC-4 induced Ser¹⁵-p-p53 occurred within 0.5 h of exposure (the earliest sampled time point), several hours ahead of detectable p-H2A.X (Figure 4B, Supplementary Figure S1A) and c-PARP (Figure 2C). Therefore, the observed increased p-H2A.X in ISC-4-exposed LNCaP cells most probably signified nucleosomal DNA fragmentation in apoptotic cells rather than early DNA double strand break damages to activate p53 signaling. Alternatively, the increased p-H2A.X might have resulted from G₂/M arrest and increased mitotic phosphorylation without DNA damage.⁵³⁻⁵⁴

To interrogate the contribution of p53 to ISC-4 induction of apoptosis and the suppression of AR and PSA, we knocked down p53 protein abundance in LNCaP cells by transfection of siRNA targeting p53 (Figure 4C). The diminished p53 expression in the LNCaP cells, as confirmed by decreased basal levels of p53 protein and p21Cip1 (lane 3 vs lane 1), attenuated the apoptosis metrics such as c-PARP and p-H2A.X (Figure 4C, lane 4 vs lane 2) and Annexin V binding to apoptotic cells (Figure 4D). Knocking down p53 in LNCaP cells did not affect the suppressing action of ISC-4 on AR and PSA (Figure 4C). As expected of a hierarchal relationship of ROS generation with p53 activation, depleting p53 by siRNA did not alter the ROS production in the ISC-4-exposed cells (M2 fraction in Figure 4E). The data

therefore supported a crucial role of p53 in mediating the apoptosis effect of ISC-4 independently of the AR axis.

3.6 | PUMA and Bax-mitochondrial intrinsic caspase cascade as p53 downstream target in ISC-4-induced apoptosis

In spite of the observed moderately increased protein abundance of p21Cip1 in ISC-4-exposed cells (Figures 3D and 4A, Supplementary Figure S1A), temporally, the ISC-4-induced p21Cip1 abundance changes fluctuated and lagged much behind the p53 changes (Figure 4B; Supplementary Figure S1B). As expected of the most studied downstream transcriptional target of p53, depleting p21Cip1 level by siRNA did not change Ser¹⁵-p-p53 level or its induction by ISC-4 (Figure 5A). However, the efficient depletion of p21Cip1 only modestly attenuated the apoptotic readouts (c-PARP and p-H2A.X) and caused a proportionally minor rebound of AR and PSA abundance in the ISC-4-exposed cells (Figure 5A, lane 4 vs lane 2).

Since PUMA and Bax were other well-known p53 downstream target proteins to mediate apoptosis signaling in various DNA damage and non-genotoxic contexts,⁵⁵ we tested the impact of down-regulating each individually by siRNA transfection on the ISC-4-induced apoptosis outcomes. As shown in Figure 5B for PUMA, ISC-4 treatment increased its protein level, and the death execution in the ISC-4-exposed cells was abolished by the siRNA knockdown approach. However, in contrast to PUMA or p21Cip1, total Bax protein level was not induced by ISC-4 (Figure 5C), yet siRNA knocking down of Bax still afforded a partial attenuation of apoptotic cleavage of PARP (Figure 5C). The data supported a crucial involvement of PUMA as a downstream target of p53-apoptosis signaling from ISC-4 in the LNCaP cells with an indirect contribution from Bax.

4 | DISCUSSION

Our data presented above established several attractive cellular and molecular action features of ISC-4 that would be relevant to the chemoprevention and/or therapy of PCa and revealed aspects of mechanisms distinct from MSeA as a reference bioactive Se compound of documented PCa inhibitory efficacy in animal models.³⁹⁻⁴¹ These included the approximately fourfold improvement in growth suppression potency of ISC-4 versus its sulfur counterpart PBITC (Figure 1) and the induction of caspase-mediated apoptosis (Figures 1 and 2D), both compounds being superior in *in vitro* potency than MSeA. Although not unexpected, comparison of the impacts of ISC-4 or PBITC with MSeA in terms of p-AKT status, AR, PSA and p53 abundance (Figure 2A) suggested closer similarities in mechanisms of actions between ISC-4 and PBITC than with the structurally distinct MSeA. In particular, MSeA exerted a more rapid suppression of PSA than AR, whereas ISC-4 and PBITC decreased AR temporally ahead of PSA reduction. Whereas MSeA induced a rapid post-transcriptional PSA protein degradation followed by down-regulation of AR abundance and transcription,⁴² ISC-4 suppressed AR and PSA

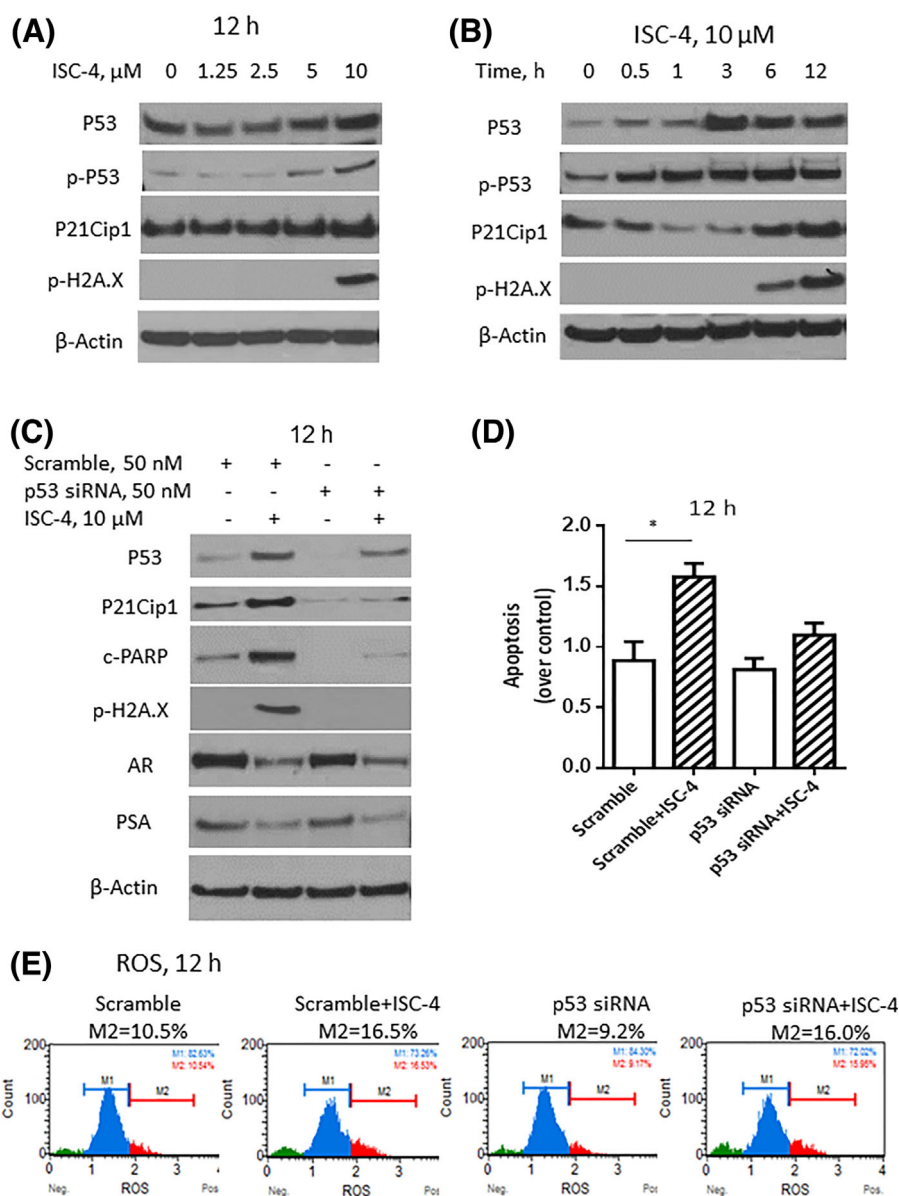


FIGURE 4 ISC-4 activated p53 as a central node for apoptosis. A, Western blot assessment of ISC-4 impact on p53 and its Ser¹⁵ phosphorylation and abundance of p21Cip1 and DNA double strand break marker protein Ser¹³⁹-p-H2A.X in a concentration-titration experiment. LNCaP cells were treated with the indicated concentrations of ISC-4 for 12 h. B, Western blot assessment of ISC-4 impact on p53, Ser¹⁵-p-p53, p21Cip1 and p-H2A.X in a time course experiment. LNCaP cells were treated with 10 μM of ISC-4 for 0.5–12 h. C, Western blot assessment of ISC-4 impact on p53, Ser¹⁵-p-p53, p21Cip1 and p-H2A.X and AR, PSA in LNCaP cells without or with siRNA targeting p53. LNCaP cells were transfected with p53 siRNA (50 nM) or scrambled RNA for 36 h, and were treated with 10 μM of ISC-4 for 12 h. D, Annexin V binding assay to assess apoptosis in cells treated as in (C). Error bar represents SD of triplicate determinations. E, Detection of ROS by dihydroethidium fluorescence in cells as treated in (C)

abundances without initially decreasing their steady state mRNA level (Figure 2E). Future work will address the post-transcriptional mechanism(s) related to increased degradation and/or decreased synthesis of AR and PSA by ISC-4.

As we had shown that MSeA exposure of LNCaP cells did not trigger ROS⁴⁵ nor p53,^{43–44} our findings in the current study revealed a crucial role of NAC-quenchable ROS to trigger and discharge these molecular (AR axis) and cellular (apoptosis) actions of ISC-4 (Figure 3) and the activation of p53 as a critical downstream

nexus for ROS-initiated apoptosis signaling (Figure 4) through PUMA and Bax (Figure 5). Presumably, PUMA might displace Bax from its complexes with anti-apoptotic Bcl-2 family proteins to allow Bax to translocate to the mitochondria and dimerize or oligomerize to activate the cytochrome C-intrinsic caspase activation cascade downstream of p53.⁵⁶ This might explain why depleting Bax would diminish the death execution efficiency of ISC-4 treatment. The finding of crucial p53 mediator role for apoptosis induction in LNCaP cells was consistent with and corroborated by the much reduced

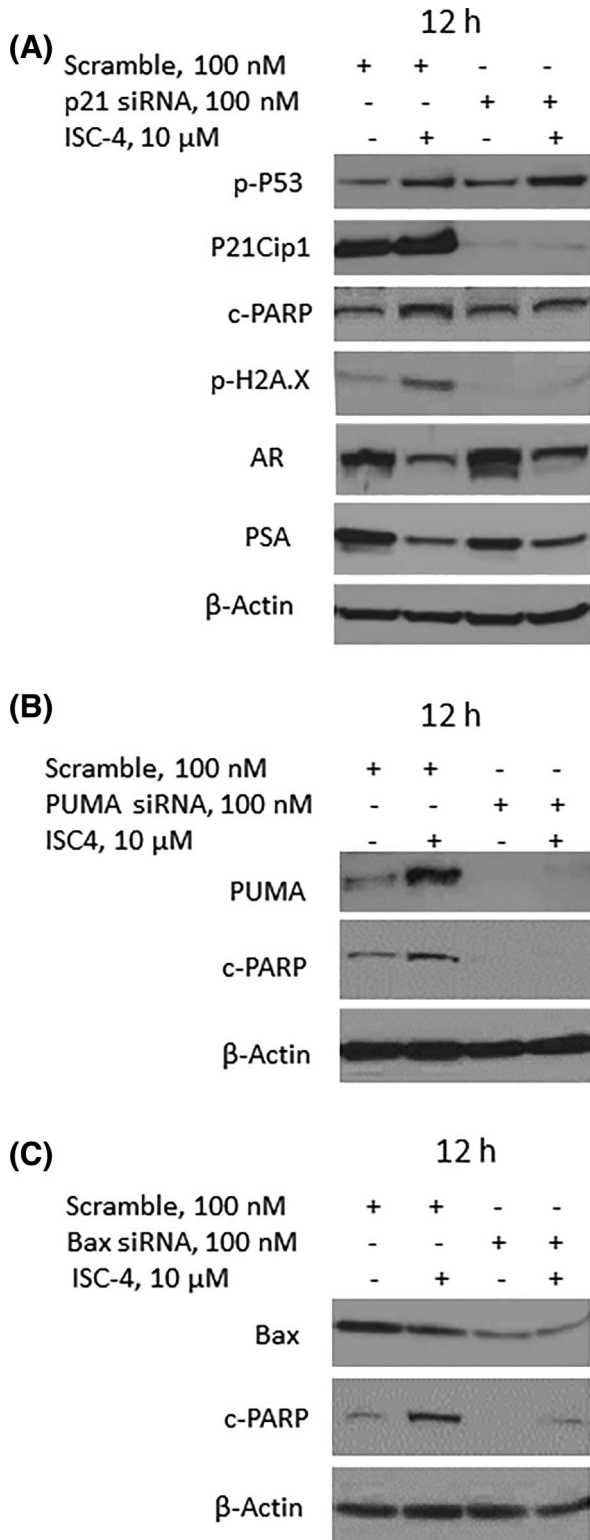


FIGURE 5 Western blot detection proteins of interest to assess the role of select p53 downstream genes in ISC-4-induced apoptosis. A, Depleting p21Cip1 by siRNA. LNCaP cells were transfected with either scrambled or p21Cip1 siRNA (100 nM) for 36 h. Cells were treated with 10 μM of ISC-4 for 12 h. B, Knocking down PUMA by siRNA. C, Knocking down Bax by siRNA. LNCaP cells were transfected with either scrambled or PUMA siRNA or Bax siRNA (100 nM) for 48 h and were treated with 10 μM of ISC-4 for 12 h

apoptosis in p53-null PC-3 cells (Figure 1E). The mechanistic distinctions between ISC-4 and MSeA suggest potential combinatorial benefits of using both types of Se agents for PCa chemoprevention or therapy by targeting crucial molecules and signaling networks through their distinctive and complementary actions.

With respect to ISC-4 mechanisms of action, the combination of dose-response and time course studies along with pharmacological and siRNA approaches enabled us to construct the likely temporal sequence of signaling events and probable cause-effect relationship among a number of molecules interrogated in the LNCaP cells. We graphically summarized these signaling events in Figure 6. However, many questions remain to be investigated over mechanistic details, for instance, what is the subcellular origin(s) of the ROS generation? How does ROS suppress AR and its signaling axis? How does ROS activate p53 axis? What are the protein kinases responsible for phosphorylative activation of p53 or H2A.X?

Given organ site specificity of oncogenesis and driver mutations, it is noteworthy of the significant molecular signaling differences among ISC-4-exposed LNCaP cells and the previously studied melanoma²⁸ and colorectal cancer cells³⁰ in spite of the ISC-4-induced anti-proliferative and apoptosis cellular responses in all these cell lines. Our study of the LNCaP cells did not detect an anticipated inhibitory impact of ISC-4 on AKT phosphorylation (Figure 2A) per inference from the reported potent decrease by ISC-4 in the melanoma cells of pAKT3²⁸ and in colorectal cancer cells of pAKT1/2.³⁰ The LNCaP cells are known not to express AKT3 protein,⁴⁸ therefore unlikely to involve any contribution of AKT3 inhibition by ISC-4 toward its induction of the observed cellular and molecular responses. The efficacy of ISC-4 as a potential chemopreventive agent or therapeutic drug candidate in PCa and its relevant “molecular targets” could not be reliably predicted from the available literature and require empirical experimental approaches for critical hypothesis testing and validation.

In summary, our findings suggest multi-targeting cancer-intrinsic potential of ISC-4 for PCa chemoprevention and therapy through intracellular ROS to discharge the AR signaling inhibition activity and

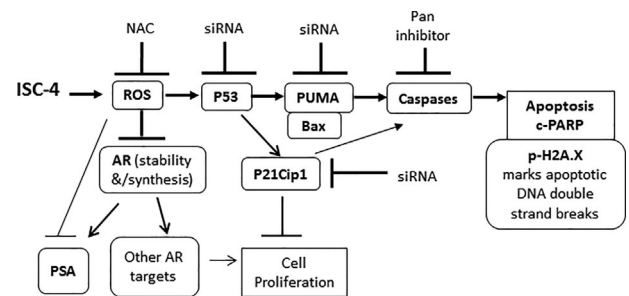


FIGURE 6 Scheme of ISC-4-induced signaling cascades in LNCaP cells. Treatment with ISC-4 rapidly induced intracellular ROS, which then suppressed AR signaling axis, and induced p21Cip1 through p53-dependent pathway to jointly contribute to anti-proliferation (cell cycle arrest, to be studied in future). The intracellular ROS also triggered p53-PUMA/Bax mitochondrial intrinsic death axis to execute caspase-mediated apoptosis, leading to DNA nucleosomal fragments marked by p-H2A.X

activation of p53-PUMA/Bax apoptosis. The data provide strong scientific rationale to justify testing the in vivo efficacy of ISC-4 to prevent or treat PCa in clinically relevant animal models involving AR and p53 signaling to assess its merit for future translation studies. The distinct modes of action of ISC-4 versus MSeA suggest potential combinatorial use of the two Se agents to achieve synergistic anti-cancer efficacy outcome for translation to human PCa patients.

ACKNOWLEDGMENTS

The authors thank Yuka Imamura and the PennState Cancer Institute Genomic Sciences Core facility for next-gen sequencing authentication of cell line and RT qPCR. The work was supported in part by National Cancer Institute, grant no. R01 CA172169.

CONFLICTS OF INTEREST

All authors declare no potential or actual conflicts of interest.

ORCID

Junxuan Lu  <http://orcid.org/0000-0002-2354-7186>

REFERENCES

- Heinlein CA, Chang C. Androgen receptor in prostate cancer. *Endocr Rev.* 2004;25:276–308.
- Petrylak DP, Tangen CM, Hussain MH, et al. Docetaxel and estramustine compared with mitoxantrone and prednisone for advanced refractory prostate cancer. *N Engl J Med.* 2004;351:1513–1520.
- de Bono JS, Oudard S, Ozguroglu M, et al. Prednisone plus cabazitaxel or mitoxantrone for metastatic castration-resistant prostate cancer progressing after docetaxel treatment: a randomised open-label trial. *Lancet.* 2010;376:1147–1154.
- Tran C, Ouk S, Clegg NJ, et al. Development of a second-generation antiandrogen for treatment of advanced prostate cancer. *Science.* 2009;324:787–790.
- Chen CD, Welsbie DS, Tran C, et al. Molecular determinants of resistance to antiandrogen therapy. *Nat Med.* 2004;10:33–39.
- de Bono JS, Logothetis CJ, Molina A, et al. Abiraterone and increased survival in metastatic prostate cancer. *N Engl J Med.* 2011;364:1995–2005.
- Ryan CJ, Smith MR, de Bono JS, et al. Abiraterone in metastatic prostate cancer without previous chemotherapy. *N Engl J Med.* 2013;368:138–148.
- Scher HI, Fizazi K, Saad F, et al. Increased survival with enzalutamide in prostate cancer after chemotherapy. *N Engl J Med.* 2012;367:1187–1197.
- Beer TM, Armstrong AJ, Rathkopf D, et al. Enzalutamide in metastatic prostate cancer before chemotherapy. *N Engl J Med.* 2014;371:424–433.
- Scher HI, Beer TM, Higano CS, et al. Prostate cancer foundation/department of defense prostate cancer clinical trials, c., antitumour activity of mdv3100 in castration-resistant prostate cancer: a phase1-2 study. *Lancet.* 2010;375:1437–1446.
- Arora VK, Schenkein E, Murali R, et al. Glucocorticoid receptor confers resistance to antiandrogens by bypassing androgen receptor blockade. *Cell.* 2013;155:1309–1322.
- Claessens F, Helsen C, Prekovic S, et al. Emerging mechanisms of enzalutamide resistance in prostate cancer. *Nature reviews. Urology.* 2014;11:712–716.
- Fahey JW, Zalcmann AT, Talalay P. The chemical diversity and distribution of glucosinolates and isothiocyanates among plants. *Phytochemistry.* 2001;56:5–51.
- Drewnowski A, Gomez-Carneros C. Bitter taste, phytonutrients, and the consumer: a review. *Am J Clin Nutr.* 2000;72:1424–1435.
- Cinciripini PM, Hecht SS, Henningfield JE, Manley MW, Kramer BS. Tobacco addiction: implications for treatment and cancer prevention. *J Natl Cancer Inst.* 1997;89:1852–1867.
- Xiao D, Zeng Y, Choi S, Lew KL, Nelson JB, Singh SV. Caspase-dependent apoptosis induction by phenethyl isothiocyanate, a cruciferous vegetable-derived cancer chemopreventive agent, is mediated by Bak and Bax. *Clin Cancer Res.* 2005;11:2670–2679.
- Xiao D, Singh SV. Phenethyl isothiocyanate-induced apoptosis in p53-deficient PC-3 human prostate cancer cell line is mediated by extracellular signal-regulated kinases. *Cancer Res.* 2002;62:3615–3619.
- Xiao D, Lew KL, Zeng Y, et al. Phenethyl isothiocyanate-induced apoptosis in PC-3 human prostate cancer cells is mediated by reactive oxygen species-dependent disruption of the mitochondrial membrane potential. *Carcinogenesis.* 2006;27:2223–2234.
- Xiao D, Powolny AA, Moura MB, et al. Phenethyl isothiocyanate inhibits oxidative phosphorylation to trigger reactive oxygen species-mediated death of human prostate cancer cells. *J Biol Chem.* 2010;285:26558–26569.
- Xiao D, Choi S, Lee YJ, Singh SV. Role of mitogen-activated protein kinases in phenethyl isothiocyanate-induced apoptosis in human prostate cancer cells. *Mol Carcinog.* 2005;43:130–140.
- Kim JH, Xu C, Keum YS, Reddy B, Conney A, Kong AN. Inhibition of EGFR signaling in human prostate cancer PC-3 cells by combination treatment with beta-phenylethyl isothiocyanate and curcumin. *Carcinogenesis.* 2006;27:475–482.
- Beklemisheva AA, Feng J, Yeh YA, Wang LG, Chiao JW. Modulating testosterone stimulated prostate growth by phenethyl isothiocyanate via Sp1 and androgen receptor down-regulation. *Prostate.* 2007;67:863–870.
- Wang LG, Liu XM, Chiao JW. Repression of androgen receptor in prostate cancer cells by phenethyl isothiocyanate. *Carcinogenesis.* 2006;27:2124–2132.
- Khor TO, Keum YS, Lin W, et al. Combined inhibitory effects of curcumin and phenethyl isothiocyanate on the growth of human PC-3 prostate xenografts in immunodeficient mice. *Cancer Res.* 2006;66:613–621.
- Powolny AA, Bommareddy A, Hahm ER, et al. Chemopreventive potential of the cruciferous vegetable constituent phenethyl isothiocyanate in a mouse model of prostate cancer. *J Natl Cancer Inst.* 2011;103:571–584.
- Sharma AK, Sharma A, Desai D, et al. Synthesis and anticancer activity comparison of phenylalkyl isoselenocyanates with corresponding naturally occurring and synthetic isothiocyanates. *J Med Chem.* 2008;51:7820–7826.
- Lipinski CA, Lombardo F, Dominy BW, Feeney PJ. Experimental and computational approaches to estimate solubility and permeability in drug discovery and development settings. *Adv Drug Deliv Rev.* 2001;46:3–26.
- Sharma A, Sharma AK, Madhunapantula SV, et al. Targeting Akt3 signaling in malignant melanoma using isoselenocyanates. *Clin Cancer Res.* 2009;15:1674–1685.
- Nguyen N, Sharma A, Sharma AK, et al. Melanoma chemoprevention in skin reconstructs and mouse xenografts using isoselenocyanate-4. *Cancer Prev Res (Phila).* 2011;4:248–258.
- Sharma AK, Kline CL, Berg A, Amin S, Irby RB. The Akt inhibitor ISC-4 activates prostate apoptosis response protein-4 and reduces colon

- tumor growth in a nude mouse model. *Clin Cancer Res.* 2011;17:4474–4483.
31. Isaacs WB, Carter BS, Ewing CM. Wild-type p53 suppresses growth of human prostate cancer cells containing mutant p53 alleles. *Cancer Res.* 1991;51:4716–4720.
 32. Carroll AG, Voeller HJ, Sugars L, Gelmann EP. P53 oncogene mutations in three human prostate cancer cell lines. *Prostate.* 1993;23:123–134.
 33. Veldscholte J, Ris-Stalpers C, Kuiper GG, et al. A mutation in the ligand binding domain of the androgen receptor of human LNCaP cells affects steroid binding characteristics and response to anti-androgens. *Biochem Biophys Res Commun.* 1990;173:534–540.
 34. Li J, Yen C, Liaw D, et al. PTEN, a putative protein tyrosine phosphatase gene mutated in human brain, breast, and prostate cancer. *Science.* 1997;275:1943–1947.
 35. Cancer Genome Atlas Research Network. The molecular taxonomy of primary prostate cancer. *Cell.* 2015;163:1011–1025.
 36. Crampsie MA, Jones N, Das A, et al. Phenylbutyl isoselenocyanate modulates phase I and II enzymes and inhibits 4-(methylnitrosamino)-1-(3-pyridyl)-1-butanone-induced DNA adducts in mice. *Cancer Prev Res (Phila).* 2011;4:1884–1894.
 37. Jiang C, Ganther H, Lu J. Methylselenium-specific inhibition of MMP-2 and VEGF expression: implications for angiogenic switch regulation. *Mol Carcinog.* 2000;29:236–250.
 38. Jiang C, Wang Z, Ganther H, Lu J. Caspases as key executors of methylselenium-induced apoptosis (anoikis) of DU-145 prostate cancer cells. *Cancer Res.* 2001;61:3062–3070.
 39. Li GX, Lee HJ, Wang Z, et al. Superior in vivo inhibitory efficacy of methylseleninic acid against human prostate cancer over selenomethionine or selenite. *Carcinogenesis.* 2008;29:1005–1012.
 40. Wang L, Bonorden MJ, Li GX, et al. Methyl-selenium compounds inhibit prostate carcinogenesis in the transgenic adenocarcinoma of mouse prostate model with survival benefit. *Cancer Prev Res (Phila).* 2009;2:484–495.
 41. Wang L, Guo X, Wang J, et al. Methylseleninic acid superactivates p53-senescence cancer progression barrier in prostate lesions of pten-knockout mouse. *Cancer Prev Res (Phila).* 2016;9:35–42.
 42. Cho SD, Jiang C, Malewicz B, et al. Methyl selenium metabolites decrease prostate-specific antigen expression by inducing protein degradation and suppressing androgen-stimulated transcription. *Mol Cancer Ther.* 2004;3:605–611.
 43. Jiang C, Hu H, Malewicz B, Wang Z, Lu J. Selenite-induced p53 Ser-15 phosphorylation and caspase-mediated apoptosis in LNCaP human prostate cancer cells. *Mol Cancer Ther.* 2004;3:877–884.
 44. Hu H, Jiang C, Li G, Lu J. PKB/AKT and ERK regulation of caspase-mediated apoptosis by methylseleninic acid in LNCaP prostate cancer cells. *Carcinogenesis.* 2005;26:1374–1381.
 45. Li GX, Hu H, Jiang C, Schuster T, Lu J. Differential involvement of reactive oxygen species in apoptosis induced by two classes of selenium compounds in human prostate cancer cells. *Int J Cancer.* 2007;120:2034–2043.
 46. Livak KJ, Schmittgen TD. Analysis of relative gene expression data using real-time quantitative PCR and the 2⁻(Delta Delta C(T)) Method. *Methods.* 2001;25:402–408.
 47. Jiang C, Wang Z, Ganther H, Lu J. Distinct effects of methylseleninic acid versus selenite on apoptosis, cell cycle, and protein kinase pathways in DU145 human prostate cancer cells. *Mol Cancer Ther.* 2002;1:1059–1066.
 48. Graff JR, Konicek BW, McNulty AM, et al. Increased AKT activity contributes to prostate cancer progression by dramatically accelerating prostate tumor growth and diminishing p27Kip1 expression. *J Biol Chem.* 2000;275:24500–24505.
 49. Crampsie MA, Pandey MK, Desai D, Spallholz J, Amin S, Sharma AK. Phenylalkyl isoselenocyanates vs phenylalkyl isothiocyanates: thiol reactivity and its implications. *Chem Biol Interact.* 2012;200:28–37.
 50. Biegging KT, Mello SS, Attardi LD. Unravelling mechanisms of p53-mediated tumour suppression. *Nat Rev Cancer.* 2014;14:359–370.
 51. el-Deiry WS, Tokino T, Velculescu VE, et al. WAF1, a potential mediator of p53 tumor suppression. *Cell.* 1993;75:817–825.
 52. Rogakou EP, Pilch DR, Orr AH, Ivanova VS, Bonner WM. DNA double-stranded breaks induce histone H2AX phosphorylation on serine 139. *J Biol Chem.* 1998;273:5858–5868.
 53. Tu WZ, Li B, Huang B, et al. γH2AX foci formation in the absence of DNA damage: mitotic H2AX phosphorylation is mediated by the DNA-PKcs/CHK2 pathway. *FEBS Lett.* 2013;587:3437–3443.
 54. Turinetti V, Giachino C. Multiple facets of histone variant H2AX: a DNA double-strand-break marker with several biological functions. *Nucleic Acids Res.* 2015;43:2489–2498.
 55. Yu J, Zhang L. PUMA, a potent killer with or without p53. *Oncogene.* 2008;27 Suppl:S71–S83.
 56. Yu J, Wang Z, Kinzler KW, Vogelstein B, Zhang L. PUMA mediates the apoptotic response to p53 in colorectal cancer cells. *Proc Natl Acad Sci U S A.* 2003;100:1931–1936.

SUPPORTING INFORMATION

Additional supporting information may be found online in the Supporting Information section at the end of the article.

How to cite this article: Wu W, Karelia D, Pramanik K, et al.

Phenylbutyl isoselenocyanate induces reactive oxygen species to inhibit androgen receptor and to initiate p53-mediated apoptosis in LNCaP prostate cancer cells.

Molecular Carcinogenesis. 2018;1–12.

<https://doi.org/10.1002/mc.22825>

亲和超滤质谱技术在 中药活性成分筛选中的研究进展

周 慧¹, 王义民¹, 郑 重², 刘 舒², 刘志强²

(1. 吉林大学珠海学院, 广东 珠海 519041;

2. 中国科学院长春应用化学研究所, 吉林 长春 130022)

摘要:亲和超滤质谱技术是 20 世纪 90 年代中期发展起来的一种快速、简单、有效的药物小分子发现模式。该技术利用配体与受体之间特异性结合,通过超滤装置快速筛选活性小分子化合物,再结合液相色谱-质谱联用技术(LC-MS),鉴定活性成分结构。亲和超滤质谱技术集药物活性成分筛选、结构鉴定于一体,尤其适用于从复杂体系中筛选潜在的活性小分子化合物。近年来,针对中药发挥药理作用具有多组分、多靶点的重要特点,亲和超滤质谱技术已被广泛用于从中药提取物中筛选与特定蛋白靶点相结合的小分子活性物质,对阐明中药药效的物质基础和以活性成分作为先导化合物的新药开发具有重要意义,是对传统药物发现方法的有利补充。本工作综述了该技术在中药活性成分筛选中的原理、特点、应用进展,以及对未来的展望。

关键词:亲和超滤质谱(AUF-MS);中药;活性成分筛选

中图分类号:O657.63 **文献标志码:**A

doi:10.7538/zpxb.2018.0033

Recent Advances of Affinity Ultrafiltration Mass Spectrometry in Screening Active Components of Traditional Chinese Medicine

ZHOU Hui¹, WANG Yi-min¹, ZHENG Zhong², LIU Shu², LIU Zhi-qiang²

(1. Department of Chemistry and Pharmacy, Zhuhai College of Jilin University, Zhuhai 519041, China;

2. Changchun Center of Mass Spectrometry, Changchun Institute of Applied Chemistry,

Chinese Academy of Sciences, Changchun 130022, China)

Abstract: Affinity ultrafiltration mass spectrometry (AUF-MS) technology is a rapid, simple and effective method for the discovery and development of small active molecule in traditional Chinese medicine (TCM). This technology was initially developed in the middle of 1990s, which was introduced to target-oriented drug discovery. Through the ligand-receptor specific binding characteristics, the affinity ultrafiltration device can facilitate the rapid screening of small-molecule ligands from the complex extracts, and

收稿日期:2018-03-27;修回日期:2018-05-03

基金项目:国家自然科学基金项目(81403077);吉林省科技发展计划国际科技合作项目(20170414008GH);广东省自然科学基金博士启动项目(2014A030310494)资助

作者简介:周 慧(1982—),女(汉族),吉林长春人,副教授,从事质谱分析研究。E-mail:zhouhuimslab@163.com

high performance liquid chromatography-mass spectrometry (HPLC-MS) assists in the structural identification of potentially active small drug molecules. Thus, AUF-MS has become a powerful tool for identifying bioactive molecules from complex chemical matrices. The general workflow of AUF-MS is not complicated: depending on the molecular weight cut-off of the semi-permeable membrane, the ligand-bound protein complexes are retained by the membrane under centrifugal force to separate the bound and unbound components of the analyte. Bound ligands are eluted from the ultrafiltration membrane by destabilizing the target-ligand complex with an organic solvent or pH change, and then the ligands are consequently subjected to analysis by LC-MS to identify and characterize the low molecular weight compounds that interact with target molecules. The classic strategies of screening active ingredients from natural product, such as the high-throughput screening methods based on ultraviolet fluorimetric or radioactive detection, the traditional phytochemical screening procedure (i. e. isolation, structure elucidation and bioactivity test), are not able to meet the urgent need of contemporary pharmacology research due to its time consumption and a high rate of false positive or negative results. In comparison with those methods, AUF-MS is easier to be operated without unnecessary isolation or purification of inactive compounds and directly screen bioactive ingredients from the Chinese herb. Also, only modest amounts of target proteins are required, which are no labeling or immobilization. We have employed AUF-LC-MS to identify inhibitors of enzymes such as α -glucosidase, xanthine oxidase, neuraminidase from Chinese herb medicine. The results showed that AUF-MS performs better reproducibility and more tolerance of interferences than classic strategies for certain targets. In this review, Firstly, a brief introduction was exhibited about the general procedures of AUF-MS, and the key factors affecting the result of AUF-MS, including the selection of ultrafiltration membrane and dissociation, the dose of receptors. Secondly, the recent applications of AUF-MS to screen potential bioactivity small molecules from the natural product in the past ten years were summarized. These results based on AUF-MS to screen active compounds were expected to be valuable for discovering drug molecules candidates from TCM and efficiently designing drugs for prevention and the treatment of diseases. Finally, the future prospects of AUF-MS were also presented. AUF-MS technology is expected to provide new research ideas for the screening of active components from TCM.

Key words: affinity ultrafiltration mass spectrometry (AUF-MS); Chinese herbal medicine; active components screening

中药活性成分筛选研究是中药现代化的重要组成部分,也是实现中药“走出去”的必经之路。较之传统的人工合成药物设计模式,中药化学成分多样性使其在新药研发方面体现出较大优势。从中药成分中筛选得到的活性物质往往结构新颖、疗效高、不良反应少,既可以直接开发为新药,也可以作为先导化合物进行结构修饰与优化后成为一代新药^[1],现已成为制

药工业中新药研发的来源之一。根据文献^[2]报道,在过去 30 多年时间里,超过 50% 已批准上市的药物直接或间接来源于天然产物。因此,以中药为来源的药物活性成分筛选受到新药研发工作者的推崇。

传统的中药活性成分筛选模式主要以多次提取、分离为基础,其基本思路是利用体外药效评估对提取分离的每一阶段组分进行活性评

价,追踪其活性组分,然后继续追踪活性显著组分,直至获得活性单体成分。但这种研究策略往往实验周期长、工作量大,无法实现大规模、高通量筛选,而且该筛选模式忽略了中药多成分、多靶点、协同作用的特点,导致筛选出的一些药物药用效果较差^[3]。因此,基于疾病靶点的、以活性为导向的高通量筛选研究十分必要。

近年来,随着“精准医疗”计划的提出,传统的药物研究模式已经转向了“精准”靶向药物分子设计策略^[4-5]。以靶标-配体精确相互作用为理论基础,通过药物活性成分与疾病相关的特定生物靶点相互作用,从而发现对靶蛋白具有亲和力、特异性强的小分子配体。亲和超滤质谱(affinity ultrafiltration mass spectrometry, AUF-MS)筛选技术符合精准医疗时代下靶向药物研究的需求,其利用小分子药物配体和靶标之间特异性结合的特性,将具有潜在活性的小分子化合物的混合物与靶标蛋白混合,得到靶标-配体复合物和未结合的小分子,通过超滤装置将未结合的小分子滤除后,将靶标-配体复合物解离,释放出与靶标蛋白结合的活性成分,再利用液相色谱-质谱(HPLC-MS)技术分析活性化合物^[6]。该技术针对特定的疾病靶标进行全面、客观的筛选,获得的天然配体具有药理活性显著、靶向清晰、机制明确等特点,可作为新药研发中具有临床开发价值的候选化合物,且由于利用该方法进行筛选时,大量无活性的化合物被洗掉,加快了活性化合物的解析速度^[7-8]。

特别是随着 HPLC-MS 技术在分子质量检测范围、灵敏度等方面的提高,使得亲和超滤质谱技术从复杂中药体系中筛选和鉴定活性成分的优势更加明显。

本工作将从亲和超滤质谱技术在中药活性成分筛选中的原理、特点、应用进展等方面进行综述。

1 亲和超滤质谱基本概述

1.1 基本原理和分类

亲和超滤是利用已知靶蛋白(受体)与未知体系小分子(配体)特异性地结合,通过超滤膜对不同大小物质选择性的差异实现活性物质的快速分离和筛选。具体操作为:首先,将待筛选体系与选定的靶蛋白进行孵育,使得有亲和活性的小分子与靶蛋白活性位点特异性结合形成受体-配体复合物,没有亲和活性的化合物则游离出来^[9]。然后,利用超滤膜的选择透过性,用缓冲液将未与靶蛋白结合的化合物洗脱下来,将超滤膜截留下来的复合物用一定比例的有机溶剂处理,或者改变体系的 pH 使受体蛋白变性,释放出小分子配体。最后,利用 HPLC-MS 技术快速分析和鉴定小分子活性物质,其原理示于图 1。

亲和超滤技术分为脉冲超滤和离心超滤^[11]。两者筛选小分子活性物质的基本原理相同,均是通过半透膜的选择特异性达到富集配体的目的^[12-13]。脉冲超滤的操作单元由超滤

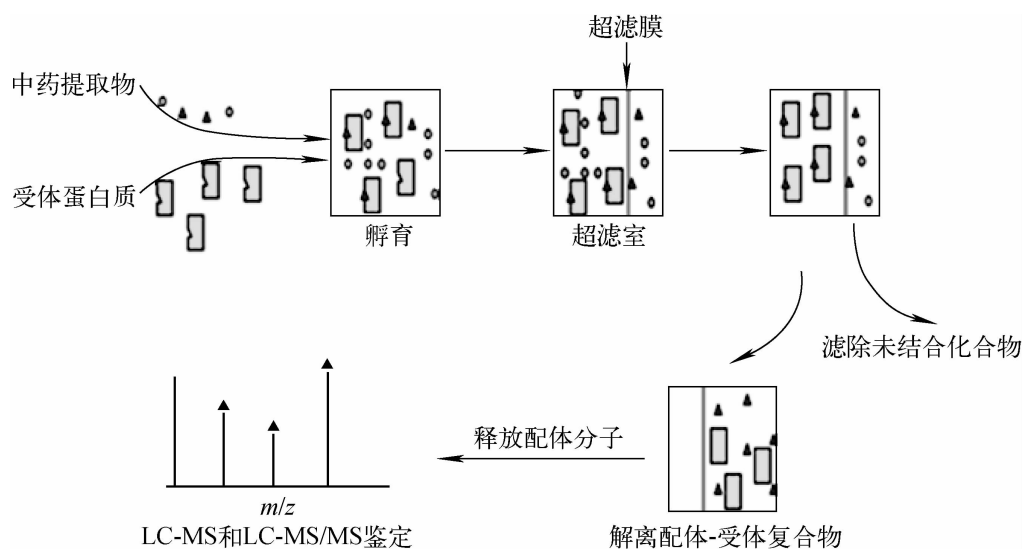


图 1 超滤质谱技术工作原理示意图^[10]

Fig. 1 Scheme of ultrafiltration mass spectrometry^[10]

室(分为上室和下室)、磁力搅拌器和超滤膜组成^[14],脉冲超滤室的两室之间被超滤膜隔开。脉冲超滤的基本筛选过程为:将受体-配体的混合物置于超滤膜上,通过施加一定的压力,选择与受体有一定亲和能力的配体,再通过液相色谱-质谱法对选择得到的配体进行结构鉴定。在脉冲超滤中,可以根据受体-配体混合液体积选择超滤室的大小,还可对超滤室进行控温,以选择最合适的受体-配体反应温度^[15]。离心超滤则采用商品化的超滤离心管,通过离心筛选化合物,不需复杂的操作程序,且实验的重现性良好。但是,较之脉冲超滤,离心超滤过程中往往存在浓差极化现象,导致超滤膜的过滤速度降低,严重的会导致蛋白在膜表面吸附和沉积,从而影响游离药物的转运。离心超滤与脉冲超滤的差异决定了它们的应用范围不同。离心超滤不能与质谱在线联用,主要用于小分子化合物的筛选,应用范围小;脉冲超滤可以实现与质谱在线连接,适用于从组合化学库和天然产物库中筛选小分子物质,尤其在计算靶标和配体的结合常数及药物代谢研究方面优势明显^[15-16]。

1.2 亲和超滤质谱的特点和优势

传统的中药成分筛选活性研究模式通常是对中药化学成分进行提取、分离、结构鉴定,然后进行生物活性测定,确定有效成分。该分离筛选过程操作繁琐、耗时长、对环境不友好,而且容易造成一些微量潜在活性物质的丢失和大量假阳性结果的干扰^[17]。相比之下,亲和超滤质谱技术在筛选活性物质时具有操作简单、效率高、成本低等特点。

首先,亲和超滤所使用的靶分子用量少,且不需要经过固定化处理,经过有机溶剂处理和多次离心即可完成分离工作。这不仅简化了实验步骤,而且避免了蛋白受体经固定化处理带来的变性与失活。其次,由于蛋白受体和小分子配体是在天然溶液状态下进行反应的,不需要进行标记,因此能够保持蛋白的天然构象;同时,能够控制受体和配体的孵育温度,使其在接近生理条件下客观地反映药物小分子和生物大分子的相互作用。另外,超滤实验所需要的靶标用量少,尤其对于价格昂贵的蛋白靶分子,实验后经处理可重复使用,节约了实验成本。最

后,超滤装置通过与具有分离能力的色谱和具有结构鉴定能力的质谱相连,使活性化合物的筛选、分离、鉴定(定性与定量)成为一个连续的过程,实现了高通量、高效率筛选。随着更多类型质谱仪的出现,超滤质谱将会更大程度地满足不同药物活性成分结构鉴定的需要^[18]。

1.3 影响亲和超滤质谱结果的关键因素

在超滤筛选实验过程中,为了减少假阳性或假阴性结果的干扰,获得理想的实验数据,实验设计时必须考虑以下因素:超滤膜的选择、受体的使用剂量、解离液的选择等。

1.3.1 超滤膜的选择 在亲和超滤过程中,超滤膜的选择决定着筛选结果的准确与否。选择超滤膜一般需要遵循2个原则:1)在选择滤膜材质时应尽可能减少靶蛋白和配体与膜的非特异性吸附,目前应用较多的材质主要有再生纤维素、甲基纤维素、聚砜类、PEEK等。2)根据分子截留量的大小选择合适孔径的超滤膜,膜的孔径过小,容易造成膜的堵塞而产生高压,影响膜的过滤效率;膜的孔径过大,容易造成漏筛,同时降低了分子间的结构强度,易导致膜的破裂^[14,17]。根据以往的实验经验,超滤膜的截留分子质量应该小于靶蛋白分子质量的1/3,例如当靶分子分子质量为25 ku时,可以选择截留量为8 ku的超滤膜^[17]。

1.3.2 受体的使用剂量 实验中受体的使用剂量会在一定程度上影响筛选结果。在反应体系中,如果受体的浓度远大于配体,则所有潜在的配体都会与受体结合,从而产生假阳性结果;如果配体浓度远大于受体,则只有结合能力强的配体才能与受体结合,从而导致结合力弱的潜在活性物质被过滤掉,产生假阴性结果。通常来说,确定受体的使用剂量时,应尽量保证靶标与配体的浓度适中,且受体的浓度与结合能力最弱配体的 K_d 值近似相等^[15]。

1.3.3 解离液的选择 在配体和受体完成特异性结合后,如何成功地将配体从复合物中解离出来,并尽可能减少非特异性吸附是影响筛选结果的关键。目前,配体的解离方法主要包括向溶液中加入一定比例的有机溶剂或者加入酸碱溶液以改变体系pH值,使蛋白变性失活,释放出配体分子。

单一使用有机溶剂解离液可能会增加非特

异性吸附,造成假阳性结果,而使用含酸的有机溶剂则能够减少配体与超滤膜的非特异性结合。Nikolic 等^[19]考察了 80% 甲醇和 10% 甲醇+2% 醋酸分别作为洗脱液时,乙嘧啶、甲氧苄氨嘧啶、双嘧达莫这 3 种存在非特异性结合的物质被洗脱下来的响应信号强度,结果表明,使用 10% 甲醇+2% 醋酸解离液比 80% 甲醇解离液获得的假阳性信号明显降低。本课题组 Xu 等^[20]利用超滤技术从中药复方二妙丸中筛选黄嘌呤氧化酶抑制剂时发现,当选择含酸的甲醇-水洗脱液时(50:50, V/V, pH3.3),对比实验组和空白组的色谱图,非特异性结合物质的响应信号较低。因此,在进行超滤筛选时,为了在一定程度上减少非特异性结合,最好选择含酸的有机溶剂作为解离液。

1.3.4 其他影响因素 对于离心超滤,除了以上 3 个重要因素外,靶蛋白与被筛选物质的孵育时间、温度、漂洗次数、离心转速与次数等都会影响筛选结果。如果蛋白与被筛选样品的孵育时间过短,相互作用不充分,容易造成漏筛;若孵育时间过长,两者可能发生反应,活性位点结构发生改变,影响结果准确性;孵育温度的选取会影响蛋白酶的活性;离心转速与次数的选取会影响蛋白与配体间的相互作用。亲和超滤方法不能完全消除假阳性实验结果,即不能完全避免配体与靶蛋白的非特异性结合。因此,在进行超滤实验时,除了增加阴性对照组以减少假阳性结果外,还可在复合物解离前用缓冲液进行多次漂洗,以最大程度减少非特异性吸附。

2 亲和超滤质谱技术在中药活性成分筛选中的应用

中药作为大自然的分子宝库,为药物研发提供了丰富的化合物来源。目前,对于中药活性物质的研究主要以大规模提取分离为基础。首先,通过多步分离、纯化获得单体化合物;然后,通过核磁、质谱等技术手段对其进行结构确认;最后,使用经典的动物、细胞模型进行生物学活性评价。这种研究策略往往实验周期长、工作量大,无法实现大规模、高通量筛选,而且难以分离和提纯具有潜在活性的微量成分。亲和超滤质谱技术不但简化了活性成分的分离、

纯化步骤,可使中药活性成分的筛选与结构鉴定一步完成,而且能够有效避免微量活性物质的漏筛和杂质干扰,可提高筛选结果的准确率,现已广泛用于中药活性成分研究。

本课题组运用亲和超滤质谱技术,从中药复杂体系中成功筛选出多种 α -葡萄糖苷酶抑制剂、黄嘌呤氧化酶抑制剂和神经氨酸酶抑制剂,并考察了中药提取物与生物大分子 DNA、人血清白蛋白的相互作用。Zhou 等^[21]利用离心超滤质谱技术成功地从刺五加叶中鉴定出 7 种具有 α -葡萄糖苷酶抑制活性的物质,包括 4 种黄酮类化合物、3 种酚酸类化合物。然后,利用体外酶活性测定方法进一步比较了刺五加叶提取物中各相关化合物的 α -葡萄糖苷酶抑制活性。结果表明,黄酮醇类糖苷与 α -葡萄糖苷酶的作用强度与糖配基的类型有关;咖啡酰奎宁酸类化合物的 α -葡萄糖苷酶抑制活性不仅与咖啡酰基的数目有关,而且与咖啡酰基和奎宁酸基团连接的位点有关。Liu 等^[22]运用超滤筛选结合超高效液相色谱-电喷雾多级串联质谱(UPLC-DAD-ESI-MSⁿ)和傅里叶变换离子回旋共振质谱(FT-ICR-MS)技术成功地从丹参提取物中筛选出 12 种具有黄嘌呤氧化酶抑制作用的物质,并运用 Nikolic 等^[19]评价 COX-2 抑制剂抑制能力的计算公式,得到这 12 种配体的富集因子。研究表明,1,2-萘醌基团是抑制剂发挥抑制作用的重要结构,脂环上的咪唑和羟基取代可以不同程度增强抑制剂的抑制能力,这一结果可为研发治疗痛风的药物提供借鉴。

超滤质谱技术以快速、灵敏、高通量的特点被广泛应用于从中药提取物中筛选活性成分。但是,目前超滤质谱技术还存在一些不足,例如,化合物与目标靶蛋白的非特异性结合会导致假阳性结果,从而使筛选出的化合物表现出活性很弱或者完全没有活性。为减少假阳性结果,在超滤筛选时可以引入变性酶作为对照组。Yang 等^[23]分别以活性酪氨酸酶和变性酪氨酸酶为靶标进行 2 个平行实验,采用 UPLC-DAD-MSⁿ 技术对实验组和对照组的滤液进行分析,从桑椹叶提取物中成功筛选鉴定出 12 种具有酪氨酸酶结合活性的物质,再通过体外酶活性实验进行验证,最后发现了槲皮素 D-吡喃葡萄糖苷和山奈酚 D-吡喃葡萄糖苷 2 种新的

酪氨酸酶抑制剂。

引入变性酶作为对照组虽然在一定程度上可以减少假阳性结果。但是,一些靶蛋白变性后溶解度会下降,影响筛选结果。为解决这一问题,Song 等^[24]引入了靶蛋白酶活性位点阻断剂,从菊花中筛选并鉴定出 4 种黄嘌呤氧化酶抑制剂。非布索坦是黄嘌呤氧化酶的强效抑制剂,当其在复杂体系中与潜在的抑制酶共存时,能够与潜在配体在黄嘌呤氧化酶活性位点上产生竞争性结合,从而间接减少化合物和靶分子的过度结合。利用这一特性,通过比较添加了竞争性配体的实验组和没有添加非布索坦的对照组解离液的色谱图,发现具有潜在抑制活性的物质在实验组的色谱图峰高要明显低于对照组,实验过程示于图 2。此实验结果表明,加入酶活性位点阻断剂可以有效减少非特异结合引起的假阳性结果,从而提高亲和超滤的准确性。在此基础上,该课题组将亲和超滤与分子芯片对接技术相结合,研究小分子与酶的相互作用,筛选潜在天然酶抑制剂^[25]。具体筛选过程为:首先,利用亲和超滤质谱技术从提取物中筛选出小分子活性物质;其次,对筛选出的小分子活性物质进行结构改造,得到一系列新的化合物;最后,利用分子芯片对接技术模拟结构改造后的新化合物与靶分子之间的相互作用,预测它们的活性,并结合体外酶活性实验进行验证。该课题组将超滤与分子芯片对接技术应用于筛选中药复方制剂脉络宁注射剂中的黄嘌呤氧化酶(XOD)抑制剂成分,成功筛选并鉴定出 3 种能够与 XOD 特异性结合的活性成分。然后,对筛选得到的 3 种成分进行结构优化,得到 14 种化合物,并利用分子对接技术模

拟了此 14 种化合物与 XOD 的结合情况,通过预测这些物质的活性并结合体外酶活性实验,最终发现 3,4-二咖啡酰奎宁酸甲酯和 3,5-二咖啡酰奎宁酸甲酯为 XOD 的强效抑制剂,且测得此二者的 IC_{50} 值低于已上市的抗痛风药别嘌醇。由此可见,利用超滤质谱技术不仅可以从中药提取物中直接筛选活性物质,还可以结合计算机模拟技术对已鉴定的活性物质进行结构改造形成组合化学库,从而进行二次筛选,可为高活性中药先导化合物的发现提供资料和思路。

线粒体不仅是细胞内能量合成的重要场所,还与氧自由基的产生、细胞死亡进程调控有关。早期研究表明^[26],帕金森病、阿尔茨海默氏症、糖尿病、肿瘤等疾病和衰老均与线粒体功能异常有关,因此,以线粒体为药理学靶点的药物筛选意义重大。不同于常见的以单一靶蛋白为靶标从复杂基质中筛选活性物质,Yang 等^[27]通过离心超滤与液相色谱-质谱联用技术建立了以线粒体为靶向的生物活性筛选平台,其使用阳性对照组对该方法的适用性进行评价,并优化了靶细胞器、样品浓度和孵育时间,成功地检测到 19 种生物活性化合物,并通过体外药理学实验证实其中 9 种物质能够与靶线粒体活性位点结合。杨兴鑫等^[28]应用基于线粒体的离心超滤-液相色谱-质谱法,从中药葛根和川芎中筛选得到了 23 种可与线粒体结合的活性化合物,并鉴定了其中 17 种化合物。在此基础上,采用体外药理学实验证实了 7 种化合物具有调节线粒体功能的作用。此外,研究人员还发现,洋川芎内 A 和 3'-羟基葛根素可抑制 HepG2 细胞增殖,提高缺氧/复氧所致损伤的心肌细胞存活率。该研究结果可为深入阐释

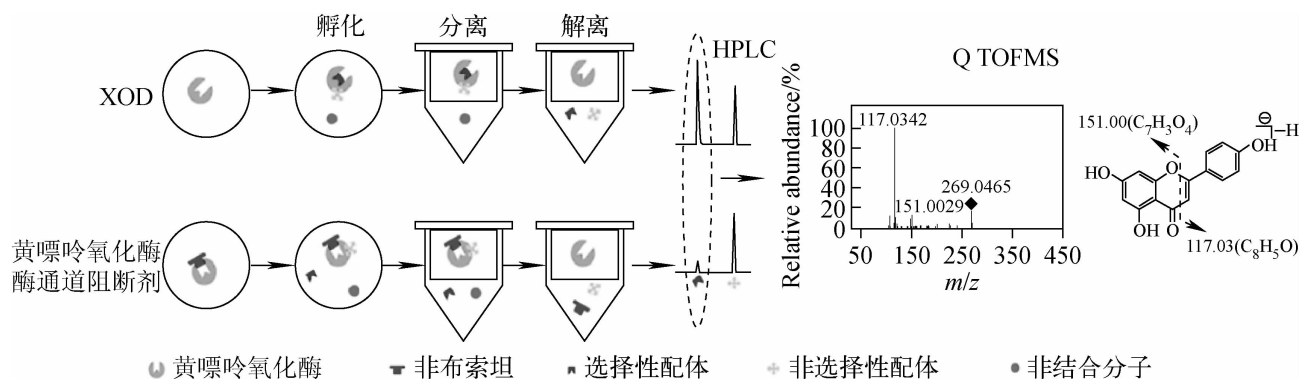


图 2 加入非布索坦阻断剂的亲和超滤筛选示意图^[24]

Fig. 2 General workflow for AUF-MS screening method combined with febuxostat^[24]

中药治疗线粒体相关疾病的机理及开发线粒体靶向新药提供重要的科学依据。

研究者还将亲和超滤和代谢组学技术相结合进行药物机制研究。Fu 等^[29]应用基于高分辨质谱的代谢组学分析技术从甘草粗提取物中发现了 30 种和 22 种分别能与埃博拉病毒核蛋白和马尔堡病毒核蛋白结合的配体,经混合物单体分离、单体活性测定法结合生物化学分析方法,最终确定 18- β 甘草次酸和甘草查儿酮 A 能够显著降低病毒核蛋白的热稳定性并诱导形成

核蛋白寡聚体,且应用生化实验证实 18- β 甘草次酸能有效阻止病毒 RNA 片段与埃博拉病毒核蛋白的结合。该研究结果揭示了中药甘草在抗病毒方面的作用机制,为抗病毒药物的开发提供了借鉴,并且为中药甘草相关的复方研究提供了实验数据。

近年来,亲和超滤质谱与细胞和生化实验相结合,已广泛应用于中药提取物活性物质筛选研究中。近 6 年来,亲和超滤质谱技术在中药有效成分筛选中的研究实例列于表 1。

表 1 亲和超滤质谱技术在中药活性成分筛选中的应用^[9,17]

Table 1 Application of AUF-MS to target-oriented drug discovery in screening active components of TCMs^[9,17]

靶标 Targets	分析物 Analytes	分析方法 Analytical methods	文献 References	
酪氨酸酶	桑叶	UPLC-DAD-MS ^a	23	
	甘草根	HPLC-DAD-ESI-ion trap MS	30	
	苍耳果实提取物	HPLC-DAD	31	
	α -葡萄糖苷酶	降香黄檀	HPLC-DAD-ESI-MS ^a	32
		黄连提取物	HPLC-DAD-ESI-MS ^a	33
		人参茎叶总皂苷	HPLC-DAD-ESI-MS ^a	34
		玉竹	HPLC-DAD, HPLC-Q/TOF MS	35
		黄芩	HPLC-DAD-ESI-MS	36
		竹节参	UHPLC-DAD-ESI-ion trap MS	37
		山竹果	HPLC-ESI-ion trap MS	38
黄嘌呤氧化酶	黄芩根提取物	HPLC-ESI-Q/TOF MS	39	
	银杏叶提取物	HPLC-DAD-ESI-ion trap MS	40	
	番石榴叶茶	HPLC-ESI-TOF MS	41	
	丹参	UPLC-DAD-ESI-MS ^a , FT-ICR-MS	22	
	卷柏	HPLC-PDA-ESI-MS, UPLC-QqQ-MS	42	
	脉络宁注射液	HPLC-ESI-Q/TOF MS	25	
	菊花	HPLC-ESI-Q/TOF MS	24	
脂肪酶	珠子参	UHPLC-DAD-ESI-ion trap MS	43	
	五苓散、泽泻、小陷胸汤、小柴胡汤	HPLC-ESI-ion trap MS	44	
神经氨酸酶	铁皮石斛	HPLC-ESI-Q/TOF MS	45	
	复方板蓝根颗粒	HPLC-PDA-ESI-ion trap MS	46	
神经氨酸酶	黄芩	HPLC-DAD-ESI-ion trap MS	47	
	女贞子	UPLC-PDA-ESI-ion trap MS	48	
环氧化酶-2	生姜	HPLC-ESI-QqQ-MS	49	
	羌活、丹参、当归、独活等 11 种草药	HPLC-ESI-Q/TOF MS, HPLC-APPI-QqQ-MS	50	
	川乌	UPLC-DAD-ESI-ion trap MS	51	
人血清白蛋白	甘草	HPLC-ESI-Q/TOF MS	52	
	丹红注射液	HPLC-ESI-Q-TOF-HRMS	53	
环氧合酶-1	羌活、丹参、当归、独活等 11 种草药	HPLC-ESI-Q/TOF MS	50	
DNA	红车轴草	HPLC-ESI-ion trap MS	54	
乙醇脱氢酶	甘草	HPLC	55	

续表 1

靶标 Targets	分析物 Analytes	分析方法 Analytical methods	文献 References
芳香化酶	延胡索	HPLC-DAD-ESI-MS ⁿ	56
线粒体	虎杖、黄芩	HPLC-DAD-ESI-IT-TOF-MS ⁿ	27
α -淀粉酶	山楂叶	HPLC-ion trap MS	57
过氧化物酶体增殖剂激活受体	艾叶	HPLC-ESI-QqQ-MS	58
蛋白酪氨酸磷酸酶 1B	中国红曲米	UPLC-ESI-Q-TOF-MS	59
乙酰胆碱酯酶	黄连根	HPLC-ESI-Q/TOF MS	60
5-脂氧合酶	防风、土茯苓、葛根和红花	HPLC-ESI-MS ⁿ	61
基质金属蛋白酶-2	土茯苓、菝葜和防风	HPLC-ESI-MS ⁿ	62
磷酸二酯酶	杜仲	HPLC-HSCCC-ESI-MS	63
马尔堡病毒	甘草	UPLC-ESI-Q/TOF MS	64
恶性疟原虫硫氧还蛋白和 谷胱甘肽还原酶	姜黄素类化合物	RRLC-ESI-Q/TOF MS	65
拓扑异构酶 I	臭李子	HPLC-ESI-MS/MS	66

3 结论与展望

中药发挥药理作用具有多成分、多靶点、协同作用的特点。因此,如何快速、一体化地实现中药多种活性成分筛选及鉴定是艰巨却意义重大的工作。基于靶标,以生物活性为导向的亲亲和超滤质谱技术的出现,提高了从复杂中药成分体系中识别目标成分的特异性和灵敏性,且能够实现大规模、高通量筛选,已被研究者广泛应用到特定靶标的活性物质筛选中。在未来的研究中,可考虑以超滤技术为核心,设计在线超滤池,通过将多个超滤池并联后与液相色谱串联,进一步实现样品的高通量超滤筛选。这样,超滤技术不但可用于研究 1 种药物与单一作用靶点或多个靶点的相互作用,还可研究多种药物与单一作用靶点或多个靶点的相互作用,符合中药治疗疾病的整体作用理论。此外,超滤技术也可用于研究中药小分子作用机制。随着基于超滤膜分离和高分辨质谱技术的发展,亲和超滤质谱技术将在中药活性成分研究,特别是高通量药物筛选方面发挥更大的作用。

参考文献:

- [1] 朱大元. 中药活性成分研究是中药现代化的重要组成部分[J]. 化学进展, 2009, 21(1): 24-29.
ZHU Dayuan. Studies on active ingredients of TCM-The essential part of TCM's modernization [J]. Progress in Chemistry, 2009, 21(1): 24-29 (in Chinese).
- [2] ATANASOV A G, WALTENBERGER B, PFERSCHY-WENZIG E M, et al. Discovery and resupply of pharmacologically active plant-derived natural products: a review[J]. Biotechnol Adv, 2015, 33(8): 1 582-1 614.
- [3] POTTERAT O, HAMBURGER M. Concepts and technologies for tracking bioactive compounds in natural product extracts: generation of libraries, and hyphenation of analytical processes with bioassays[J]. Nat Prod Rep, 2013, 30(4): 546-564.
- [4] 展鹏, 王学顺, 刘新泳. “精准医疗”背景下的分子靶向药物研究-精准药物设计策略浅析[J]. 化学进展, 2016, 28(9): 1 363-1 386.
ZHAN Peng, WANG Xueshun, LIU Xinyong. Contemporary molecular targeted drug in the context of “Precision medicine”: an attempting discussion of “Precision drug design”[J]. Progress in Chemistry, 2016, 28(9): 1 363-1 386 (in Chinese).
- [5] NEWMAN D J, CRAGG G M. Natural products as sources of new drugs from 1981 to 2014[J]. J Nat Prod, 2016, 79(3): 629-661.
- [6] 周慧, 宋凤瑞, 刘志强, 等. 超滤质谱技术在药物小分子与生物靶分子相互作用研究中的应用进展[J]. 化学进展, 2010, 22(11): 2 207-2 214.
ZHOU Hui, SONG Fengrui, LIU Zhiqiang, et al. Applications of ultrafiltration mass spectrometry in the studies on interaction between small drug molecule and biological target[J]. Progress in Chemistry, 2010, 22(11): 2 207-2 214 (in Chinese).

- Chinese).
- [7] QIN S S, REN Y R, FU X, et al. Multiple ligand detection and affinity measurement by ultrafiltration and mass spectrometry analysis applied to fragment mixture screening[J]. *Analytica Chimica Acta*, 2015, 886: 98-106.
- [8] ZHANG G, GUO X H, WANG S S, et al. Screening and identification of natural ligands of tyrosinase from *Pueraria lobata Ohwi* by combination of ultrafiltration and LC-MS[J]. *Analytical Methods*, 2017, 9(33): 4 858-4 862.
- [9] WEI H, ZHANG X, TIAN X, et al. Pharmaceutical applications of affinity-ultrafiltration mass spectrometry: recent advances and future prospects[J]. *J Pharm Biomed Anal*, 2016, 131: 444-453.
- [10] LIU D, GUO J, LUO Y, et al. Screening for ligands of human retinoid X receptor- α using ultrafiltration mass spectrometry[J]. *Anal Chem*, 2007, 79(24): 9 398-9 402.
- [11] CHEN C J, CHEN S, WOODBURY C P, et al. Pulsed ultrafiltration characterization of binding [J]. *Analytical Biochemistry*, 1998, 261(2): 164-182.
- [12] WHITLAN J B, BROWM K F. Ultrafiltration in serum protein binding determinations[J]. *Journal of Pharmaceutical Sciences*, 1981, 70(2): 146-150.
- [13] WIEBOLDT R, ZWEIGENBAUM J, HENION J. Immunoaffinity ultrafiltration with ion spray HPLC/MS for screening small-molecule libraries [J]. *Analytical Chemistry*, 1997, 69(9): 1 683-1 691.
- [14] 赵宏艳,张勇忠,肖春玲. 亲和超滤 HPLC-MS 法的研究进展[J]. *药学学报*, 2009, 44(10): 1 084-1 088.
- ZHAO Hongyan, ZAHNG Yongzhong, XIAO Chunling. Advance in the study of affinity selection ultrafiltration HPLC-MS[J]. *Acta Pharmaceutica Sinica*, 2009, 44(10): 1 084-1 088 (in Chinese).
- [15] GEOGHEGAN K F, KELLY M A. Biochemical applications of mass spectrometry in pharmaceutical drug discovery[J]. *Mass Spectrometry Reviews*, 2005, 24(3): 347-366.
- [16] GHOSH R, PAN S, WANG L J, et al. A pulsed tangential-flow ultrafiltration technique for studying protein-drug binding [J]. *J Pharm Sci*, 2013, 102(8): 2 679-2 688.
- [17] 郭思琪,杨华,李萍. 亲和超滤结合液质技术在中药有效成分发现中的应用[J]. *药学学报*, 2016, 51(7): 1 060-1 067.
- WU Siqu, YANG Hua, LI Ping. Application of the affinity ultrafiltration coupled with LC-MS technology in screening active components of traditional Chinese medicines[J]. *Acta Pharmaceutica Sinica*, 2016, 51(7): 1 060-1 067 (in Chinese).
- [18] 王兆伏,宋凤瑞,刘志强,等. 质谱技术在中药小分子与生物大分子相互作用研究中的应用 [J]. *质谱学报*, 2010, 31(3): 129-137.
- WANG Zhaofu, SONG Fengrui, LIU Zhiqiang, et al. Application of mass spectrometry in the study of binding interactions between small molecules in chinese medicinal herbs and biomacromolecules [J]. *Journal of Chinese Mass Spectrometry Society*, 2010, 31(3): 129-137 (in Chinese).
- [19] NIKOLIC D, HABIBI-GOUDARZI S, CORLEY D G, et al. Evaluation of cyclooxygenase-2 inhibitors using pulsed ultrafiltration mass spectrometry [J]. *Analytical Chemistry*, 2000, 72(16): 3 853-3 859.
- [20] 徐晨,刘舒,刘志强,等. 离心超滤质谱法筛选中药复方二妙丸中黄嘌呤氧化酶抑制剂[J]. *高等学校化学学报*, 2014, 35(8): 1 640-1 645.
- XU Chen, LIU Shu, LIU Zhiqiang, et al. Screening of xanthine oxidase inhibitors in traditional Chinese herbal formulae ermiaowan using ultrafiltration UPLC-MSⁿ [J]. *Chemical Journal of Chinese Universities*, 2014, 35(8): 1 640-1 645 (in Chinese).
- [21] ZHOU H, XING J P, LIU S, et al. Screening and determination for potential alpha-glucosidase inhibitors from leaves of *Acanthopanax senticosus* harms by using UF-LC/MS and ESI-MSⁿ [J]. *Phytochem Anal*, 2012, 23(4): 315-323.
- [22] LIU Y, LIU S, LIU Z Q. Screening and determination of potential xanthine oxidase inhibitors from *Radix salviae Miltiorrhizae* using ultrafiltration liquid chromatography-mass spectrometry [J]. *J Chromatogr B Analyt Technol Biomed Life Sci*, 2013, 923-924(4): 48-53.
- [23] YANG Z Z, ZHANG Y F, SUN L J, et al. An

- ultrafiltration high-performance liquid chromatography coupled with diode array detector and mass spectrometry approach for screening and characterising tyrosinase inhibitors from mulberry leaves[J]. *Anal Chim Acta*, 2012, 719(6): 87-95.
- [24] SONG H P, ZHANG H, FU Y, et al. Screening for selective inhibitors of xanthine oxidase from Flos Chrysanthemum using ultrafiltration LC-MS combined with enzyme channel blocking[J]. *Journal Chromatography B*, 2014, 961: 56-61.
- [25] SONG H P, CHEN J, HONG J Y, et al. A strategy for screening of high-quality enzyme inhibitors from herbal medicines based on ultrafiltration LC-MS and in silico molecular docking[J]. *Chem Commun (Camb)*, 2015, 51(8): 1 494-1 497.
- [26] MURPHY M P, SMITH R A. Drug delivery to mitochondria: the key to mitochondrial medicine[J]. *Advanced Drug Delivery Reviews*, 2000, 41(2 000): 235-250.
- [27] YANG X X, XU F, WANG D, et al. Development of a mitochondria-based centrifugal ultrafiltration/liquid chromatography/mass spectrometry method for screening mitochondria-targeted bioactive constituents from complex matrixes: herbal medicines as a case study[J]. *J Chromatogr A*, 2015, 1 413: 33-46.
- [28] 杨兴鑫,周瑜珍,徐凤,等. 基于线粒体的离心超滤/液相色谱/质谱法筛选中药线粒体靶向活性成分[EB/OL]. 北京:中国科技论文在线[2017-07-10]. <http://www.paper.edu.cn/releasepaper/content/201707-29>.
- [29] FU X, WANG Z H, Li L X, et al. Novel chemical ligands to ebola virus and marburg virus nucleoproteins identified by combining affinity mass spectrometry and metabolomics approaches[J]. *Sci Rep*, 2016, 6: 1-13.
- [30] LIU L L, SHI S Y, CHEN X Q, et al. Analysis of tyrosinase binders from *Glycyrrhiza uralensis* root: evaluation and comparison of tyrosinase immobilized magnetic fishing-HPLC and reverse ultrafiltration-HPLC[J]. *Journal of Chromatography B*, 2013, 932(Suppl C): 19-25.
- [31] WANG Z Q, HWANG S H, HUANG B, et al. Identification of tyrosinase specific inhibitors from *Xanthium strumarium* fruit extract using ultrafiltration-high performance liquid chromatography [J]. *Journal of Chromatography B*, 2015, 1 002(Suppl C): 319-328.
- [32] ZHAO C F, LIU Y Q, CONG D I, et al. Screening and determination for potential alpha-glucosidase inhibitory constituents from *Dalbergia odorifera* T. Chen using ultrafiltration-LC/ESI-MSⁿ [J]. *Biomed Chromatogr*, 2013, 27(12): 1 621-1 629.
- [33] ZHOU H, JIANG T, WANG Z Y, et al. Screening for potential α -Glucosidase inhibitors in *Coptis chinensis* franch extract using ultrafiltration LC-ESI-MSⁿ [J]. *Pak J Pharm*, 2014, 27(6): 2 007-2 012.
- [34] 何忠梅,王晓慧,李国峰,等. 靶向亲和液质联用技术对人参茎叶总皂苷中 α -葡萄糖苷酶抑制剂的快速筛选[J]. *分析化学研究报告*, 2013, 41(11):1 694-1 698.
- HE Zhongmei, WANG Xiaohui, LI Guofeng, et al. Screening and structures characterization of α -Glucosidase inhibitors from total saponins of ginseng stems and leaves by ultrafiltration LC-MSⁿ[J]. *Chinese Journal of Analytical Chemistry*, 2013, 41(11): 1 694-1 698(in Chinese).
- [35] ZHOU X I, LIANG J S, ZHANG Y, et al. Separation and purification of α -glucosidase inhibitors from *Polygonatum odoratum* by stepwise high-speed counter-current chromatography combined with Sephadex LH-20 chromatography target-guided by ultrafiltration-HPLC screening[J]. *Journal of Chromatography B*, 2015, 985(Suppl C): 149-154.
- [36] ZHAO H D, ZHANG Y P, GUO Y, et al. Identification of major α -glucosidase inhibitors in Radix Astragali and its human microsomal metabolites using ultrafiltration HPLC-DAD-MSⁿ [J]. *J Pharm Biomed Anal*, 2015, 104: 31-37.
- [37] LI S N, TANG Y, LIU C M, et al. Development of a method to screen and isolate potential α -glucosidase inhibitors from *Panax japonicus* C. A. Meyer by ultrafiltration, liquid chromatography, and counter-current chromatography[J]. *J Sep Sci*, 2015, 38(12): 2 014-2 023.
- [38] 唐英,刘春明,任浚萁,等. 山竹果中 α -葡萄糖苷酶和黄嘌呤氧化酶抑制剂的超滤质谱分析[J]. *时珍国医国药*, 2015, 26(10): 2 322-2 325.

- TANG Ying, LIU Chunming, REN Junqi, et al. Screening of α -glucosidase and xanthine oxidase inhibitors from *Garcinia mangostana* extract using ultrafiltration HPLC-ESI-MS [J]. *LiShiZhen Medicine and Materia Medica Research*, 2015, 26(10): 2 322-2 325(in Chinese).
- [39] YANG J R, LUO J G, KONG L Y. Determination of α -glucosidase inhibitors from *Scutellaria baicalensis* using liquid chromatography with quadrupole time of flight tandem mass spectrometry coupled with centrifugal ultrafiltration [J]. *Chinese Journal of Natural Medicines*, 2015, 13(3): 208-214.
- [40] 刘洋,周慧,刘舒,等. 银杏叶中 α -葡萄糖苷酶抑制剂的超滤质谱筛选[J]. *高等学校化学学报*, 2013,34(4):813-818.
- LIU Yang, ZHOU Hui, LIU Shu, et al. Screening of α -glucosidase inhibitors in *Ginkgo biloba* extract using ultrafiltration LC-ESI-MSⁿ [J]. *Chemical Journal of Chinese Universities*, 2013, 34(4): 813-818(in Chinese).
- [41] WANG L, LIU Y F, LUO Y, et al. Quickly screening for potential α -glucosidase inhibitors from *Guava leaves* tea by bioaffinity ultrafiltration coupled with HPLC-ESI-TOF/MS method [J]. *J Agric Food Chem*, 2018, 66(6): 1 576-1 582.
- [42] WANG J, LIU S, MA B, et al. Rapid screening and detection of XOD inhibitors from *S-tamariscina* by ultrafiltration LC-PDA-ESI-MS combined with HPLC [J]. *Anal Bioanal Chem*, 2014, 406(28): 7 379-7 387.
- [43] LI S N, TANG Y, LIU C M, et al. Development of a method to screen and isolate potential xanthine oxidase inhibitors from *Panax japonicus* var *via* ultrafiltration liquid chromatography combined with counter-current chromatography [J]. *Talanta*, 2015, 134: 665-673.
- [44] XIAO S, YU R R, AI N, et al. Rapid screening natural-origin lipase inhibitors from hypolipidemic decoctions by ultrafiltration combined with liquid chromatography-mass spectrometry [J]. *Journal of Pharmaceutical and Biomedical Analysis*, 2015, 104(Suppl C): 67-74.
- [45] TAO Y, CAI H, LI W D, et al. Ultrafiltration coupled with high-performance liquid chromatography and quadrupole-time-of-flight mass spectrometry for screening lipase binders from different extracts of *Dendrobium officinale* [J]. *Analytical and Bioanalytical Chemistry*, 2015, 407(20): 6 081-6 093.
- [46] LIU S, YAN J, XING J P, et al. Characterization of compounds and potential neuraminidase inhibitors from the *n*-butanol extract of Compound Indigowoad Root Granule using ultrafiltration and liquid chromatography-tandem mass spectrometry [J]. *J Pharm Biomed Anal*, 2012, 59(1): 96-101.
- [47] 刘舒,邢俊鹏,闫峻,等. 中药黄芩中神经氨酸酶抑制剂的超滤质谱筛选研究 [J]. *化学学报*, 2011,69(11):1 570-1 574.
- LIU Shu, XING Junpeng, YAN Jun, et al. Screening and structures characterization of neuraminidase inhibitors from Radix *Scutellaria* extract by ultrafiltration LC-MSⁿ [J]. *Acta Chimica Sinica*, 2011, 69(11): 1 570-1 574(in Chinese).
- [48] ZHANG Y C, HE Y, LIU C Y, et al. Screening and isolation of potential neuraminidase inhibitors from leaves of *Ligustrum lucidum* Ait. based on ultrafiltration, LC/MS, and online extraction-separation methods [J]. *Journal of Chromatography B*, 2018, 1 083: 102-109.
- [49] VAN BREEMEN R B, TAO Y, LI W K. Cyclooxygenase-2 inhibitors in ginger (*Zingiber officinale*) [J]. *Fitoterapia*, 2011, 82(1): 38-43.
- [50] CAO H M, YU R, CHOI Y S, et al. Discovery of cyclooxygenase inhibitors from medicinal plants used to treat inflammation [J]. *Pharmacological Research*, 2010, 61(6): 519-524.
- [51] ZHU H B, LIU S, LI X, et al. Bioactivity fingerprint analysis of cyclooxygenase-2 ligands from Radix *Aconiti* by ultrafiltration-UPLC-MSⁿ [J]. *Analytical and Bioanalytical Chemistry*, 2013, 405(23): 7 437-7 445.
- [52] 王献,喻花,潘子昂,等. 超滤质谱法研究人血清白蛋白与甘草提取物的相互作用 [J]. *中南民族大学学报*, 2015,34(3):25-28.
- WANG Xian, YU Hua, PAN Ziang, et al. Study on the interaction between human serum albumin and licorice extracts by ultrafiltration mass spectrometry [J]. *Journal of South-Central University for Nationalities*, 2015, 34(3): 25-28(in Chinese).

- [53] ZHU J F, YI X J, HUANG P, et al. Drug-protein binding of Danhong injection and the potential influence of drug combination with aspirin: insight by ultrafiltration LC-MS and molecular modeling[J]. *Journal of Pharmaceutical and Biomedical Analysis*, 2017, 134: 100-107.
- [54] 马蕾,王兆伏,陈丽娜,等. 红车轴草总异黄酮成分 DNA 结合剂的超滤质谱筛选[J]. *高等学校化学学报*, 2013, 34(2): 331-335.
MA Lei, WANG Zhaofu, CHEN Lina, et al. Screening DNA binders from isoflavone extracts of red clover by centrifugal ultrafiltration-LC-MSⁿ[J]. *Chemical Journal of Chinese Universities*, 2013, 34(2): 331-335(in Chinese).
- [55] CHEN M, LIU L L, CHEN X Q. Preparative isolation and analysis of alcohol dehydrogenase inhibitors from *Glycyrrhiza uralensis* root using ultrafiltration combined with high-performance liquid chromatography and high-speed counter-current chromatography[J]. *Journal of Separation Science*, 2014, 37(13): 1 546-1 551.
- [56] SHI J, ZHANG X Y, Ma Z J, et al. Characterization of aromatase binding agents from the dichloromethane extract of *Corydalis yanhusuo* using ultrafiltration and liquid chromatography tandem mass spectrometry[J]. *Molecules*, 2010, 15(5): 3 556-3 566.
- [57] 陶益,陈锥,张玉峰. 亲和超滤耦联液相色谱质谱快速检测山楂叶中的 α -淀粉酶抑制剂[J]. *分析化学研究报告*, 2013, 41(2): 229-234.
TAO Yi, CHEN Zhui, ZHANG Yufeng. Characterization of α -Amylase binding agents from Hawthorn leaf using ultrafiltration and liquid chromatography tandem mass spectrometry[J]. *Chinese Journal of Analytical Chemistry*, 2013, 41(2): 229-234(in Chinese).
- [58] CHOI Y S, JUNG Y J, KIM S N. Identification of Eupatilin from *Artemisia argyi* as a selective PPAR α agonist using affinity selection ultrafiltration LC-MS[J]. *Molecules*, 2015, 20(8): 13 753-13 763.
- [59] JIN Y, CHENG X H, JIANG F Q, et al. Application of the ultrafiltration-based LC-MS approach for screening PTP1B inhibitors from Chinese red yeast rice[J]. *Anal. Methods*, 2016, 8(2): 353-361.
- [60] ZHAO H Q, ZHOU S D, ZHANG M M, et al. An in vitro AChE inhibition assay combined with UF-HPLC-ESI-Q-TOF/MS approach for screening and characterizing of AChE inhibitors from roots of *Coptis chinensis* Franch[J]. *J Pharm Biomed Anal*, 2016, 120: 235-240.
- [61] ZHAO A Q, LI L, LI B, et al. Ultrafiltration LC-ESI-MSⁿ screening of 5-lipoxygenase inhibitors from selected Chinese medicinal herbs *Saposhnikovia divaricata*, *Smilax glabra*, *Pueraria lobata* and *Carthamus tinctorius*[J]. *Journal of Functional Foods*, 2016, 24: 244-253.
- [62] LI L, LI B, ZHANG H R, et al. Ultrafiltration LC-ESI-MSⁿ screening of MMP-2 inhibitors from selected Chinese medicinal herbs *Smilax glabra* Roxb., *Smilax china* L. and *Saposhnikovia divaricata* (Turcz.) Schischk as potential functional food ingredients[J]. *Journal of Functional Foods*, 2015, 15(1117): 389-395.
- [63] SHI S Y, PENG M J, ZHANG Y P, et al. Combination of preparative HPLC and HSCCC methods to separate phosphodiesterase inhibitors from *Eucommia ulmoides* bark guided by ultrafiltration-based ligand screening[J]. *Analytical and Bioanalytical Chemistry*, 2013, 405(12): 4 213-4 223.
- [64] 付旭,李利新,汪志华,等. 利用亲和质谱技术从中药材提取物中筛选马尔堡病毒核蛋白的小分子配体[J]. *南开大学学报*, 2016, 49(5): 1-7.
FU Xu, LI Lixin, WANG Zhihua, et al. Ligand screening from TCM extracts against marburg virus nucleoprotein using affinity mass spectrometry[J]. *Acta Scientiarum Naturalium Universitatis Nankaiensis*, 2016, 49(5): 1-7 (in Chinese).
- [65] MULABAGAL V, CALDERON A I. Development of binding assays to screen ligands for plasmodium falciparum thioredoxin and glutathione reductases by ultrafiltration and liquid chromatography/mass spectrometry[J]. *J Chromatogr B Analyt Technol Biomed Life Sci*, 2010, 878(13/14): 987-993.
- [66] CHEN G L, GUO M Q. Screening for natural inhibitors of topoisomerases I from *Rhamnus davurica* by affinity ultrafiltration and high-performance liquid[J]. *Frontiers in Plant Science*, 2017, 8(1 521): 1-11.